A STUDY OF THE PHENOMENON OF BRIDGING OF SUGARCANE BAGASSE

by

HERBERT WOLFGANG BERNHARDT M.Sc.(Chem.Eng.)

A thesis submitted in partial fulfilment of the requirements for the degree of Doctor of Philosophy in the Department of Chemical Engineering, University of Natal.

Durban

December 1996

The experimental work described in this thesis was carried out with the assistance of staff members of the Biotechnology Division of the Sugar Milling Research Institute, as formally acknowleged herein. The thesis, except where specific mention is made in the text to the contrary, is my own original work.

No part of this work has been submitted to any other university or institution for degree purposes.

H.W. Bernhardt

H.W. BERNHARDT

ABSTRACT

This work reports the results of a systematic study of the factors that affect the bridging behaviour of bagasse. It shows that traditional bulk solids theory is inappropriate for predicting bagasse flow mainly because of the impossibility of obtaining a reliable measure of internal friction. It demonstrates the significant influence of fibre length and moisture content on its handling charateristics.

Correlations of pertinent bulk properties such as compactibility, tensile strength, surface friction and translation of vertical into horizontal pressure have been developed. These were derived as a result of measurements in equipment that was designed for the purpose.

Finally, an empirical model utilising these correlations is proposed by which the likelihood of bridge formation in any piece of bagasse handling equipment can be determined. The validity of the model is assessed by comparison with bridging tests that were performed under controlled conditions.

ACKNOWLEDGEMENTS

The work reported in this thesis was carried out as an official research project of the Sugar Milling Research Institute (SMRI). I would like to thank Dr. Brian Purchase, the director, for suggesting it and giving me his wholehearted support and encouragement throughout. I also wish to thank the SMRI Board of Control who approved the necessary funds to execute it.

The enthusiasm of my first supervisor, Professor Robin Judd, formerly from the University of Durban-Westville and the encouragement and guidance of my subsequent supervisor, Professor Brian Loveday, from the Unversity of Natal, are acknowledged with gratitude.

I wish to thank Mr. Conrad Klüsener of the Illovo Sugar Sezela By-products factory for allowing me to set up my bagasse shear cell at his factory and contributing to the costs of the installation and experiments.

I would also like to give special thanks to Mr. Anton Winterbach of the new Komati Mill who made it possible for me to be present during commissioning of this factory and to study the performance of its bagasse handling system.

Numerous discussions took place between myself and factory engineers at all the South African and Swaziland sugar mills on bagasse handling problems. I would like to thank them all for giving me their time and sharing much of their hard-earned experience.

The SMRI workshop team of Messrs. Don McFarlane, Solly Chinsamy and Dave Joseph deserve special mention for the meticulous way in which

they constructed the different items of equipment. Similarly, the electronics experts, Messrs. Vaughn Stone and Mike Gooch, did excellent work in making new instruments, like the bagasse pressure transducer, and data capture hardware.

I am indebted to Mrs. Sue Wienese, Messrs. Paul Notcutt and Seppy Ramsuraj, as well as Miss Vanessa Ochse and Miss Keren Zelinka for doing most of the tedious work of measuring bagasse particle dimensions, and assisting in various ways with the experiments.

I wish to record my gratitude to Dr. Michael Murray from the mathematical statistics department of the University of Natal for assisting me with statistical analysis of the data and to Mrs. Patsy Clarke from the computer services division for helping me with Statgraphics 5.0.

Special thanks are due to Messrs. Rick Hoekstra, John Field, Anton Winterbach, Bruce Moor, Allan Ferguson, Mick Sugden and Rob Bodger as well as to Dr. Brian Edwards for reading, and making helpful comments on, sections of the text, and to Dr. Maurice Kort for his thorough proof reading.

My wife Lucille deserves a medal for patiently continuing to live with the hope that, once the thesis is finished, the multitude of jobs on the house and in the garden will be tackled.

Finally, I want to thank my God for giving me the faith that enabled me to bring this work to a conclusion, and for providing treasured inspiration at crucial stages.

TABLE OF CONTENTS

NOMENCLATURE

Symbol	Description	Units
a, b	Constants	-
b_1,... b_n	Parameters in regression equations	-
c	Coarse-fine ratio	-
d	Volume surface mean particle diameter	m
dM	Differential mass fraction	-
f_c	Unconfined yield strength	Nm^{-2}
g	Acceleration due to gravity	ms^{-2}
h	Bed height, depth	m
h_{arch}	Height of arching zone	m
$h_{arch,eff}$	Effective height of arching zone	m
h_c	Critical bridging height	m
l	Length of bagasse bridge	m
	distance between vertical plates	m
n	Number of particles measured	-
n	Shear index	-
t	Thickness of bagasse bridge	m
x, x_i	Mean sieve interval size,	mm
	mean particle size	mm
x_m	Mean particle size by mass	mm
y	Fibre length	mm
B	Breadth of bagasse particle	mm
C	Cohesion, bridge collapsing	Nm^{-2}, -
C_w	Cohesion at wall	Nm^{-2}
F_{arch}	Friction force due to arching	N
F_{norm}	Normal friction force	N
F_{tot}	Total friction force	N

Symbol	Description	Units
F_{flow}	Flow factor $d\sigma_1/df_c$	-
G	Weight of bagasse	N
H	Adhesion force	N
K, K_i	Ratio of horizontal to vertical stress σ_h/σ_v	-
K_a	Rankine active stress ratio	-
K_p	Rankine passive stress ratio	-
K_o	Zero lateral strain stress ratio	-
L	Length of bagasse particle, mean fibre length	mm
M_i	Mass of particles retained on ith sieve	g
N	Normal component of inter-particle force, no ridge	N -
P	Pressure, bridge persisting	Nm^{-2}, -
P_h	Horizontal pressure	Nm^{-2}
P_v, P_{v2}	Vertical pressure	Nm^{-2}
PR	Parallel ridges	-
R	Radius of cylindrical silo	m
RR	Rectangular ridges	-
S_1, S_2	Surface parameters	-
T	Thickness of bagasse particle	mm
W	Moisture content	%
X, X_1,..,X_i	Sieve aperture size	mm

Symbol	Description	Units
$\beta_0,\ldots,\beta_n$	Regression coefficients	-
Δ	Angle of internal friction (Definition by Williams and Birks, 1967)	-
δ	Effective angle of internal friction	-
ε	Error term	-
κ	Material parameter determining interparticle adhesion forces	-
λ	Length index	-
μ, μ_w	Coefficient of surface friction	-
ρ	Density	kgm^{-3}
ρ_b	Bulk density	kgm^{-3}
ρ_d	Bulk density : dry basis	kgm^{-3}
ρ_p	Particle density	kgm^{-3}
ρ_w	Bulk density : wet basis	kgm^{-3}
Σ	Notation for summation	-
σ, σ_N	Normal stress	Nm^{-2}
σ_h	Horizontal normal stress	Nm^{-2}
σ_T	Tensile strength	Nm^{-2}
σ_v	Vertical normal stress	Nm^{-2}
σ_w	Normal stress at wall	Nm^{-2}
σ_1	Unidirectional (compacting or tensile) stress	Nm^{-2}
σ_ε^2	Variance of error term	-
τ	Shear stress	Nm^{-2}
τ_w	Shear stress at wall	Nm^{-2}
τ_S	Shear strength	Nm^{-2}
ϕ	Angle of internal friction	-
ϕ_W	Angle of wall friction	-

LIST OF FIGURES

LIST OF TABLES

CHAPTER ONE

THE NEED FOR A STUDY ON

THE BRIDGING BEHAVIOUR OF BAGASSE

1.1 INTRODUCTION

Bagasse is the fibrous residue left after sugar has been extracted from sugar cane. The main use of bagasse is that of fuel for boilers which generate steam for the sugar extraction process. Bagasse is, however, also a potentially valuable raw material for a range of by-products including pulp and paper, charcoal briquettes, and a number of useful chemicals such as furfural, xylitol, ethanol, carboxymethyl cellulose and others (Paturau, 1989). As a particulate solid it is notoriously difficult to handle. No systematic study is documented of the fundamental properties of bagasse.

The main reason why this study was undertaken was to obtain a clearer understanding of the variables which affect its flow characteristics, and to provide a basis for the design of equipment which handles and processes bagasse.

In section 1.2 a very brief description of the situations in cane sugar factories that can give rise to bagasse handling problems is presented. Some of the articles in the literature which deal with bagasse handling difficulties are highlighted in section 1.3. The methodology of the study and thesis structure are outlined in section 1.4.

1.2 PROBLEMS OF BAGASSE HANDLING

Modern cane sugar factories employ either a milling tandem or a diffuser to extract sugar from shredded cane. The last stage of the extraction process involves de-watering the fibrous residue using one or two heavy-duty de-watering mills. The de-watered fibrous residue is called bagasse.

The bagasse has to be conveyed from the de-watering mills and fed in a controlled, metered manner to boiler furnaces which utilise it as fuel to generate steam which is used for evaporation. The conventional equipment used for bulk conveying of bagasse is either a slat carrier or a belt conveyor. Pneumatic conveying is used in a number of sugar factories to convey the finer particles of bagasse (called bagacillo) to the filter station where they are used as a filter aid, or to transport the very fine particles (called pith), which are separated from whole bagasse in a depithing operation, to a manufacturing step in which a by-product is made from the bagasse. The principles of pneumatic transport are entirely different from those governing bulk transport of bagasse and will not be considered in this work.

The problems associated with the handling of bagasse can be summarised by a single word: "chokes". A choke involves the excessive accumulation of bagasse in a restricted space such as, for example, a transfer chute. To clear a bagasse choke can be very laborious and often results in an interruption of fuel supply to the boiler furnace. This may give rise to an unsteady steam supply which adversely affects many key operations throughout the factory.

There can be many causes for such an accumulation to commence, some of which are described below. Once an accumulation has started it builds up so quickly because of the rapid speed of the conveyor which continuously keeps bringing large masses of bagasse that it is ususally impossible to stop the conveying system before full development of the choke has taken place. Most chokes are accompanied by firm compaction because the conveyor will continue to feed bagasse into the restricted space until the friction force between the compacted mass and the conveyor causes the motor to trip from an overload signal. The aim of the study was to try and understand why local accumulations take place and to enable equipment to be designed in a way that minimises the chances of their occurrence.

Bagasse conveying (i.e. bulk conveying) normally involves a change in elevation as well as direction. This often necessitates the use of transfer chutes. These chutes often choke up as a result of inadequate design or excessive belt loading.

Close-fitting skirting is usually mounted to the ends of transfer chutes to contain the dust generated as bagasse falls onto the next belt. Accumulation of bagasse can occur at points of attachment of the skirting and initiate a choke.

Special devices such as ploughs are needed to feed bagasse evenly into boiler chutes from a conveyor belt. The design of ploughs which feed adequate amounts of bagasse into all of the boiler chutes without periodically causing local accumulations is no easy matter.

Most factories have a bagasse shed which serves as a temporary storage area to facilitate an uninterrupted bagasse supply for the boiler. The operation of storage involves controlled deposition in, as well as reclamation from, this shed. A special continuous scratcher device, which can be tilted according to the direction of travel to achieve uniform reclamation, is

commonly employed. Nevertheless, bagasse avalanches at the edge of the storage pile occur frequently. These result in overloading of the return belt and the development of chokes at transfer chutes. Avalanche screws (Jackson, 1984) fitted to the scratcher minimise this occurrence, but their effectiveness depends on their setting in relation to the natural angle of repose of the bagasse. This angle can vary significantly for bagasse which originates from different cane varieties. It is also dependent on the length of time for which the bagasse has been stored and the degree of compaction to which it has been subjected by higher layers of bagasse.

Another potential choking point is the feeder device at the bottom end of the boiler feed chute which supplies a steady, metered amount of bagasse to the boiler furnace.

A successful bagasse handling system must be able to convey the required amounts of bagasse from the source to its destination without periodic accumulation occurring at points along this route which would obstruct continuous flow. The reason why transient accumulations of bagasse can become so problematic and cause serious chokes is because of bagasse's extraordinary tendency to form self-supporting bridges. Bagasse, unlike a free-flowing solid like sand in which a momentary accumulation would dissipate itself rapidly, can form a solid mass of considerable strength because of the matting and interlocking behaviour of its particles.

A knowledge of the factors that contribute to the formation of bridges, and what minimum conditions are required under which permanent bridges cannot form, would be helpful in eliminating persistent trouble spots in an existing bagasse handling system and in designing a new system. Examples where such knowledge would find application include

* *design of bagasse chutes and deflector plates*
* *calculations of power consumption for bagasse handling*

equipment

* *design of bagasse ploughs*
* *determination of minimum distance between slats in slat carriers*
* *determination of clearance of slats from carrier decks*
* *design of bagasse screw feeders*
* *design of levelling devices on conveyor belts.*

1.3 REPORTED STUDIES WHICH INVESTIGATED BAGASSE FLOW BEHAVIOUR

Literature that deals with bagasse handling falls into two categories. There are a number of PhD theses which investigate specialised aspects of cane processing, such as milling and diffusion, on a fundamental level. Then there are journal articles and textbook descriptions that report on bagasse handling problems, and offer possible solutions. These generally deal with the effects of one factor on the handling characteristics. The effects are usually described in qualitative terms and the solution offered has been reached by a process of trial and error.

Examples of the first kind are theses by Bullock (1957), Murry (1960), Munro (1964), Solomon (1967) and Russell (1968) who have made in-depth studies of sugar extraction by milling. Rein (1972) presented a study of sugar extraction by cane diffusion. The data on bagasse handling contained in these works is not applicable to the elucidation of the problem of bridging since the experimentation reported was performed under conditions very different from those which pertain to ordinary bagasse handling in chutes, on carriers or on conveyor belts. For example, the pressures investigated in the milling studies were at least one order of magnitude higher than those normally encountered in stored, or loosely poured, bagasse. The diffusion

study of Rein (1972) concentrated on the percolation behaviour of liquids through beds of shredded cane. In bridging studies one is concerned with the flow of bagasse as a bulk solid without the interaction of interstitial liquid.

The following overview of journal articles and textbook descriptions that report on bagasse handling problems will illustrate that, in general, these articles propose solutions to specific problems, based on experience.

The handling characteristics of bagasse are dependent on the degree of preparation. Hugot (1986, p. 100) mentions that the friction properties of bagasse, which affect its handling characteristics, are related to the fineness of preparation. A surface friction coefficient of 0.25 - 0.30 is quoted by Hugot (p. 87) for de-watered bagasse on smooth plates. It is a well established fact that bagasse from a milling tandem has different handling characteristics to that from a diffuser. Mill bagasse generally has fibres of shorter length than diffuser bagasse because in a milling tandem the shearing effect due to the differential speeds of the top and bottom of deep grooves tend to break up the long fibres (Jenkins, 1966, p.75). Bullock and Murry (1957) show that the value of the friction coefficient depends on surface roughness, moisture content, degree of preparation, pressure and speed of movement. Different cane varieties, with their different mean fibre lengths, and different relative proportions of pith particles to stringy fibres, are also considered a cause of differing handling properties (Ramanujam, 1956). Furthermore, temperature can influence handling properties. Farmer (1977) mentioned that hot bagasse is softer than cold.

Chute geometry is considered an important determinant of flow characteristics of bagasse. Long chutes and steep angles assist feeding of bagasse to mills and furnaces (Murry and Hutchinson, 1958). Donnelly chutes are generally 3-4 m long and nearly vertical. The inclination of the front plate of the chute is generally 1° less than the back plate to make the chute slightly diverging. This will counteract the tendency of bagasse to

form arches in the chute (Hugot, 1986, p. 88).

Luxford *et al.* (1977) provide design specifications for a rotary feeder device at the bottom end of the boiler chute based on empirical measurements. They furthermore relate the experience of increased choking occurring in bagasse boiler feeders with increasing amounts of extraneous matter (particularly leaves) in the cane.

Bagasse bridges can form between adjacent slats in a slat carrier if slats are too close together. Ferguson (1957) recommends a gap of 61 cm. Incorrect clearance between slats and the carrier deck can cause slat breakage at the edges of boiler feed chute openings because of the extremly high shearing strength of bagasse. Allan (1970) notes that boiler feed chutes should have openings on slat carrier decks which have an inclined lead-in depression in front of the opening and a similarly inclined lead-out section at the distal end of the opening. This adaptation is said to prevent bridging. The recommended clearance between the tynes of a rake conveyor and the deck is 22 mm (Hugot, 1986, p. 77).

Stored bagasse tends to compact with the passage of time. Knights and Perreira (1966) state that bagasse can pack so tightly under its own weight that reclamation from the storage pile becomes difficult. Ednie (1967) writes that bagasse stored in silos can form bridges which, in the equipment described, were approximately 9 m wide. Collapse of the bridges will inevitably lead to bagasse conveying problems. During storage microbial activity leads to the partial breakdown of the original chemical structure consisting mainly of cellulose, hemicellulose and lignin (Bruijn, 1973). This partial breakdown alters the physical characteristics of the bagasse particles such as fibre length and rigidity. The angle of repose of bagasse affects the reclamation of bagasse from the shed. This angle can vary according to the time of storage, the bagasse type and the degree of compaction. Jackson (1984) quotes a typical angle of repose of 51°.

Carliell (1984) states that ploughs which deflect bagasse off the top of a conveyor belt into a boiler feed chute need to be designed according to the type of bagasse (in terms of moisture content and fibre length). Miyagawa (1975) mentions the difficulty that ploughs have in cutting into bagasse on a conveyor belt when they descend vertically into the bagasse stream to commence diverting it into a boiler chute.

From this overview of the literature on bagasse handling problems it appears that there seems to be no record of a systematic study of the properties of bagasse on which the design of handling equipment can be based. This thesis represents an attempt at such a study.

1.4 METHODOLOGY OF THE STUDY AND STRUCTURE OF THE THESIS

The properties of the aggregate of particles which make up bagasse determine its behaviour, or more specifically, its tendency to form self-supporting bridges. It is therefore necessary to define these properties, and to specify the techniques whereby they are measured.

Possible characteristics that have an influence on the flow behaviour of bagasse are:

* *mean particle size*
* *ratio of coarse fibres to fine pith particles*
* *shape of particles*
* *particle rigidity*
* *particle hardness*
* *moisture content*
* *bulk density*
* *compactibility*
* *soil content*

* *surface friction coefficient*
* *internal friction or shear strength*
* *tensile strength.*

This list of properties would take account of variations in handling behaviour caused by different processing methods (milling or diffusion, degree of preparation, de-watering efficiency) and harvesting techniques or conditions, as well as those produced by different cane varieties. In this study an attempt was made to take measurements of most of these properties - with the exception of particle rigidity and hardness, and soil content. Rigidity and hardness were not measured because the author could not conceive a valid technique for doing this. The bagasse used for the measurements included samples from milling tandems and diffuser factories, as well as samples of pith and de-pithed fibre. This was done so as to provide information that would cover the widest range of particle size encountered in industrial bagasse handling operations. Soil content was ignored because the measured average ash content in bagasse for the whole South African sugar industry is 1.5% of which 1.0% represents the soil content. Although the soil content can increase markedly during a prolonged rainy harvesting period, it was assumed that excessive soil contents are rare and that normal soil contents would not affect the overall bagasse properties significantly.

In essence therefore, an attempt has been made to measure the specified bagasse properties and to establish a theoretical model predicting the bridging behaviour based on these measurements. A bagasse bridge measuring apparatus was designed and built to test the validity of the model. The definitions as well as the techniques used to measure the stated bagasse properties are given in appropriate sections of the thesis.

The thesis is structured as follows. Chapter 1 gives a general introduction and lists potential as well as reported bagasse handling problems. In chapter 2 the conventional analysis techniques used to predict flow behaviour of

most bulk solids are examined critically in terms of their usefulness in predicting the flow characteristics of bagasse. Chapter 3 gives a detailed account of particle size, shape and pith:fibre ratio measurement techniques that were employed together with corresponding results. Chapter 4 deals with the measurement of bulk properties such as surface friction, compactibility, internal friction, tensile strength and the translation of vertical pressure to lateral pressure. Multilinear regression is used extensively to correlate these measurements with particle properties and moisture content. Chapter 5 presents the results of bridging experiments as well as the theoretical model which attempts to predict bridging behaviour in terms of the various bagasse properties measured. Chapter 6 is a summary of the main results of this work. Construction details of some of the specialised experimental equipment and calibration graphs are given in the appendices.

The literature overview presented in section 1.3 of this chapter is not exhaustive. It was thought prudent to refer to relevant writings in places of the text where the different topics are covered at greater depth rather than compile a "stand-alone" literature survey.

CHAPTER TWO

EXISTING THEORY ON FLOW OF BULK SOLIDS AND BAGASSE

2.1 INTRODUCTION

The aim in this chapter is to review the theories that have been proposed for understanding and predicting the flow behaviour of general bulk solids, and to establish whether or not these are appropriate in analysing bagasse flow.

The term "bulk solids" includes a wide variety of solid materials that can be considered to have commercial value, and therefore need to be handled on a regular basis in bulk. The list includes powders like cement, clay or spray-dried coffee, as well as ores, ground rocks and mineral concentrates, crystalline substances like salt, sand and sugar, particulate agricultural products like maize or grains and extraction end-products such as soy bean shreds. It can be appreciated that these solids represent a large diversity of particle size, shape and hardness. Additional properties that significantly influence handling characteristics include moisture content, temperature and biological degradation on storage. To indicate flowability, bulk solids are usually divided into cohesive and free-flowing solids.

From this very brief reference to some of the characteristics of bulk solids it is readily appreciated that the formulation of an all-embracing theory that may accurately predict the conditions under which any of these materials will flow under the influence of gravity alone, is likely to be a monumental task. Extensive narrowing of some, if not many, of the variables is probably necessary before one can hope for success in this field. The review that follows attempts to give a description of the narrowing that has been done in the theories that have been propounded.

2.2 HISTORICAL DEVELOPMENT OF BULK SOLIDS THEORY

Cowin (1974) states that there are two general approaches in the formulation of a theory on bulk solids flow: the particulate and the continuum. The particulate approach deduces the properties of the bulk solid from those of an aggregate of its particles, which for analysis purposes are usually assumed to be of uniform shape and size. In the continuum approach the properties of the bulk solid are regarded as continuous funtions of position. The particulate approach may be useful in understanding the behaviour of individual particles during flow, but it has not yielded reliable results that can be used for design purposes, such as the calculation of the required angle of a hopper or the prediction of flow rates. The continuum approach which uses "bulk" concepts such as pressure, friction and stress has been more successful in achieving agreement between theory and observation. The early development of bulk solids theory relied solely on continuum concepts. In recent years attempts are being made (Molerus, 1975) to marry the two approaches.

Many analyses that predict the flow behaviour of bulk solids through openings in the bottom of hoppers or silos start with expressions for the vertical and horizontal stress distribution throughout the mass of material. The horizontal stress determines the magnitude of the friction between the

material and the wall of the container, and the vertical stress determines the magnitude of the horizontal stress. These stresses are likely to determine whether or not the material is going to yield (flow).

Nedderman (1982) detailed the essential elements of some of the historical achievements in the evolution of bulk solids theory. As early as 1776 Coulomb attempted to calculate the forces on retaining walls in fixed soils. His method of wedges, which was subsequently refined, is used in soil mechanics today. It uses a triangular element in which the failure surface (along which motion of the bulk material takes place) is assumed to be a plane. Nedderman showed that a failure surface is usually curved. Coulomb's method may be used to predict pressures in bunkers and hoppers of rectangular cross sections but appears to be inadequate for those with circular cross-section.

Most analyses assume the bulk solid to behave as an ideal Coulomb solid. For such a solid corresponding sets of values of normal stress (σ) and shear stress (τ) at a point of failure or yield, called a yield locus, follow a linear relationship of the form

$$\tau = \mu\sigma + C . \qquad (2.1)$$

μ is called the coefficient of internal friction and C the cohesion (Nedderman 1982). The wall yield locus, which describes the conditions of failure or sliding at a wall, similarly has the form

$$\tau_w = \mu_w\sigma_w + C_w \qquad (2.2)$$

where the corresponding variables written with the subscript "w" are those operating at the wall. The coefficients μ and μ_w are often written as $\tan\phi$ and $\tan\phi_w$ where ϕ and ϕ_w are referred to as the angles of internal and wall friction respectively. Where the relationships between τ and σ, or τ_w and σ_w are non-linear (as in Figure 2.1 below), ϕ and ϕ_w are the angles which the gradients to the curves make with the horizontal direction. Coulomb's

analysis of wedges relies on the knowlege of the two bulk solid properties ϕ and ϕ_w.

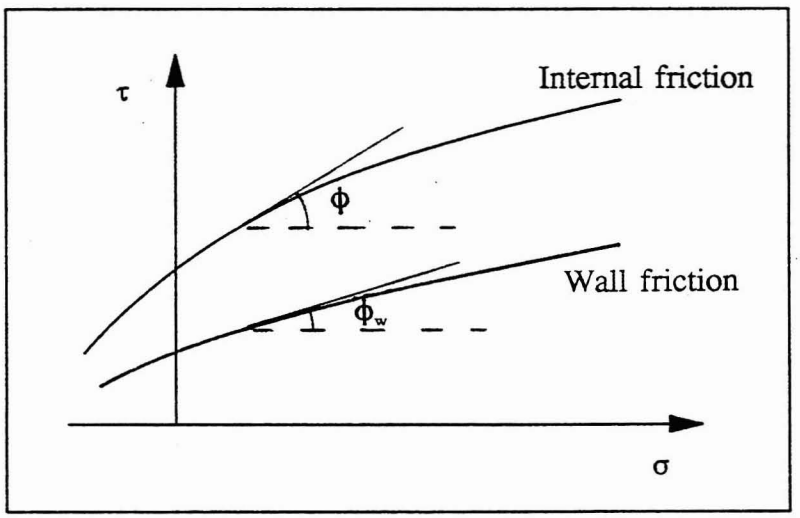

Figure 2.1 Angle of internal friction and angle of wall friction

The next major advance in the understanding of bulk solids behaviour was made by Janssen (1895). His famous equation (equation 2.3, derivation in McCabe *et al.*, 1985) used a horizontal differential slice as the basis for analysis.

$$P_v = \frac{Rg\rho_b}{2\phi_w K}\left[1 - e^{-2\phi_w Kh/R}\right] \qquad (2.3)$$

The equation calculates the vertical pressure P_v for a granular material of bulk density ρ_b at a depth h below its surface in a cylindrical silo whose radius is R. K is the ratio of horizontal to vertical stress which Janssen assumed to be constant for a given material and g is the acceleration due to gravity. The relationship (equation 2.3) has been shown to give reliable results in static loadings of silos and is particularly suited to those with circular cross-section. Subsequent workers (McCabe *et al.*, 1985) have expressed the ratio K as a function of ϕ, the angle of internal friction, namely

$$K = \frac{1 - \sin\phi}{1 + \sin\phi}. \qquad (2.4)$$

The pioneering work of Jenike and his co-workers (Jenike *et al.*, 1960) laid the foundation of modern bulk solids theory and formed the basis of much of the subsequent theoretical development. They used the term "rigid-plastic Coulomb solid" the flow behaviour of which could be described in terms of a limiting yield function (yield locus) depicted on a shear stress (τ) - normal stress (σ) system of axes shown in Figure 2.2. For any plane surface within the bulk solid the normal stress σ acts at right angles to and the shear stress τ tangential to the surface respectively.

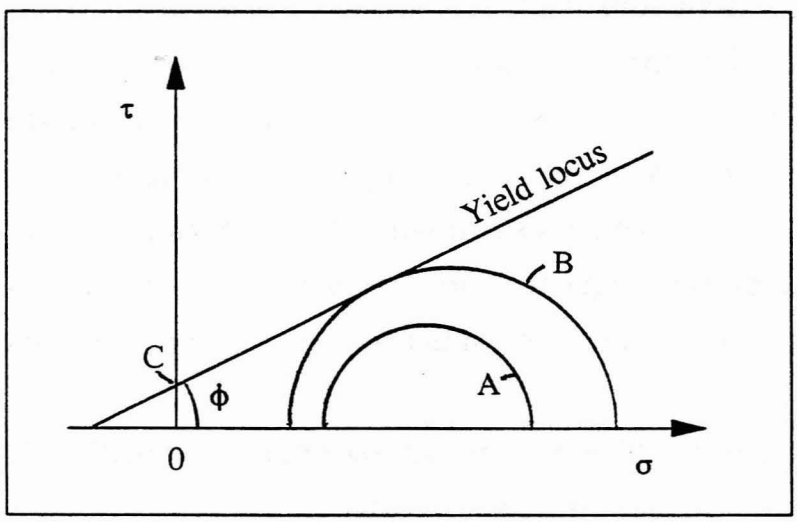

Figure 2.2 Yield locus of a Coulomb solid

Stresses lower than those represented by the function result in a static equilibrium (i.e. no flow) whereas those equal to the values of the function result in plastic yield or flow. The method of analysis makes extensive use of Mohr's stress circle (for derivation see, for example, Ryder, 1969) which represents the shear and normal stresses acting at a point in any material under consideration. The points of intersection of Mohr's stress circle with the normal stress (σ) axis represent the major and minor principal stresses acting at the point. If the stress state at a particular point in the solid material is represented by a Mohr circle situated below the yield locus (circle A) then the solid will remain rigid - in other words, no flow will occur.

A stress condition represented by a Mohr circle touching the yield locus (circle B) results in plastic deformation (i.e. flow) whereas stress conditions corresponding to Mohr circles intersecting the yield locus are, according to the theory, indicative of states of stress that cannot exist. This method of depicting flow conditions also gave a quantitative meaning to the term cohesion, C, as being the shear stress on the yield locus at zero normal stress.

For the determination of the yield locus Jenike developed a special apparatus called the Jenike shear cell by which the shear properties of the material could be measured. A strict procedure for doing the measurements was stipulated, as documented in Jenike *et al.* (1960). The range of particle sizes was restricted to particles that passed through an 840 μm sieve. The rationale given for this is that it is the fine particles that mainly determine the flow characteristics of the solid. The procedure also specifies steps to ensure a uniform specimen and a repeatable degree of consolidation.

Jenike *et al.* (1960) conceded that the limiting yield function or yield locus is not unique for a given material. Its position depends on the degree of consolidation of the material. Furthermore, the locus does not extend indefinitely, but ends at a well-defined point E called the terminus which is the point where the Mohr circle corresponding to the applied consolidating stress σ_1 touches the yield locus (see Figure 2.3).

The yield locus can be used to determine another material property called the unconfined yield strength, f_c. The method of its determination is described below with reference to Figure 2.3.

At a free surface of the material the normal stress is zero. The unconfined yield strength is the maximum pressure the solid can sustain at a free surface, and from first principles of stress analysis (see Ryder, 1969) this must be the major principal stress acting at that point (the minor principal

stress being zero), and it must act tangential to the surface. Thus the point of intersection with the σ axis (point D in Figure 2.3) of the Mohr circle which passes through the origin of the τ-σ plane and touches the yield locus gives the unconfined yield strength f_c. This is also a function of consolidating pressure σ_1.

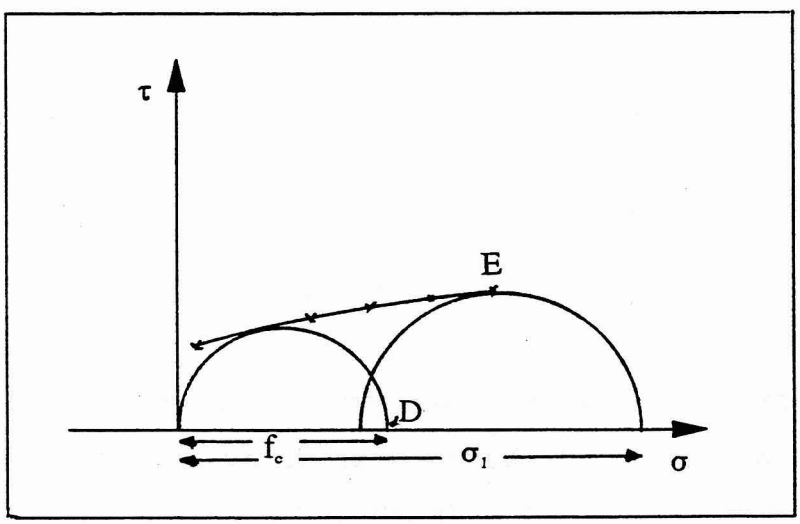

Figure 2.3 Determination of unconfined yield strength

A plot of f_c against σ_1 is called the flow function, an example of which is shown in Figure 2.4. Jenike regards this function as the most important flow property of a bulk solid. In many cases this function can be adequately approximated by a straight line through the origin. The reciprocal of the gradient of that line

$$F_{flow} = \left(\frac{d\sigma_1}{df_c}\right) \qquad (2.5)$$

is called the flow-factor F_{flow}. When $F_{flow} = \infty$, $f_c = 0$ and the solid is perfectly free-flowing. When $F_{flow} < 1$ then the unconfined yield strength f_c is greater than the major consolidating pressure σ_1, and this solid will not flow by gravity only.

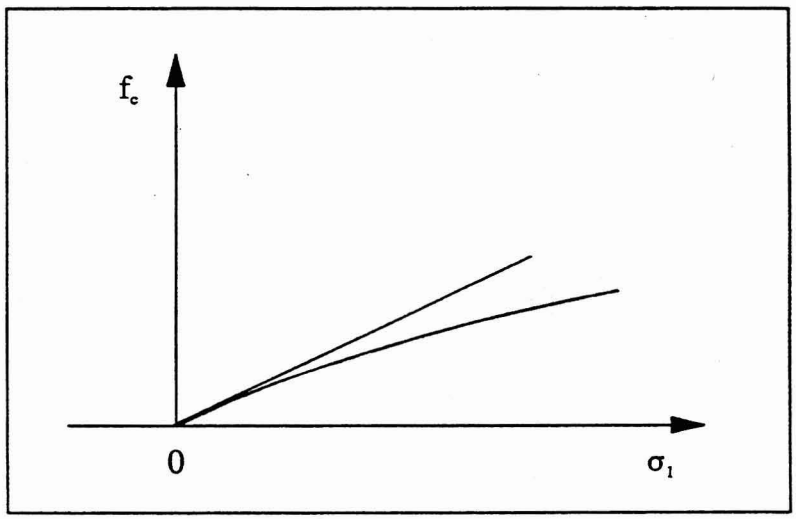

Figure 2.4 A typical flow-function plot

Jenike also defined a derived quantity which he called the "effective angle of internal friction", δ, which is depicted in Figure 2.5. For each consolidating stress σ_1 there is a unique Mohr circle. The envelope of these Mohr circles is called the "effective yield locus" (EYL) which has been found to approximate a straight line passing through the origin. The angle δ (that is, the effective angle of internal friction) which this line makes with the σ axis is a characteristic property of the bulk solid. It is frequently used in mathematical analyses investigating continuous flow. A Jenike shear cell (Jenike *et al.*, 1960) is used to determine δ for a particular material.

Carr and Walker (1967) developed an annular ring shear cell to determine the same property. Walker (1966) combined Janssen's method of stress analysis with the ideas of Jenike. He used the effective yield locus (EYL) and the wall yield locus (WYL - see description below) to develop formulae whereby the average vertical stress at any level in a silo as well as the corresponding horizontal stress are determined. His contribution was to show how wall friction affects the values of vertical and horizontal stress in the vicinity of the wall. Using his theoretical analysis he developed formulae which could determine the minimum size opening to prevent arching or bridging of the

material to occur during discharge. His analysis requires a knowledge of the angle of wall friction ϕ_w and the effective angle of internal friction δ.

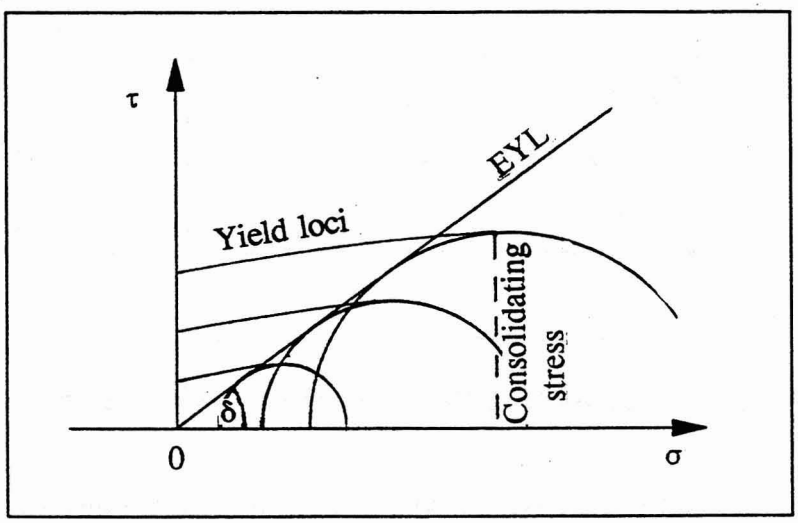

Figure 2.5 Effective angle of internal friction.

The wall yield locus (see Figure 2.6), which is also plotted on the τ - σ diagram, represents the shear stresses required to move the bulk material over a given surface for different normal stresses. Its position depends both on the bulk solid and the wall material. It can often be approximated by a straight line passing through the origin and the angle which this line makes with the σ axis is called the angle of wall friction ϕ_w. The angle of wall friction ϕ_w is invariably less than the effective angle of internal friction δ, except for so-called rough walls for which ϕ_w is taken as being equal to δ, the implication being that the surface of a rough wall is assumed to consist of the same material as the bulk solid.

In his theoretical development Walker (1966) implies that there are two possible stress values that a flowing material can assume, depending on the conditions of flow. At the wall these two possibilities are shown as P_1 and P_2 in Figure 2.6 as elaborated more precisely by Walters (1972).

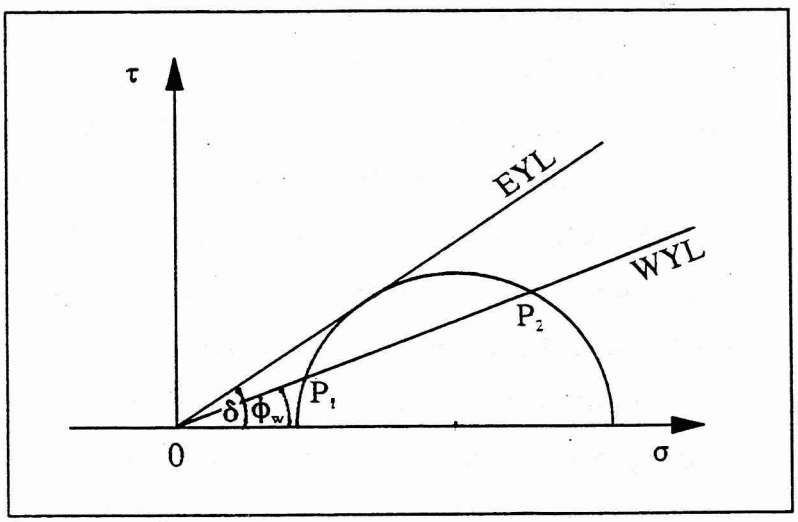

Figure 2.6 Two possible stress conditions during material yield at the wall

Walters distinguishes between the static case (point P_1) which pertains during filling of a silo without any material being withdrawn at the same time, and the dynamic case (point P_2) when bulk material is discharged from the silo. He postulates that these two cases give rise to two widely divergent stress distributions in the silo. The analysis for the two different stress distributions is based on the soil mechanics concepts of "Rankine active" and "Rankine passive" states (see Terzaghi, 1943). They are illustrated in Figure 2.7 and represent two extreme cases of plastic equilibrium.

Consider a semi-infinite layer of soil which at one end is prevented from sliding and forming its natural angle of repose by a retaining wall. The Rankine active case refers to the situation where the retaining wall moves outwards and the soil slides along a failure surface as shown in Figure 2.7 (a). In the Rankine passive case the retaining wall is subjected to an inward movement causing a portion of the soil to be compressed and pushed upwards as shown in Figure 2.7 (b). The yield stresses are those that occur at the failure surfaces. Walters uses the Mohr stress circle, in conjunction with the appropriate values for δ and ϕ_w to derive expressions for these. He argues that during filling of a silo the active state prevails as the material

flows to fill available space, while during emptying, particularly if there is a tapering hopper section in which the cross-sectional area diminishes, the passive case applies because of the continuous compression which the material undergoes as it flows towards the outlet. At inception of flow a change occurs from the static to the dynamic state. This results in a switch of the stresses from the active to the passive case. This switch, which moves as a pressure wave upwards through the silo from the discharge opening, may result in forces on the silo wall several times larger than those predicted by Janssen's formula. Other investigators (for example Blight, 1988) deny that this occurs.

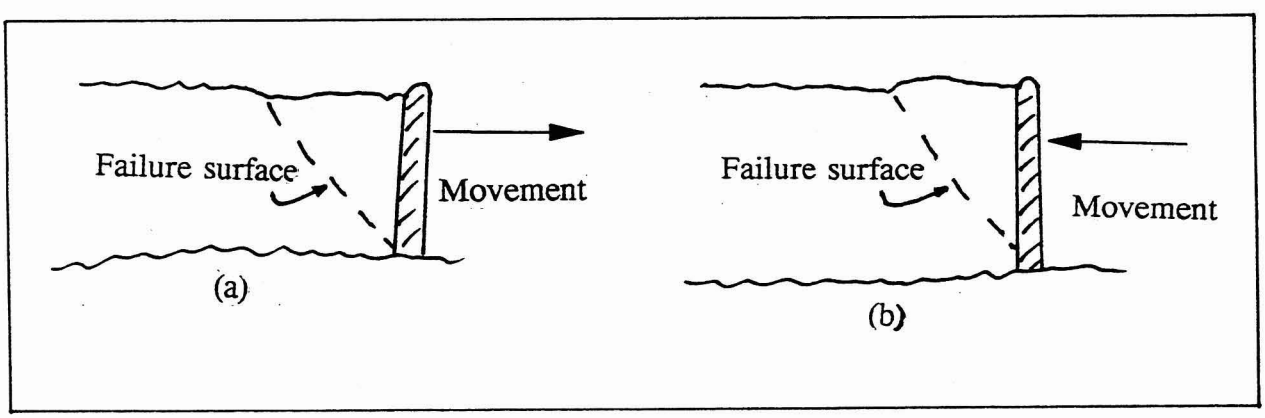

Figure 2.7 (a) Rankine active and (b) Rankine passive failure

In a critical examination of the Jenike yield locus Williams and Birks (1967) conclude that the tensile strength σ_T of a powder plays a significant role. The determination of the tensile strength is illustrated in Figure 2.8. When a material yields under a shear force some of the work done by the force is used to overcome internal friction of the material while the remainder is absorbed in producing a change of volume during the failure. For a rational separation of these two components it is necessary to re-plot the stress-strain diagram so that the yield locus intersects the σ-τ axis at the origin instead of at the value σ_T. This can be done by plotting compound normal

stress (defined as $\sigma_T + \sigma_N$) against shear stress τ. The end-points of the yield loci thus plotted lie on a straight line which passes through the origin, as shown in Figure 2.9.

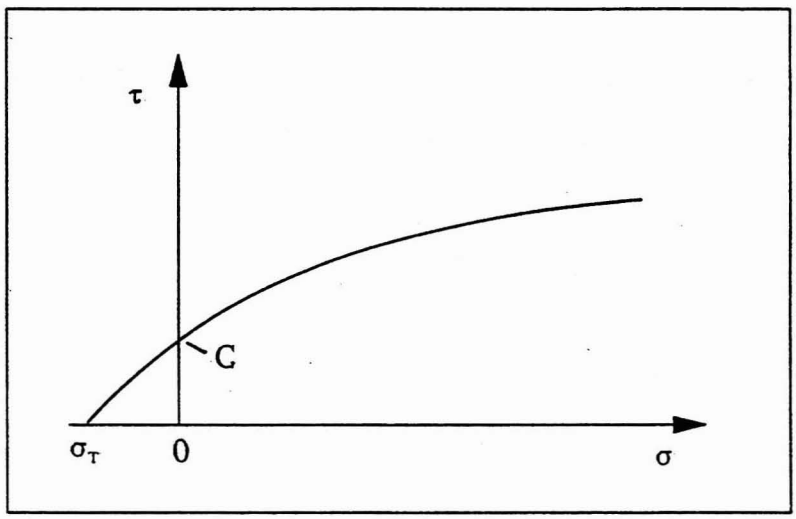

Figure 2.8 Determination of tensile strength of a bulk solid

Each end-point of a yield locus represents a point for which yield occurs without change of volume, and therefore represents the condition where the shear force does work against friction only. In other words, the angle , Δ, which the line through the end-points of the yield loci makes with the compound stress axis would be the true angle of internal friction. The analysis presented by Williams and Birks assumes that the material mass is isotropic and that its bulk density uniquely defines its state of compaction.

The Warren Spring equation quoted by Williams and Birks (1967) has been used to model the yield locus at constant bulk density. This equation has the form

$$\left(\frac{\tau}{C}\right)^n = \frac{\sigma_N + \sigma_T}{\sigma_T} . \qquad (2.6)$$

C and σ_T are the cohesion and tensile strength indicated in Figure 2.8 respectively and σ_N is the applied normal stress. The so-called shear index n is claimed by Farley and Valentin (1968) to be related to the volume surface mean particle diameter d by the relation

$$n = 1 + \frac{B}{d^{\frac{2}{3}}} \qquad (2.7)$$

where B is a constant. The tensile strength σ_T is correlated with the bulk density, ρ_b, and the particle density, ρ_p, by the equation

$$\sigma_T = A\left(\frac{\rho_b}{\rho_p}\right)^m \qquad (2.8)$$

where A and m are constants. The above equations are based on measurements conducted on five different powders that had been chosen for their relatively constant particle shape but wide range of particle size and specific gravity.

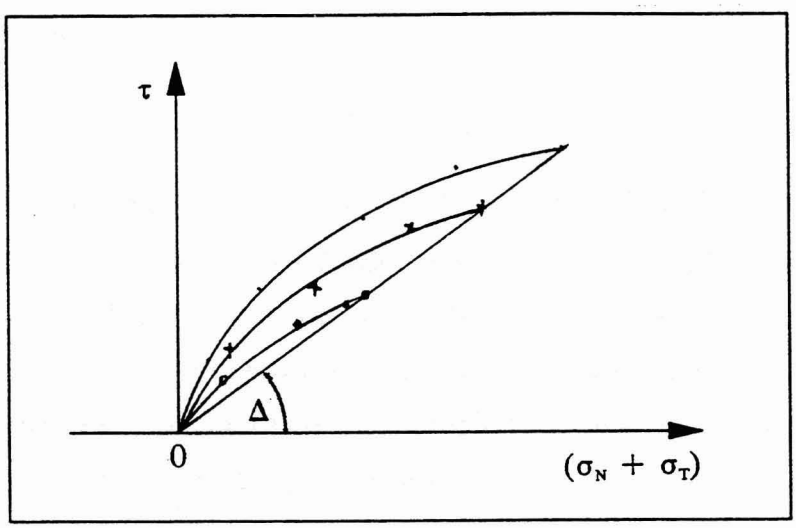

Figure 2.9 Yield loci with shear stress plotted against compound stress

Further development in bulk solids theory took place by adopting a different elementary surface on which the stress analysis was based. Janssen had used a horizontal slice of material on which a force balance was performed. This balance assumed that the stresses on any horizontal plane are uniform (Nedderman, 1982). The method of characteristics (described by Wilms, 1985) does not require such an assumption, and yields an exact solution according to Nedderman. It uses a small rectangular element, on which a force balance is executed, to represent the stress conditions at any point in the material. Although this method is reputed to give more accurate answers, the calculation procedure is far more onerous than the other methods described so far. It does assume, however, that the material is in a state of incipient failure at all points and, like the other methods, it requires a value for δ, the effective angle of internal friction.

The theories described so far require two material parameters, namely an internal friction measure (ϕ,δ or Δ) and a wall friction measure (ϕ_w) for solution. Molerus (1975), in formulating a theory of yield for cohesive powders, combined the continuum concept of stress with the forces transmitted at interparticle contacts. He postulated that the cohesive behaviour of fine powders is due to the adhesion forces generated between particles. These adhesion forces vary in proportion to the normal component of the inter-particle forces, i.e.

$$N = \kappa H \qquad (2.9)$$

where N is the normal component of the interparticle force and H the adhesion force. The constant of proportionality, κ, for fine powders has a value of approximatley 0.3 and is considered to be a material parameter. The degree of consolidation therefore influences significantly the magnitude of the adhesion forces. The increase in adhesion forces caused by increased consolidation is considered to be a consequence of plastic deformation, or flattening, of the contact points. The resultant increase in contact area between touching particles produces an increase in the van der Waals forces

between the contacted areas. The theory further postulates that the effective angle of internal friction, δ, is an invariant material property which is a function of ϕ, the angle of internal friction, and κ, according to the following relationship:

$$\tan \delta = (1 + \kappa) \tan \phi \; . \qquad (2.10)$$

An interesting consequence of this theory, which, reportedly, is supported by experimental measurements, is that anisotropic mechanical properties can be generated in the bulk solid by different combinations of principal stresses, even though the degrees of consolidation are identical. This contradicts the continuum mechanics notion that a bulk solid consolidated to a uniform degree is regarded as an isotropic, homogeneous medium and that bulk density only determines the states of stress within the solid.

The idea that the consolidating technique may affect the slope and position of the yield locus, due to the relative position of the particles, was also mentioned by Jenike *et al.* (1960) and they consequently stipulate their very precise "two-step consolidation" procedure. Molerus (1975) furthermore concludes that the results of tests on material properties, such as yield loci, generated by different measuring devices are not necessarily comparable.

Janssen's formula (equation 2.3) contains the factor K which represents the ratio of horizontal to vertical stress, σ_h/σ_v, at any point in a bulk solid. Blight (1988) defines three different values of this ratio for cohesionless solids. Their relationship is illustrated in Figure 2.10.

The distinguishing feature which determines the appropriate value of the ratio is what restriction applies to the horizontal strain of the material. If the material can expand laterally without limit when loaded vertically then the Rankine active ratio, K_a, applies. This is related to the angle of internal friction , ϕ, by

$$K_a = \frac{1 - \sin\phi}{1 + \sin\phi} . \qquad (2.11)$$

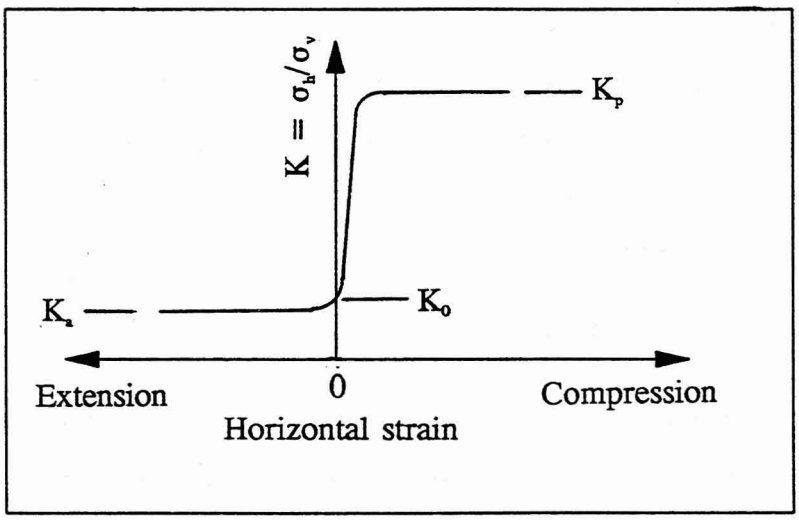

Figure 2.10 Definition of the different values of the stress ratio, K

The "at rest" or "zero lateral yield" ratio, K_0, applies when all lateral strain is prevented as the material is loaded vertically, as in the case of filling a silo with rigid walls such as reinforced concrete. Blight (1988) says that this is related empirically to ϕ by

$$K_0 = 1 - \sin\phi . \qquad (2.12)$$

The third ratio is called the passive stress ratio, K_p, which applies to the material being compressed laterally while the vertical stress is kept constant. The relation between K_p and ϕ is

$$K_p = \frac{1 + \sin\phi}{1 - \sin\phi} . \qquad (2.13)$$

Blight investigated the horizontal pressures in two model and ten full size structures, in particular the increases in horizontal pressure occurring during the change from filling to emptying, with specific emphasis on the transition between the cylindrical to the converging part of the silo. Walker's (1966)

and Jenike's (1964) theories predict a possible nine-fold increase in the K ratio from the active (filling) to the dynamic (emptying) condition at the transition point between vertical and converging walls. Blight maintains that, for $\phi = 50°$, for example, his analyses indicate a much smaller increase in the K ratio, namely by a factor not larger than 1.8. In other words, the excessively large stresses predicted by Jenike and Walker to occur at commencement of flow (called the switch stresses) were not substantiated by the measurements presented by Blight. The following relationship adequately provided the appropriate limit for the horizontal stress

$$\sigma_h = K_0 \rho_b h . \qquad (2.14)$$

The few instances of non-adherence to the limit defined by equation 2.14 seemed to be related to silo expansion or contraction caused by diurnal temperature variations, or posssible inaccuracies in silo construction. Blight further recommends that actual measurements of particle properties, such as bulk density and angle of friction, be used for accurate design instead of tabulated values given in codes of practice.

Other bulk solid theories are reported in the literature, but these seem to have gained limited acceptance. In order that a balanced perspective be presented it is considered appropriate to highlight some of the shortcomings of the "main-line" theories, as outlined by the main proponents of these same theories.

Roberts (1991) who lists several of the achievements of modern bulk solids theory says: "the level of sophistication required by industry demands in many cases a better understanding of the behaviour of bulk solids.... It becomes progressively clearer that there are many gaps in the present state of knowledge where further research is necessary." Carson (1991) writes: " the inadequacy of bulk solids flow theory is reflected in the significant number of silo failures that occurred in the 1980's". Molerus wrote in 1985: "Well proven design procedures are available ... only for a few problems of

practical importance. ... It has to be considered that, so far, only qualified answers have been given to limited questions with respect to material properties. These questions are essentially

- what is the mechanism of steady-state flow and
- what are the limiting states of stress for incipient yield of a previously consolidated particulate material."

Nedderman (1982) also concedes that the understanding of bulk solids flow is rather limited. In particular, he maintains that one cannot adequately describe regions of elastic equilibrium and how these affect adjoining regions of critical equilibrium where flow is about to commence. In real flow situations, particularly those involving fine or angular materials, flow is often irregular. This indicates an oscillating interplay of different kinds of dynamics which are not fully understood. Jenike *et al.* (1960) are quick to point out that "the present state of knowledge precludes a complete analysis of the flow of such (bulk) solids".

What further complicates the accurate prediction of flow behaviour is the fact that it is very difficult to achieve agreement on measured properties of the bulk solids. Schwedes (1983) shows that wall friction measurements of identical bulk solid/wall combinations can vary by as much as 10°. Wall friction τ is generally considered to be a linear function of consolidating stress σ. In a series of carefully controlled measurements on coal McLean (1988) showed that as consolidating stress decreases the wall friction angle increases, even to the extent of exceeding the internal angle of friction. To fit this curve he proposes an equation of the form:

$$\tau = A - \frac{B}{\sigma + C} \qquad (2.15)$$

where A, B and C are constants.

Arnold and Reed (1987) who compared shear results from a Jenike shear

cell with those from a Walker ring shear apparatus found significant differences. Hoeckman and Meulewaeter (1988) found it necessary to design a special shear apparatus to measure the required shear properties of soy shreds. Their measurements furthermore showed that the properties of the material changed considerably after being stored for some time.

It is thus clear that the accurate prediction of the flow behaviour of bulk solids is not a simple matter. In the following section an assessment will be made of the extent to which existing bulk solids theory is useful in analysing the flow characteristics of sugarcane bagasse.

2.3 EXISTING BULK SOLIDS THEORY AND BAGASSE

The applicability of existing theory to the flow behaviour of bagasse is directly linked to the characteristics of the particles which comprise bagasse. In most bulk solids for which properties have been measured the particles are of relatively uniform size and shape, as well as hardness. None of these properties applies to bagasse. Bagasse particles can range in length from 0.2 to more than 100 mm. Furthermore, the stringy nature of the material causes the particles to interlock and form mats of considerable tensile strength, which is not the case with most other bulk materials. There is also a considerable range in particle hardness for bagasse. The pith particles are soft and spongy whereas the fibres derived from the rind of sugarcane stalks are relatively hard and unyielding. The diversity of particle hardness, size and shape result in bagasse exhibiting unusual flow characteristics. It seems that existing bulk solids theory is inadequate for establishing bagasse flow criteria. Some additional reasons why the author believes this to be the case are given below.

In the previous section it was made clear that there were two measurements that were essential for the prediction of flow behaviour, namely the wall

friction and the internal friction. It is relatively simple to perform wall friction measurements for bagasse, as shown in section 4.2. However, existing shear testers, such as the Jenike shear cell, or the Walker annular ring apparatus are totally inadequate for measuring the shearing characteristics, or internal friction, of bagasse. The reason is that when an attempt is made to shear bagasse, instead of yielding, which would result in one portion of the bagasse sliding relative to another, it tends to compress and form a tight, compact, unyielding mass the strength of which increases with increasing shear force. It appears that it is not possible to obtain a meaningful measure for one of the key input variables, namely internal friction, using conventional test equipment.

McLean (1988) does make the observation that some materials do not exhibit the freedom to shear, and bagasse seems to be one of these. The author designed an apparatus to investigate the shear strength of bagasse which is described in section 4.4. The results of these investigations indicate that bagasse does not exhibit shearing behaviour in the sense that shear is normally understood.

Plaza and Edwards (1994) describe shearing tests carried out on shredded sugarcane at pressures normally encountered during milling (200 kPa to 20 MPa), in other words, much higher pressures than are normally found in bagasse flow situations. The type of shear in those tests involves partial, if not total, particle shear.

Molerus (1975) postulates that the cohesive behaviour exhibited by fine powders whose particles are of the order of 1-10 μm are due to adhesion forces occurring at interparticle contacts. Bagasse certainly does appear to exhibit cohesive behaviour, but most of its particles are much larger than those for which adhesive forces are significant. It is suggested that the cohesive behaviour of bagasse is due to the interlocking of the fibres of which it is constituted. The reason for the cohesive nature of bagasse is

therefore structural, not due to adhesion forces between the particles. Existing theory makes no provision for this phenomenon.

As described earlier, existing bulk solids theory relies on the phenomena of Rankine active and Rankine passive yield. By simply taking a mass of bagasse between two hands and pressing it together it is observed that the more it is compressed, the stronger it becomes, with a decreasing tendency to yield. In other words, it appears that bagasse does not yield significantly under Rankine passive conditions. Thus, an analysis which is based on the active and passive forms of yield cannot be applied to bagasse.

It therefore seems evident that a totally different approach from that by which bulk solids flow is normally analysed, be applied in order to predict the conditions under which bagasse will flow. In this thesis (see chapter 4) multivariate expressions have been developed for surface friction, compactibility, tensile strength and translation of vertical to horizontal pressure as functions of mean fibre length, bulk density and moisture content. These expressions are used to predict the tendency of bagasse to form self-supporting bridges in rectangular chutes by applying an empirical model which is presented in chapter 5.

CHAPTER THREE

CHARACTERISATION OF BAGASSE PARTICLES

3.1 INTRODUCTION

The particle characteristics of a bulk solid, such as size and shape distribution, have a profound influence on its handling behaviour. For this reason it was considered essential that repeatable methods of particle size and shape analysis be available for bagasse in order to express differences quantitatively. Considerable effort was invested in this area and the results of the work performed on particle characterisation are summarised in this chapter under the following headings:

Problems of particle size and shape determination
Sieve analysis
Shape characterisation
Calculation of "mean fibre length"
Coarse-fine ratio.

3.2 PROBLEMS OF PARTICLE SIZE AND SHAPE DETERMINATION

The main difficulty with attempting to quantify the size and shape of bagasse particles concerns the tremendous diversity of these properties exhibited by bagasse. The particles can be broadly classified into "fibres" and "pith", but the range of sizes and shapes within these classes, particularly in the case of fibres, is excessive, as is clear from Figure 3.1. For example, bagasse fibre lengths can vary from approximately 0.5 mm to 150 mm. Pith sizes do not cover such a wide range, but the shape of pith particles varies widely, as shown in the photograph in Figure 3.2.

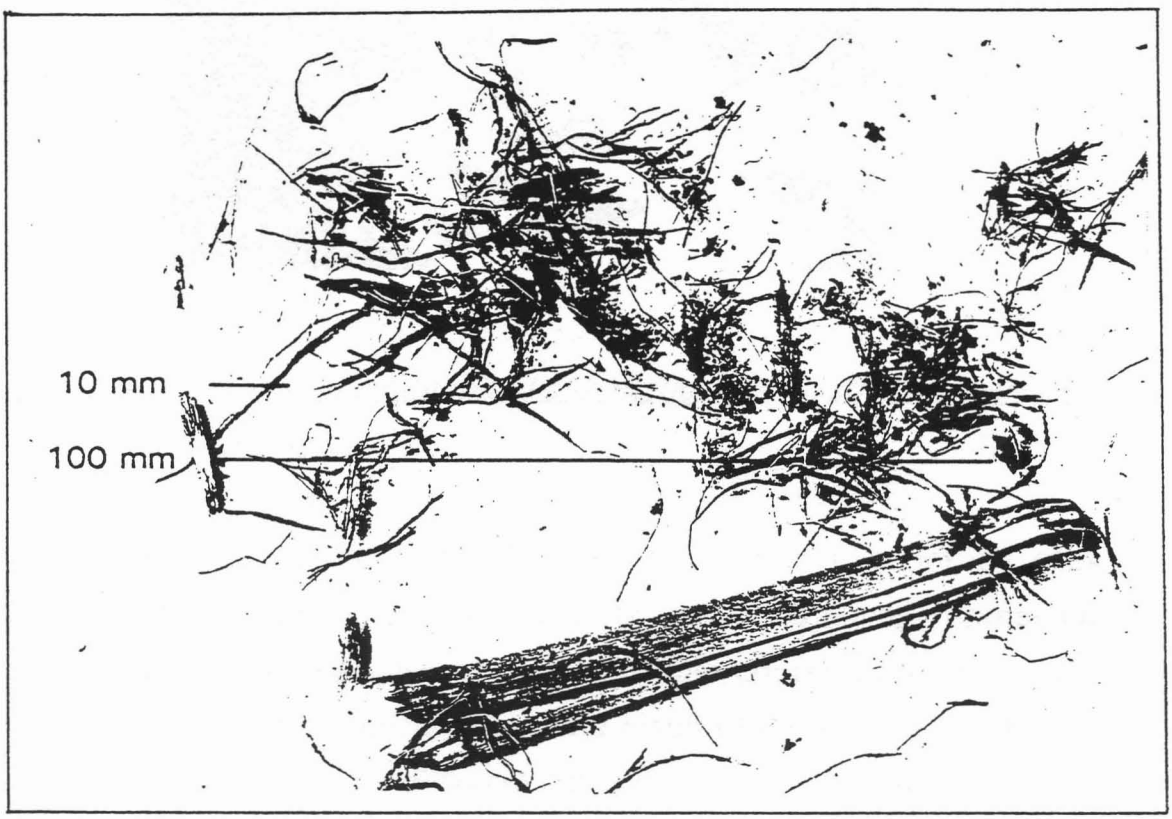

Figure 3.1 *A selection of bagasse particles to illustrate the ranges of size and shape*

Possible methods of size analysis include microscopic or laser scanning, sieve fractionation and pneumatic classification. Whatever method of particle

characterisation is adopted, it should preferably be simple so that it does not consume much analyst time and can be carried out routinely by factory operating staff. An automatic on-line technique would be ideal - but such a technique has not been invented yet. Furthermore, the method must be repeatable.

Figure 3.2 *A photomicrograph of pith particles to illustrate the diversity of shapes*

Repeatability of bagasse particle size determination is not so easy to achieve. This is partly due to the difficulty of obtaining representative samples. If mill-run samples (at 50% moisture content) are used then the particle analysis is subject to error as a result of differential mass loss due to water evaporation for different sizes during the analysis. If oven-dried bagasse is used, then selection of representative samples becomes difficult because of the tendency for the finer particles to migrate to the bottom of the container. Furthermore, an oven-dried sample is likely to re-absorb moisture from the atmosphere during analysis and this again introduces errors. To allow an oven-dried sample to attain moisture equilibrium with the atmosphere is time-consuming (at least four hours are required). Generally

it is desirable to have analysis results as soon as possible. Another reason for the difficulty of achieving repeatability is the tendency of bagasse fibres to interlock or mat. Such matting interferes with the passage of particles through a nest of sieves, makes microscopic analysis almost impossible and affects pneumatic classification.

The determination of particle shapes is fraught with similar obstacles. The wide variety of shapes makes the selection of a "characteristic particle shape" impossible. The technique of shape determination is also problematic. Manual measurement of the larger particles is probably the most accurate. The smaller particles need to be scanned by microscope. A pneumatic shape determination technique may be possible, but fibre interlocking is likely to present difficulties.

3.3 SIEVE ANALYSIS

The method adopted in this work for the quanititative expression of particle size was sieve analysis, for the following reasons. It gave relatively good repeatability as opposed to pneumatic classification, which was found by Rein (1972) to be less efficient and reproducible than sieving. Furthermore, sieving is a simple technique which can easily be performed in an ordinary factory laboratory. It provides an analysis by mass, which is considered more appropriate than one by number that would be obtained by direct particle size measurement and microscopic examination. Although it is possible to convert an analysis by number into one by mass (see Allen, 1990) an analysis by number is extremely time-consuming. The disadvantage of sieving as a technique suitable for bagasse, namely that fibrous particles often tend to lie horizontally on the screen and do not pass through the screen because of their length, even though their width and thickness are smaller than the sieve aperture, will be dealt with in section 3.4 where the shape characteristics of bagasse particles are evaluated and in section 3.6

where these results are utilised in the determination of mean particle size. The tendency of bagasse to interlock or mat is minimised if the size of sample which is being analysed is kept sufficiently small. The results of work performed in the field of sieve analysis will be covered under the headings

Different sieving techniques
Typical bagasse particle size distributions
"Mean" particle size
Sub-sampling
Repeatability.

Different sieving techniques

A number of South African companies uses sieving as a means of particle size determination. The following description shows the variety of techniques used.

The SASTA Laboratory Manual (1985) recommends the use of approximately 200 g mill-run bagasse which is dried in an oven at 105 °C for one hour. This is then allowed to cool and reach moisture equilibrium with ambient air for about four hours. The dried sample is then transferred to a stack of three sieving boxes (300 mm x 300 mm) with screen apertures of 12.7, 6.4, and 3.2 mm respectively in which it is shaken for two minutes with lateral movements. The portion that passes the last screen is transferred to a set of four screens of 200 mm diameter with apertures of 1.7, 1.0, 0.6, and 0.4 mm followed by a catch pan. This set of sieves is placed on a mechanical shaker, which executes vertical vibrations the amplitude of which can be adjusted, for 10 minutes. From the different fractions the surface area per g dry sample is calculated as an indicator of the degree of preparation.

MONDI BOARD MILLS LTD have the following method (Hoekstra, 1987). A meticulous sampling procedure is described whereby daily composited samples are collected. To obtain representative sub-samples the problem of migration of fines is dealt with by adding and thoroughly mixing an equal mass of water to a given sample of mill-run bagasse which is assumed to have a moisture content of 50%. The resulting mixture then has an approximate moisture content of 75% which is judged sufficient to stop transmigration of fines. Small handfuls of this artificially wetted bagasse are then picked randomly from the large composite sample until about 100 g have been collected. This sample is then dried at 105°C for four hours. To scatter clumps of fines and dislodge pith from fibres the dried sample is transferred to a small ball mill (pot diameter 162 mm) containing 12 stainless steel balls (25 mm diameter) and milled for 25 minutes. The ball-milling procedure is based on an investigation carried out by Burger and Gonin (1975).

At the conclusion of ball-milling the sample, which has a mass of approximately 25 g, is assumed to be in equilibrium with the surrounding atmosphere and is transferred to a nest of sieves with apertures of 1.000, 0.500 and 0.355 mm followed by a catch pan using the full set of sieves. Mechanical sieving for five minutes is followed by a second five-minute period of mechanical sieving of the particles collected in the 0.355 mm sieve and the catch pan. The pan contents are then added to the particles retained on the 0.355 mm sieve and this is then hand-sieved until only the fine fibres are left on the 0.355 mm screen. The fractions retained by the 1.000, 0.500 and 0.355 mm sieves are added to give the coarse fraction while that collected in the pan is the fine fraction (pith). The fractionation procedure adopted by this company is clearly very elaborate.

SAPPI FINE PAPERS LTD (Mouton, personal communication, 1992) fractionate pre-dried bagasse (drying executed at 110°C for 2-3 h) with sieves having apertures 8, 4, 2, 1 and 0.85 mm using a mechanical shaker

for 10 minutes. The percentage of fines is that portion collected in the pan (i.e. the fraction that passes through the 0.85 mm sieve). The sieves are approximately 700 mm in diameter and the sample size is about 100 g oven-dry.

TRANSVAAL SUGAR LTD (Kriek, personal communication, 1992) use a sample size of approximately 5 kg mill-run bagasse and rectangular screens measuring 570 mm x 870 mm. The aperture size of each of the screens is shown in Table 3.1 as well as the sieving time applied to each screen. Hand-sieving, where two people execute a horizontal motion on the sample in one sieve for the time span indicated in Table 3.1, is used. The percentage pith is the mass percent of sample that passes the last screen.

TABLE 3.1

Apertures and shaking times for sieves (Transvaal Sugar)

Sieve Number	Aperture mm	Shaking time min
1	22.0	1
2	10.0	2
3	6.0	2
4	3.0	5

The bagasse fractionation method used by ILLOVO SUGAR LTD, Byproducts at Sezela (Govender, personal communication, 1992) uses a set of standard (Tyler) sieves with the following aperture sizes (in mm): 2.36, 1.40, 1.00, and 0.71.

Cone and quartering is used on mill-run bagasse to obtain a representative sample of approximately 80 g mass (at 50% moisture). This sample is then

fractionated by passing through the set of sieves which are clamped together in a holding device while being manually rocked on a rubber mat for 10 minutes. Cognisance is taken of the fact that a mass loss can be expected due to moisture evaporation.

To evaluate the quality of bagacillo as filter aid for rotary vacuum filters the SASTA Laboratory Manual (1985) recommends the use of a 0.85 mm sieve (200 mm diameter) with catch pan and a bagacillo sample mass of 100 g (50% moisture). After drying at 105°C for one hour and subsequent cooling in ambient air for a further one hour the dried sample is then sieved manually for four minutes using a rotary motion. The minimum requirement for acceptable quality is that at least 80% of the sample should pacs through the 0.85 mm sieve.

The literature gives brief descriptions of the sieving procedures that have been used by some researchers.

Behne (1940, quoted in Anon., 1958) used sieve analysis to derive a "fineness figure" of prepared cane. The sieve sizes used by him had openings of 26, 18, 10, 5.5, 3.5, 2.5, 1.2, and 0.6 mm respectively. The fineness figure is calculated according to the formula

$$Fineness = \sum \frac{mass\ \%\ retained\ on\ each\ sieve}{length\ of\ opening\ of\ sieve\ in\ mm} . \quad (3.1)$$

Anon. (1958) calculated the same fineness figure on prepared cane in an attempt to correlate degree of preparation with bulk density at a standard pressure of 15.4 psig and five minute consolidation time. In this case the sieve sizes used were 12.7, 7.9, 4.8, 3.2, 1.2, 0.7 and 0.4 mm. He reports a disappointingly large scatter about the regression line. However, the sieving procedure used a mixture of manual and mechanical sieving, and oven-drying was only applied to particles which passed the 4.8 mm sieve

because it was recognised that "moist particles tended to stick to the finer sieves". Hence evaporation during sieving undoubtedly reduced the accuracy of the results.

Sockhill (1956) showed that the distribution of pol (residual sugar) in final bagasse varied with particle size. He generated four size fractions using rectangular sieves the apertures of which were 12.7, 6.3 and 3.2 mm respectively. Manual sieving was used where each sieve was given a standard number of shakes, this number ranging from 50 to 125 from the coarsest to the finest sieves. No attempt was made to calculate a mean particle size. The fineness of preparation was expressed in terms of the relative mass fractions of the particles that passed through the three screens.

Foster and Hill (1966) describe the determination of "mean particle thickness" of prepared cane using three sieves with square openings of 12, 7 and 4 mm respectively. The sizes applied to the four mass fractions that were thus generated were taken as 12, 9, 5 and 2 mm thick and the mean thickness was determined by

$$Mean\ thickness = \sum \frac{(mass\ \%\ of\ fraction)\ (its\ nominal\ thickness)}{100} . \qquad (3.2)$$

Foster and Shann (1968) used this method to measure the degree of cane preparation which, they showed, had a profound influence on pol extraction. The method was also used by Pastega (1971).

Rein (1972), who investigated liquid flow through a bed of bagasse, recommended a sample of oven-dried bagasse not exceeding 30 g. He used apertures of 10.6, 5.0, and 2.8 mm employing hand-sieving of two minutes per sieve, followed by mechanical sieving for 10 minutes in a JEL shaker through a series of Tyler screens with openings of 1.65, 1.00, 0.589 and

0.351 mm. The size corresponding to the 50% value of a cumulative size distribution plotted on log-normal co-ordinates is used as the representative particle size. Rein stresses the importance of using a uniform sieving procedure.

The method described by White (personal communication, 1992) is the one detailed in the SASTA Laboratory Manual (1985) using hand-sieving with aperture sizes of 12.7, 6.4, and 3.2 mm and a mechanical shaker on a nest of sieves with apertures of 1.7, 1.0, 0.6 and 0.4 mm.

Burger and Gonin (1975) investigated particle analysis of bagasse from the point of view of determining the quantity of useful fibre for paper-making. They recommend that the pre-dried bagasse sample be ball-milled for 25 minutes using 25 mm diameter stainless steel ball bearings to separate the pith particles from the fibres prior to mechanical sieving for 10 minutes. The sieve sizes used were 1.204, 0.595, 0.354, 0.250 and 0.105 mm. Particles larger than 0.354 mm (i.e. those retained by the 0.354 mm and coarser sieves) were classified as useful fibre while those that passed through the 0.354 mm sieve were considered pith.

Marson (1980) used a grading device containing five sieves with the coarsest one having 12.5 mm diameter apertures, successive sieve aperture diameters reducing by a factor of approximately 0.5. Mechanical shaking with horizontal motion only was applied. The drying procedure involved the use of a heated forced air draft causing partial fluidisation.

Ponce *et al.* (1983) report a study of the geometric properties and density of several bagasse fractions. The following screen sizes (in mm) were used: 22.4, 16.0, 11.2, 8.0, 5.6, 4.0, 2.36, 1.19, 0.841, 0.595 and 0.354. Air dried bagasse samples were fractionated for 20 minutes using an electric vibrator.

In an investigation into the pith and fibre content of sugarcane Moodley (1991) used a rectangular wire mesh basket (2 mm apertures) with a removable lid to separate the pith from the fibres. This basket, which contained the sample of finely shredded cane, was made to rotate in a water bath at 23 rpm for 20 minutes. After this pith-washing operation the water from the bath was filtered through a 1.651 mm sieve to retain the fibres that had passed through the basket screen and then through a 100 micron screen to collect the pith. The particles that passed through the 100 micron screen were assumed to be soil particles. The fibres retained on the 1.651 mm sieve were added to the portion of the sample that remained in the basket after rotation in the water bath to give the fibre fraction. The fibre and pith fractions were subsequently dried and weighed.

Aralde *et al.* (1993) made a determination of the heat transfer coefficient in pneumatic conveying bagasse drying. The bagasse fractions were obtained from sieves of 19.0, 9.50, 4.75, 2.36, 1.18, 0.85, 0.60 and 0.30 mm apertures.

The large diversity of methods of bagasse particle size analysis practiced within the sugar (and related) industries reflects the uncertainty there exists about a reliable technique. The problems which have to be addressed are the following:

* What is the best method of dividing a bagasse sample that is too large for one set of sieves into portions that fairly represent the whole sample?
* Does sieve analysis of bagasse provide repeatable answers?
* Is hand sieving to be preferred to mechanical sieving?
* What range of sieve apertures should form part of the screen series?

An attempt will be made in the succeeding paragraphs of this section to provide answers to these questions.

A potential problem that has not been investigated in this study is the adhesion of particles which results in the formation of aggregates that do not disintegrate during sieving (both in the wet and in the dry state). To break up such aggregates Hoekstra (1987) recommended ball-milling as described above. It is the author's experience that such aggregates comprise a rather small portion of the total mass of a sample. It is therefore debatable whether ball-milling, which almost certainly will alter the particle size distribution, can be considered a valid technique forming part of the size analysis of bagasse.

Typical bagasse particle size distributions

The method of sieving that was adopted used standard laboratory test sieves of 200 mm diameter with the following apertures (in mm): 6.7, 4.0, 2.8, 2.0, 1.4, 1.0, 0.85, 0.60, 0.425 and 0.30. In a later set of trials (see p. 70) an additional sieve was added, namely with 13.2 mm openings. This was done to provide a more even distribution of size fractions for particularly the coarser samples such as diffuser bagasse and depithed fibre. As far as possible an attempt was made to keep the resolution (i.e. the ratio of apertures of two adjacent sieves in the series) constant at $\sqrt{2}$ as recommended by Allen (1990). Mechanical sieving of 10 minutes' duration on a laboratory shaker was used. The equipment was not large enough to accommodate the whole nest of sieves in one operation so the sieving was carried out in two steps using the coarse sieves down to 1.4 mm first, followed by the remaining fine sieves. Each step lasted 10 minutes.

Figure 3.3 shows block diagrams of size distributions obtained from three samples of diffuser bagasse and three samples of mill bagasse. These samples indicate that bagasse does not follow a normal distribution. In fact, it is probably best described as a multimodal distribution. The difference between diffuser bagasse and mill bagasse is also evident with a much higher proportion of large particles (fibres) in the diffuser bagasse.

"Mean" particle size

It is desirable to obtain a single figure that gives an indication of the "average" size of the particles in a bagasse sample under investigation.

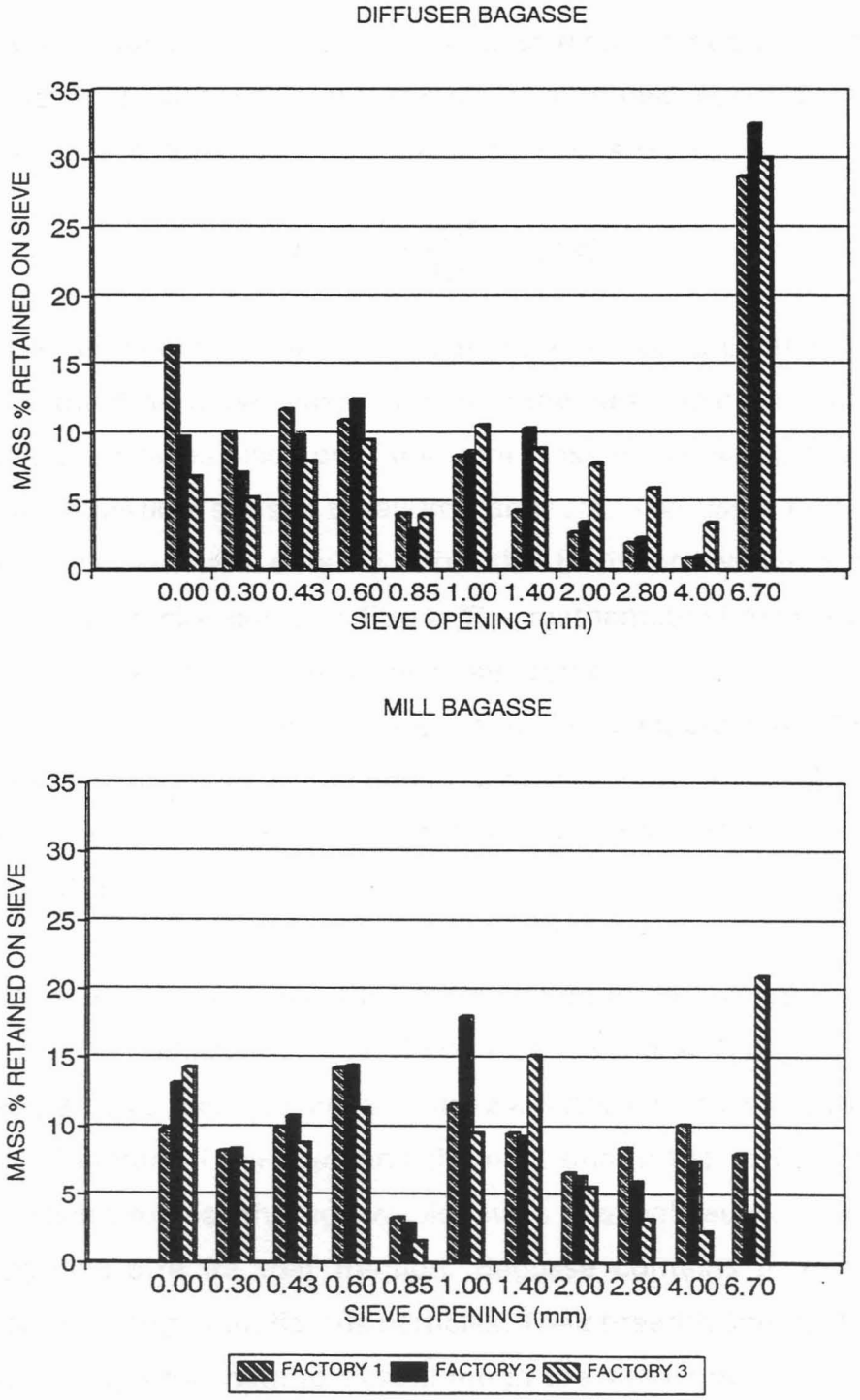

Figure 3.3 Size distributions for a variety of different bagasse types

Furthermore, the determination of the mean particle size should be relatively simple and not require a laborious technique such as, for example, manual plotting of a graph to find a median value.

Since one is dealing with a multimodal particle size distribution this figure will probably not coincide with the largest mass fraction but it will be a composite figure describing the sample as a whole. For a distribution by mass the general formula for the mean particle size, x_m, is

$$x_m = \frac{\int x dM}{\int dM} \qquad (3.3)$$

where x is the average size of particles (in mm) over a limited size interval and dM is the differential mass fraction of the particles in that size interval. The integration takes place over the total mass of the sample, and the full spectrum of particle sizes is taken into account. The usual technique is to use sieve fractionation data to form the basis on which a theoretical cumulative undersize curve is fitted. The mathematical expression of this curve is then used to determine the mean particle size. If a large number of sieves is used and the size intervals are well spaced out then the raw data can be used to give a relatively accurate estimate of the mean particle size. Details of the technique adopted to calculate the mean particle size are given in section 3.5.

A comment is appropriate on the determination of the average particle size, x, between two adjacent sieves. If one was dealing with uniformly shaped, rounded particles then the average sieve aperture of the sieve that retained the mass fraction of particles and the next one in the series that allowed these particles to pass through would give a relatively accurate value of the mean particle size for that fraction. Bagasse contains a relatively large percentage of long, thin, fibrous particles. Their breadth and thickness might be small enough for them to pass through the sieve openings if they were orientated in a vertical direction, but their excessive length prevents them

from going through because the shaking action of the mechanical shaker is not sufficently vigorous to achieve that orientation. Hence a significant proportion of fibrous particles are often retained on a sieve because of their shape, even though their breadth and thickness would allow them to pass through the sieve if they were shorter. Thus an adjustment of the mean sieve aperture needs to be made which takes the typical fibre length into account in the detemination of the particle size of the mass fraction. The determination of fibre length will be described in section 3.4 and its incorporation into sieving data to arrive at the mean particle size for a bagasse sample in section 3.5.

Sub-sampling of bagasse

One of the problems associated with the quantitative analysis of bagasse particle size and shape, as mentioned in section 3.2, is that of obtaining representative sub-samples. The process of obtaining valid bagasse samples from the production stream for routine process control has been extensively investigated and the resultant procedure used in South African factories is documented in the SASTA Laboratory Manual (1985, p. 215). The sample that is obtained by this method is generally subdivided by cone-and-quartering for moisture, brix and pol determinations.

The moisture analysis sample is ideal for subsequent use in particle size analysis, because the particles are dry. Currently most bagasse moisture analyses are done by oven drying. It is essential that a bagasse sample is at least air-dry before sieve analysis is executed because moist bagasse particles tend to adhere to each other and separation would then be incomplete. The difficulty about the standard bagasse moisture analysis sample is that it is too bulky to be used for a sieve analysis in which standard laboratory 200 mm diameter test sieves are used. This sample must therefore be subdivided so as to yield representative sub-samples.

It was found that the normal cone-and-quartering method used to subdivide mill-run bagasse samples is inadequate for dry bagasse because the fine particles tend to migrate towards the bottom of the container. Once this has occurred it is virtually impossible to split the sample reliably by the cone-and-quarter method.

Some work was done to find a better sample splitting method. The technique that gave acceptable results involved a three-step process. The first step consisted of separating the coarse fibres from the fine particles by using a screen with 5 mm round apertures and moving the bagasse by hand over the screen several times. The coarse particles are retained on the screen and the fines pass through the apertures. In the second step the coarse and the fine portions are divided separately into equal sub-fractions. For the coarse particles cone-and-quartering was adequate, whereas a riffler was used for the fine portion. In the third step equivalent fractions of the coarse and the fine particles were recombined to form a sample of suitable size for sieve analysis. It was found that 20-30 g of oven-dried bagasse gave a sample that could be fractionated well in standard 200 mm diameter laboratory test sieves. One of the advantages of this method is that it is easy to obtain a sample of suitable size .

To compare the effectiveness of the aforementioned three-step procedure with the cone-and-quarter method, five pairs of sub-samples were generated for each of the sample splitting methods. These were subjected to the normal sieve analysis used in this work (see page 43). The aperture sizes of some of the sieves used, however, were slightly different from the procedure described on page 43 because this evaluation was carried out in a different laboratory. This, of course, does not affect the validity of the result. The standard deviation of the difference between duplicate mass fraction percentages for each sieve size was used as the comparison criterion. Table 3.2 indicates the calculation details.

TABLE 3.2

Comparison of two different sample splitting methods

SIEVE APER-TURE µm	Three-step sub-sampling			Cone and quarter sub-sampling		
	i	ii	Diff	i	ii	Diff
	%	%	%	%	%	%
6000	11.2	11.0	0.2	3.5	9.9	-6.4
4000	9.1	12.4	-3.3	6.5	13.3	-6.8
2800	9.5	9.6	-0.1	6.0	9.9	-3.9
2000	5.6	4.7	0.9	6.2	9.4	-3.2
1400	7.5	7.8	-0.3	5.9	8.7	-2.8
1000	10.1	10.2	-0.1	8.3	10.5	-2.2
850	6.7	5.8	0.9	5.7	6.7	-1.0
600	13.9	13.2	0.7	13.4	11.6	1.8
425	8.5	8.9	-0.4	13.0	7.3	5.7
300	7.5	7.2	0.3	12.8	5.1	7.7
<300	10.3	9.4	0.9	18.9	7.5	11.4
Std Deviation			1.20			5.93

The difference becomes more apparent in graphical form, as shown in Figures 3.4 and 3.5. The closer agreement between corresponding mass fractions for the three-step splitting method is evident. The combined standard deviation of the differences of the five duplicate samples split by the three-step procedure was 1.95 and for the cone-and-quarter method 4.99, showing that the three-step method gives more consistent results. The F-ratio test indicated a significant difference at the 1% level between the

two procedures for three out of the five pairs of samples. It is fairly certain therefore that the three-step method of bagasse sample splitting yields more representative sub-samples than the cone-and-quarter method.

Repeatability of bagasse sieving

The factors which can affect the repeatability of sieving results are sub-sampling and sieving procedure. In an attempt to eliminate the influence of sub-sampling, duplicate sievings were conducted on the same sample. The possibility that abrasion caused by the first sieving can affect the result of the second one cannot be excluded, but it is estimated that bagasse abrasion is minimal, particularly for sieving times of 10 or 15 minutes. Sieving procedure is concerned with aspects such as mechanical or manual sieving and sieving time.

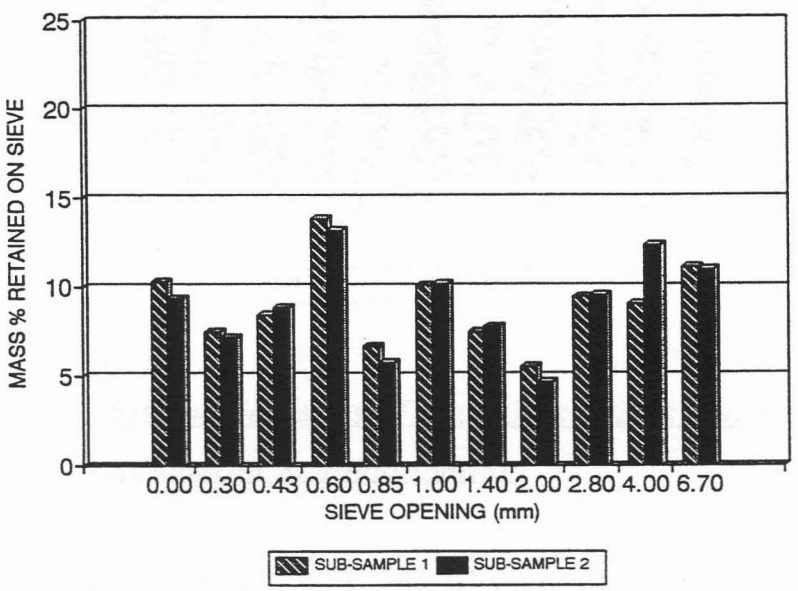

Figure 3.4 *Mass percentages of two sub-samples generated by the three-step splitting method*

Rein (1972) suggests hand sieving for two minutes for the coarse fractions. Allen (1990) recommends that hand sieving can be considered complete

when the rate of passage of material through the sieve is less than 0.1% of the total sample mass per minute. The author found that it is possible to achieve this, but it will take approximately five hours' continuous hand sieving if 10 different sieve sizes are used, because this rate of passage will have to be achieved for each sieve. Furthermore, the average discrepancy of the mean particle size obtained by hand sieving in duplicate determinations was 1.2 mm which is ten times higher than was achieved in corresponding sieving trials using a mechanical shaker. Thus hand sieving appears to be far less accurate than mechanical sieving.

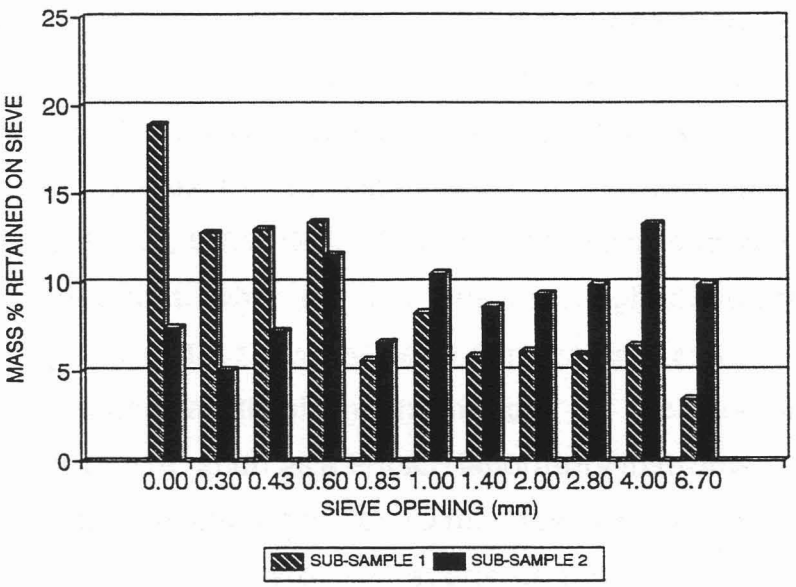

Figure 3.5 *Mass percentages of two sub-samples generated by the cone-and-quarter splitting method*

The factors influencing the results of mechanical sieving are the type of shaker and the sieving time. It is obviously desirable to standardise on both. A Fritsch laboratory shaker with an amplitude setting of 7 and a continuous shaking action was used. Such an instrument is standard equipment in many South African sugar factory laboratories for sugar crystal size analysis. The advantage of a mechanical shaker is that the same type of shaking action can be reproduced, which is hardly possible for hand sieving. Automatic

timers permit standardisation of sieving time. It was found that the standard deviation of differences of mass fractions obtained by duplicate sievings for a 10 minute sieving period did not differ significantly from that obtained from 15 minutes, and it was therefore concluded that a 10 minute sieving time on that particular mechanical shaker was adequate. The average deviation of mean particle size achieved on five bagasse samples which were each subjected to duplicate sievings by the mechanical shaker was 0.13 mm which can be considered relatively good.

To conclude this section on bagasse sieving, it is recommended that 20-30 g oven-dry bagasse be used which has been obtained by the three-step sample splitting method described on p. 47 and that has been allowed to attain moisture equilibrium with the atmosphere. Standard laboratory 200 mm diameter test sieves are suggested with the following apertures: 13.2, 6.7, 4.0, 2.8, 1.4, 1.0, 0.85, 0.60, 0.425 and 0.30 mm followed by a pan. It is recommended that, when the fractions are weighed, no attempt is made to pull through fibres that have partially penetrated a sieve. Such a procedure would introduce artificial inconsistency. A well-known, widely used mechanical shaker, such as a Fritsch laboratory instrument at a setting of 7, on continuous shaking action for 10 minutes, is considered to give adequate separation. Due to the size limitations of the type of mechanical shaker mentioned, it is probably necessary to carry out the sieving in two stages of 10 minutes each. Hand sieving is considered too inaccurate.

3.4 SHAPE CHARACTERISATION

The variety of particle shapes present in ordinary bagasse is illustrated in Figure 3.1. The purpose of quantifying the shape characteristics of bagasse is to obtain values which play a role in predicting its handling behaviour. The topic will be dealt with under the headings

Review of published data on bagasse particle shapes

Allen (1990) gives a comprehensive list of techniques that have been used to make quantitative shape determinations for a range of particulate materials. Heywood (1970) gives a precise definition of length (L), breadth (B) and thickness (T) of particles which serves as a basis of measurement and he introduces the quantities "elongation ratio" (L/B), and "flakiness ratio" (B/T). Foster and Hill (1966) evaluate a "mean particle thickness" for bagasse particles from sieve apertures. Cullen (1967) mentions that the value of the drag coefficient which affects pneumatic conveying depends on the geometry of the bagasse particles, but does not deal with its determination. Anderson (1988) gives an expression of the drag force on bagasse particles in pneumatic conveying in terms of their length, width and thickness. Holliday (1990) expressed the size of bagasse particles in terms of spheres (of similar density) which would have equivalent settling velocities in air. Singh *et al.* (1993) quote a mass to surface ratio range for bagasse particles of 0.02 - 0.04 g/cm^2, but do not elaborate on how this was measured. Love and Rein (1980) provide a formula for determining the specific surface area of a bagasse sample, but do not give figures of actual determinations.

Rein (1972, pp. 132-135) gives some data on elongation and flakiness ratios for different size fractions of bagasse, but does not utilise this information in any subsequent calculation. Bernhardt (1993) gives correlations for volume and surface shape factors for different bagasse size fractions and applies these in the determination of specific surface area. Ponce *et al.* (1983) measured the length, breadth and thickness of 4000 bagasse

particles from 9 size fractions. From these measurements equations were developed that expressed these, and related variables like volume and surface area, in terms of sieve aperture.

Method of shape analysis

Oven dried bagasse which had been allowed to reach moisture equilibrium with the atmosphere was fractionated with a mechanical shaker according to the method described in section 3.2. The sieve sizes used were 6.7, 4.0, 2.8, 2.0, 1.4, 1.0, 0.85, 0.60, 0.425 and 0.30 mm with the particles passing the 0.30 mm sieve being collected in a pan. The materials that were analysed included two samples of shredded cane from two different factories (Felixton and Gledhow) , one sample of diffuser bagasse (from Illovo), and three samples of bagasse from milling tandems (Mount Edgecombe, Maidstone, using burnt cane, and Maidstone, using unburnt (trash) cane). From each sieve fraction 200 particles, randomly selected, were analysed, except for some of the coarsest fractions (those retained by the 6.7 mm sieves) where not sufficient numbers of particles were obtained from the sample used in the fractionation. In that case at least 100 particles were analysed per coarse fraction. The total number of particles measured exceeded 12 600.

The geometrical model adopted as the basic particle shape was the rectangular block. Thus for each particle the length (L), breadth (B) and thickness (T) were determined. Manual measurement using vernier callipers capable of measuring to the nearest 0.02 mm was used for the bigger particles, namely those retained by the 0.6 mm or coarser sieves. For particles too small to be measured in this way a Kontron microscopic image analyser using a 44 times magnification was used. These measurements were recorded to the nearest µm. Because of the deviation of most bagasse particles from the strict rectangular block shape it was not possible to

conform totally to Heywood's (1970) definition of length, breadth and thickness as being dimensions in mututally perpendicular planes. Where fibres were bent or twisted, an attempt to straighten them before measurement was made, or an estimate of their length was obtained. It was, of course, not possible to rotate particles during microscopic analysis for the determination of breadth and thickness. Hence the thickness was taken as the shortest dimension at right angles to the length and the breadth as the longest dimension, again at right angles to the length. Images of some bagasse particles analysed microscopically are shown in Figure 3.2. The fraction retained by the 0.60 mm sieve contained a large number of particles that were too long to be adequately measured on the Kontron analyser but also many particles that were too small to be measured manually. It was therefore decided to analyse 100 particles manually and 100 particles microscopically from this fraction.

Results

The length, breadth and thickness data described above were recorded in spreadsheet files. The listing of all these measurements would consume excessive space and therefore only the results that are derived, and used, will be reported. From the spreadsheet data derived quantities such as volume, surface area, and shape factors can easily be determined by suitable numerical manipulation.

Since fibre length is the most significant shape characteristic affecting the bridging behaviour of bagasse it was decided to use length-related measures. Three measures were evaluated, namely the fibre length (in mm), the elongation ratio (L/B) and, what the author calls, the *length index* (λ). The last-mentioned gives, in non-dimensional form, a quantitative expression of the length of the particles as compared with the breadth and thickness, and is defined as follows. For each particle a dimensionless "length factor", l,

was determined from the average of the ratios L/B and L/T. The length index for a particular size fraction is the average of all these (200) length factors. In other words,

$$l_i = 0.5(L_i/B_i + L_i/T_i) \qquad i = 1,...n \qquad (3.4)$$

where n = number of particles measured, and

$$\lambda = \frac{\sum_{i=1}^{n} l_i}{n} \qquad (3.5) \ .$$

The fibre length and the elongation ratio was also evaluated as an average of the values obtained from each of the 200 particles measured in each size fraction. The results are given in Table 3.3.

The column headed "Interval Mean" in Table 3.3 represents the mean size, X_i, between the aperture size X_1 of the sieve above a size fraction of bagasse and the sieve aperture X_2 of the sieve that retained that fraction, calculated according to equation 3.6 (from Herdan, 1960, p. 33).

$$x_i = \sqrt[3]{\frac{(X_1^2 + X_2^2)(X_1 + X_2)}{4}} \qquad (3.6)$$

The last figure in that column (9.147 mm) is obtained by assuming that all particles would have passed a sieve with apertures of 11.2 mm which is, of course, a slight over-simplification. The figure of 11.2 mm is obtained on the assumption that the apertures of the sieve following the last one in the series would follow the $\sqrt{2}$ progression as most of the other sieves in the series. ***Since the length measurement is the most direct indication of fibre size it was decided to use this in subsequent calculations.***

For this purpose curves that relate sieve aperture to average fibre length were fitted to the measured values. A number of different mathematical expressions gave curves that approximated the measured data acceptably.

Table 3.3

Fibre length, length index (λ) and elongation ratio results for different bagasse types

Bagasse Type	Sieve Size mm	Interval Mean mm	Length Index I	Ave Length L mm	Elong. Ratio L/B	Bagasse Type	Sieve Size mm	Interval Mean mm	Length Index I	Ave Length L mm	Elong. Ratio L/B
Illovo	0.000	0.189	3.9	0.5	3.3	Maidst	0.000	0.189	5.1	0.6	3.8
Diff	0.300	0.366	5.1	0.8	4.1	Trash	0.300	0.366	3.2	0.6	2.4
	0.425	0.517	5.2	1.5	4.3		0.425	0.517	3.7	1.0	2.6
	0.600	0.732	17.9	4.9	13.2		0.600	0.732	24.3	5.5	15.3
	0.850	0.927	36.4	9.9	24.9		0.850	0.927	38.9	9.8	23.9
	1.000	1.211	45.5	13.3	30.9		1.000	1.211	43.5	12.1	27.2
	1.400	1.717	43.4	17.7	28.9		1.400	1.717	35.3	15.2	18.6
	2.000	2.422	36.5	15.4	25.6		2.000	2.422	27.1	16.2	11.3
	2.800	3.435	40.9	20.2	26.0		2.800	3.435	14.6	15.5	6.3
	4.000	5.461	40.9	27.4	11.8		4.000	5.461	16.1	22.4	6.6
	6.700	9.147	33.4	37.9	16.3		6.700	9.147	23.6	24.4	6.9
Mt	0.000	0.189	3.2	0.4	2.4	Felixt	0.000	0.189	2.9	0.5	2.1
Edge	0.300	0.366	3.3	0.6	2.4	Shredd	0.300	0.366	3.5	0.7	2.6
Mill	0.425	0.517	20.9	3.9	15.7		0.425	0.517	7.8	1.7	6.0
	0.600	0.732	22.5	4.7	16.9		0.600	0.732	17.5	4.1	13.4
	0.850	0.927	29.1	6.9	14.3		0.850	0.927	34.7	9.7	26.7
	1.000	1.211	39.5	12.0	24.0		1.000	1.211	41.2	13.8	25.9
	1.400	1.717	18.5	9.7	10.1		1.400	1.717	26.5	11.4	18.1
	2.000	2.422	31.0	11.0	13.6		2.000	2.422	41.6	19.8	25.7
	2.800	3.435	17.4	17.0	9.3		2.800	3.435	17.2	16.6	8.9
	4.000	5.461	27.3	17.4	9.9		4.000	5.461	66.4	26.5	44.6
	6.700	9.147	16.4	23.7	6.3		6.700	9.147	83.7	37.2	59.2

The form of the expression, shown in equation 3.7, that will be presented here was suggested by Hoekstra (personal communication, September 1994). In it y represents fibre length and x the mean sieve interval size.

$$y = b_1 \left[1 - e^{-b_2 \frac{x}{b_1}} \right] \qquad (3.7)$$

Table 3.3 (continued)

Fibre length, length index (λ) and elongation ratio results for different bagasse types

Bagasse Type	Sieve Size mm	Interval Mean mm	Length Index I	Ave Length L mm	Elong. Ratio L/B	Bagasse Type	Sieve Size mm	Interval Mean mm	Length Index I	Ave Length L mm	Elong. Ratio L/B
Maid-	0.000	0.189	4.5	0.6	3.5	Gledho	0.000	0.189	3.7	0.5	2.9
stone	0.300	0.366	2.9	0.5	2.2	Shredd	0.300	0.366	3.3	0.7	2.3
Burnt	0.425	0.517	3.5	0.8	2.4		0.425	0.517	6.7	1.6	4.7
	0.600	0.732	22.4	5.5	15.7		0.600	0.732	27.7	6.5	19.8
	0.850	0.927	43.7	10.9	23.6		0.850	0.927	21.4	8.1	13.6
	1.000	1.211	23.6	7.9	18.7		1.000	1.211	39.5	12.0	24.0
	1.400	1.717	19.1	8.6	11.6		1.400	1.717	39.4	16.4	20.9
	2.000	2.422	20.2	15.3	10.1		2.000	2.422	35.5	16.8	16.7
	2.800	3.435	17.8	16.9	7.9		2.800	3.435	56.8	21.9	21.7
	4.000	5.461	16.9	17.9	9.6		4.000	5.461	36.6	24.6	18.6
	6.700	9.147	24.7	17.6	14.9		6.700	9.147	58.9	50.4	24.3

It is an asymptotic curve with the value of the asymptote being given by b_1. The asymptote, whose dimension is that of length, represents the limiting (maximum) fibre length which is believed to be a real figure related to the structural properties of sugarcane. The use of b_1 again in the quotient of the argument of the exponential term serves to make the equation dimensionally consistent, both sides having the dimension of length. The parameter b_2, which is dimensionless, affects the steepness of the curve, a larger value giving a steeper curve.

A curve fitting programme called "Precision curve fitter" (1994) was used to determine the values of the parameters b_1 and b_2. These are listed in Table 3.4. The curve fitting programme uses the Levenberg-Marquardt method described by Press *et al.* (1990). Instead of using the data listed in Table 3.3 as point values in any calculation which uses fibre length as a significant variable, the mathematical expression of the curve is applied. The measured values, together with the fitted curves are shown in Figures 3.6 to 3.8.

Figure 3.6 depicts the data for one sample of diffuser bagasse from Illovo sugar factory as well as two samples of shredded cane (one from Felixton and the other from Gledhow). The Felixton shredded cane fibre length distribution seems similar to that of the diffuser bagasse from Illovo. Table 3.4 also indicates the similarity of the maximum fibre length as calculated by parameter b_1 (42.6 and 43.8 mm respectively). The maximum fibre length determined for Gledhow shredded cane is much higher (99.2 mm). For the three mill bagasse samples (Figure 3.7) the maximum fibre length appears to be significantly less than that for the diffuser sample, as expected (19.0, 24.5 and 23.5 for mill versus 42.6 mm for diffuser bagasse). It is also interesting to note the lower maximum fibre length of mill bagasse derived from burnt cane (19.0 mm) compared with that from trash cane (24.5 mm). The trash cane contains a greater percentage of leaves with long fibres which tend to be shredded to a lesser extent than the burnt cane stalks. Figure 3.8 presents curves for combined data sets. The first curve is fitted to the two shredded cane samples, the second to three mill bagasse samples and the third curve to the data for all four bagasse samples analysed.

It is suggested that when calculations involving diffuser bagasse are done where fibre length is one of the significant variables one uses the parameters obtained for the Illovo diffuser bagasse (in the absence of additional diffuser fibre length measurements). In other words, the following relationship (3.8) between mean sieve size x and fibre length y is proposed for diffuser

bagasse

$$y = 42.6 \left[1 - e^{-9.10 \frac{x}{42.6}} \right] \qquad (3.8) \ .$$

For mill bagasse the parameters obtained for the combined data set of all three mill samples is suggested, namely equation 3.9:

$$y = 22.1 \left[1 - e^{-9.18 \frac{x}{22.1}} \right] \qquad (3.9) \ .$$

Ponce *et al.* (1983) used the linear equation 3.10

$$y = 1.59x + 11.37 \qquad (3.10)$$

to fit length data for bagasse particles retained by sieves whose apertures ranged from 1.02 to 19.2 mm and the non-linear equation 3.11

$$y = 3.16\ x^{0.70} \qquad (3.11)$$

for particles retained by screens of sizes 1.02 to 9.6 mm. In these equations x represents the arithmetic average of the apertures of screens which retain a particular fraction and the previous screen through which it has passed. In the work presented here it was considered important to cover the full range of particle sizes, i.e. even those that pass through a 1 mm screen.

The advantage of using either equations 3.8 or 3.9 is that for one type of bagasse (mill or diffuser bagasse) a single equation is sufficient to estimate the fibre length of the whole range of bagasse particles. It is postulated that the data presented in this section, which can be considered to be summarised by equations 3.8 and 3.9, are largely independent of cane variety and that selection of particles of a certain fibre length distribution on a sieve is primarily a function of the action of the mechanical shaker, the sieving time, the sample size and the sieve aperture. This assumption may have to be confirmed in a separate investigation.

Section 3.5 will deal with the ***determination of a representative fibre length for a particular bagasse sample from sieving data and the appropriate fibre length equation.***

Table 3.4

Values of parameters for fibre length curve fitting equations

Bagasse type	b_1	b_2	r^2
Illovo Diffuser	42.6	9.10	.95
Maidstone mill burnt	19.0	9.38	.91
Maidstone mill trash	24.5	10.29	.94
Mount Edgecombe mill	23.5	7.78	.94
Felixton shred cane	43.8	8.24	.94
Gledhow shred cane	99.2	7.11	.95
All three mill bagasse types	22.1	9.18	.90
All four bagasse types	26.3	9.07	.85
Two shredded cane types	61.3	7.63	.92

Curves have also been fitted to the length index data. Equation 3.12 gives the form of equation which provided an acceptable fit to all the data. The equation requires six parameters $b_1, \ldots b_6$ the values of which are listed in Table 3.5. Since the fitting equations are not used anywhere in this thesis the resulting curves are not shown.

$$\lambda = b_1 + b_2 x + \frac{b_3 x^{b_4}}{b_5 + b_6(x-1)^2} \qquad (3.12) \quad .$$

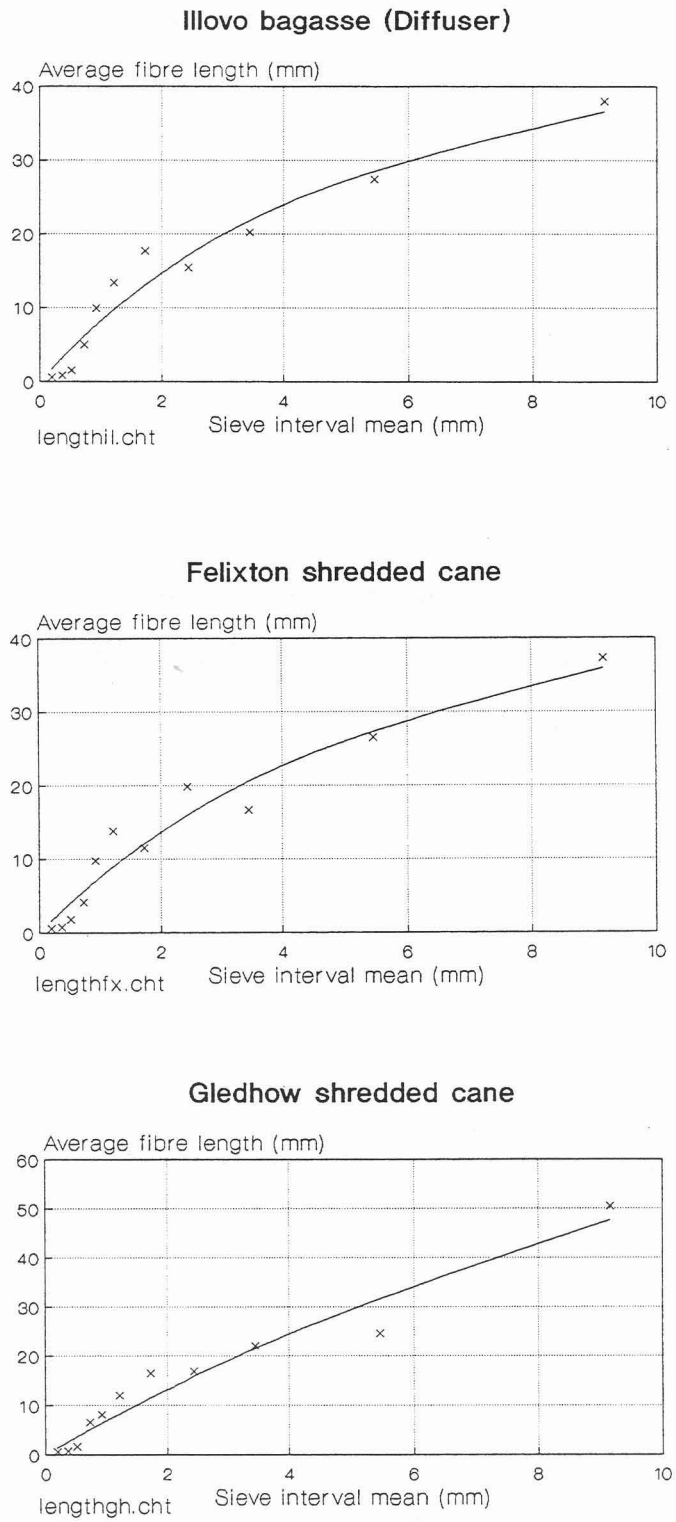

Figure 3.6 Fibre length for one sample of diffuser bagasse and two samples of shredded cane

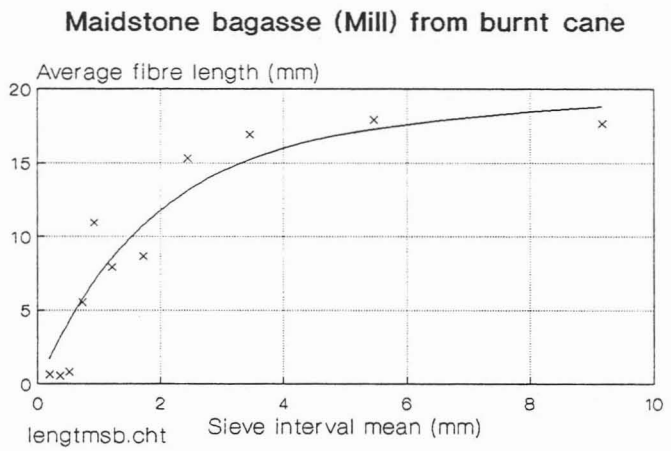

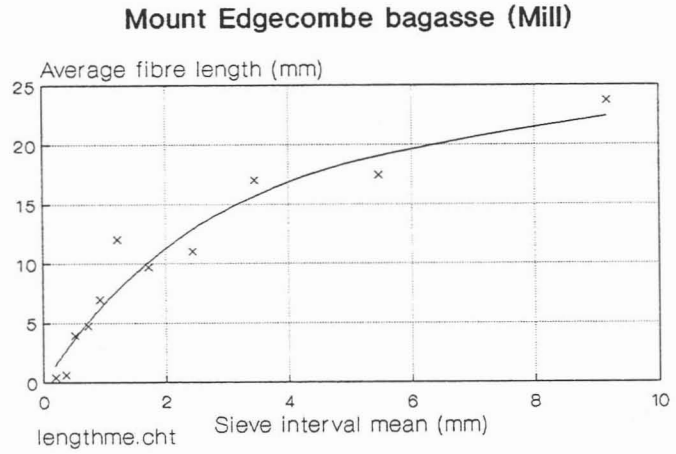

Figure 3.7 Fibre length for three samples of mill bagasse

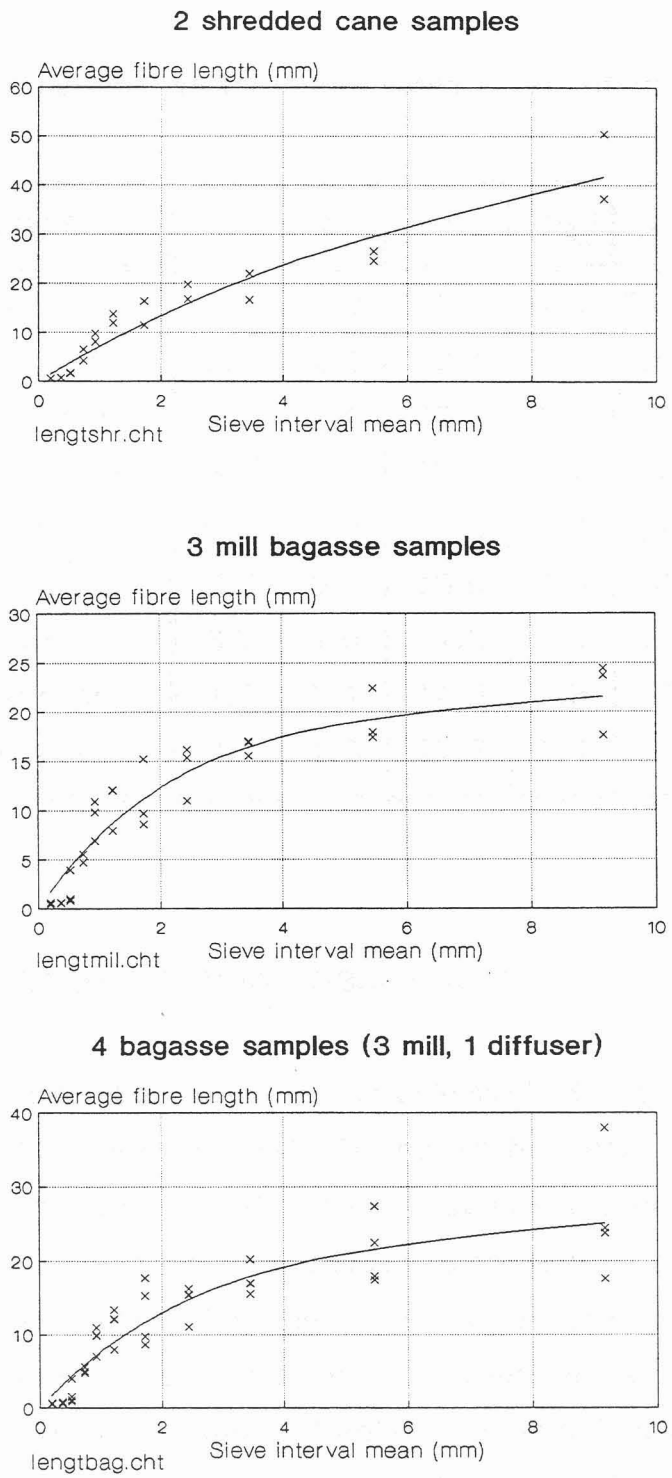

Figure 3.8 *Combined fibre length data for two shredded cane samples, three mill bagasse samples and four miscellaneous bagasse samples*

Table 3.5

Values of parameters for length index curve fitting equations

Bagasse type	b_1	b_2	b_3	b_4	b_5	b_6	r^2
Illovo Diffuser	5.3	-.12	19.2	2.5	.62	2.3	.94
Maidstone mill burnt	5.7	2.3	18.6	1.2	.51	9.4	.80
Maidstone mill trash	-0.7	2.1	22.7	1.4	.58	1.7	.95
Mount Edgecom. mill	8.3	1.1	17.5	1.7	.71	3.4	.64
Felixton shred cane	0.3	9.2	15.3	1.8	.49	5.1	.90
Gledhow shred cane	-1.8	5.7	19.6	1.0	.82	0.3	.86
All 3 mill bagasse	3.7	1.9	17.3	1.4	.56	2.3	.72
Two shredded cane	1.9	7.1	14.5	1.9	.62	2.0	.82
All 4 bagasse types	4.1	2.0	17.7	1.7	.59	2.3	.66

3.5 CALCULATION OF "MEAN FIBRE LENGTH"

There are many definitions of "mean particle size". Some of these are given by Herdan (1960), Heywood (1970) and Allen (1990). The purpose for which the mean size is used generally determines which definition is appropriate. Since fibre length is perceived to be a particle property that significantly affects the bridging behaviour of bagasse, the aim is to find a valid technique that can determine an average value for this. The fundamental equation on which the determination of "mean fibre length" is based has already been stated in equation 3.3, which, for ease of reference, is reproduced on the next page.

In this equation x represents the mean fibre size of a mass fraction dM of

$$x_m = \frac{\int x dM}{\int dM} \quad (3.3)$$

particles within a narrow size limit. It is the determination of this value x that needs some particular attention. The topic of this section will be covered under the following sub-headings:

Combination of fibre length data with sieve analysis data
Results.

Combination of fibre length data with sieve analysis data

Sieve analysis provides information on the fractions of the total mass of the sample that are retained on each sieve in the series. The problem that sieve aperture is not a good indicator of bagasse particle size, particularly of fibre length, was mentioned in section 3.4. An adjustment of the value of the sieve aperture, which reflects more realistically the average fibre length of bagasse particles that have passed through that sieve, must be applied.

In section 3.4 the results of fibre length measurements for different size fractions and different types of bagasse were summarised in the form of equations that relate average fibre length to mean sieve aperture. It was suggested that equation 3.8 was appropriate for use with diffuser bagasse and 3.9 for mill bagasse. Thus the sieve interval mean, which is calculated according to equation 3.6, is used as the x value in equation 3.8 or 3.9 to calculate the corresponding mean fibre length y for each size interval. The values obtained are shown in column 3 ("mean fibre length X_i") of Table 3.6 which shows a sample calculation for diffuser bagasse. The mean fibre length values will be different for mill bagasse where the parameters b_1 and b_2 are 22.1 and 9.18 respectively.

Results

To determine the "mean fibre length" for a bagasse sample an approximation to equation 3.3 is used, namely equation 3.13. This equation, in which n is the number of sieves used and M_i the mass of particles retained on the ith sieve, calculates an arithmetic mean fibre length based on mass. The spreadsheet data manipulation is indicated in Table 3.6. This Table also shows the detail of how the coefficient of variation (CV) for the bagasse sample is determined, using the formula given in equation 3.14.

$$x_m = \frac{\sum_{i=1}^{n} X_i M_i}{\sum_{i=1}^{n} M_i} \qquad (3.13)$$

$$CV = \frac{\sqrt{\sum_{i=1}^{n} X_i^2 M_i - x_m^2}}{x_m} \qquad (3.14)$$

The mean fibre lengths obtained for the samples used to measure the bulk properties of bagasse that are described in chapter 4 are shown in Figure 3.9 and their values, together with the respective CVs, are tabulated in Table 3.7. From this table it can be seen that there is little variation in the CV value for the different types of bagasse. It is therefore likely that the CV has little use in correlations between particle characteristics and bulk properties, whereas mean fibre length is expected to play a dominant role. A different ratio, which the author calls the "coarse-fine ratio", was used as a measure of the relative mass proportions of long fibres and small pith particles. Its values for the different types of bagasse are shown in Table 3.7 and its definition is given in section 3.6.

The possibility of using a theoretical particle size distribution such as the log-normal, Gamma, Weybull, Rosin-Rammler or Extreme value function, or other suitable equation, was investigated extensively for the purpose of deriving a mean fibre length and CV. It was ultimately decided, however, that these techniques would offer little advantage over the direct arithmetic calculation of mean fibre length as presented above, because the latter utilises the raw sieving data. Furthermore, the calculation of the arithmetic mean is simple and can be done with a standard spreadsheet programme. As long as the number of sieves being used is sufficiently large the determination of the mean should be sufficiently accurate.

TABLE 3.6

Determination of mean fibre length and coefficent of variation for a bagasse sample

SAMPLE NO: FX1 BAGASSE TYPE: DIFFUSER
MOISTURE : 53.5 %

SIEVE SIZE mm	INT MEAN mm	MEAN FIB. LENGTH Xi mm	EMPTY g	+SAMPL g	MASS g	MASS Mi %	Xi*Mi	Xi^2*Mi /100
6.700	9.147	36.563	609.25	623.85	14.60	44.55	1629.01	595.62
4.000	5.461	29.333	614.85	615.06	0.21	0.64	18.80	5.51
2.800	3.435	22.147	598.74	599.24	0.50	1.53	33.79	7.48
2.000	2.422	17.207	581.83	583.00	1.17	3.57	61.43	10.57
1.400	1.717	13.083	551.43	552.85	1.42	4.33	56.69	7.42
1.000	1.211	9.710	553.40	556.27	2.87	8.76	85.04	8.26
0.850	0.927	7.653	537.26	538.18	0.92	2.81	21.49	1.64
0.600	0.732	6.167	497.47	500.38	2.91	8.88	54.77	3.38
0.425	0.517	4.458	502.68	505.45	2.77	8.45	37.68	1.68
0.300	0.366	3.204	491.40	493.49	2.09	6.38	20.44	0.65
0.000	0.189	1.686	602.08	605.39	3.31	10.10	17.03	0.29

ARITHMETIC MEAN = 20.36 mm
COEFF. OF VARN. = 0.74

FIBRE LENGTH CURVE FIT PARAMETERS
b1 42.60
b2 9.10

FILE: MEANCALC.WQ2

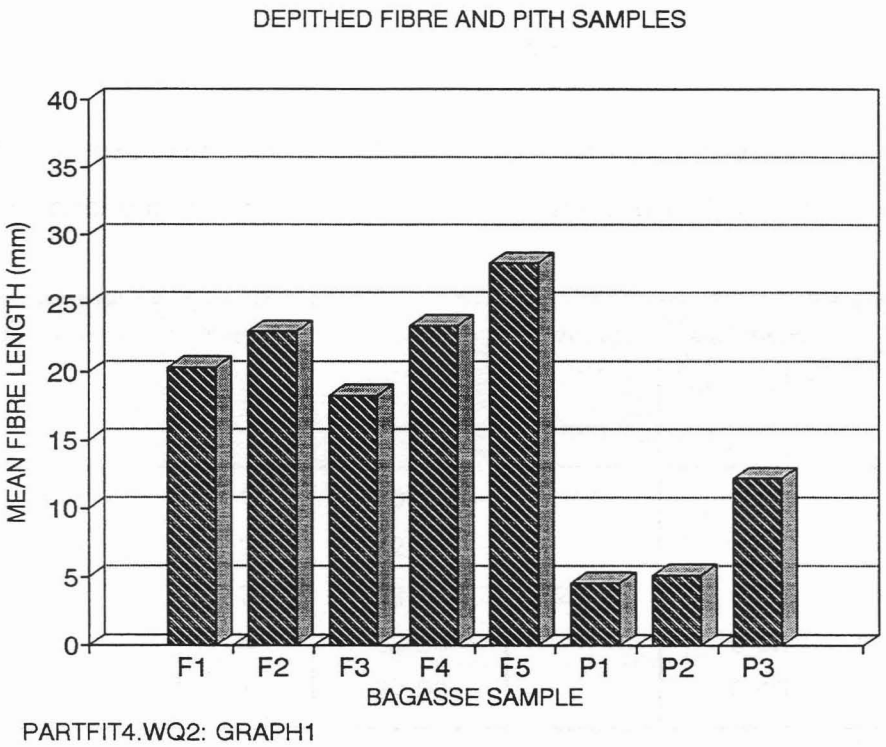

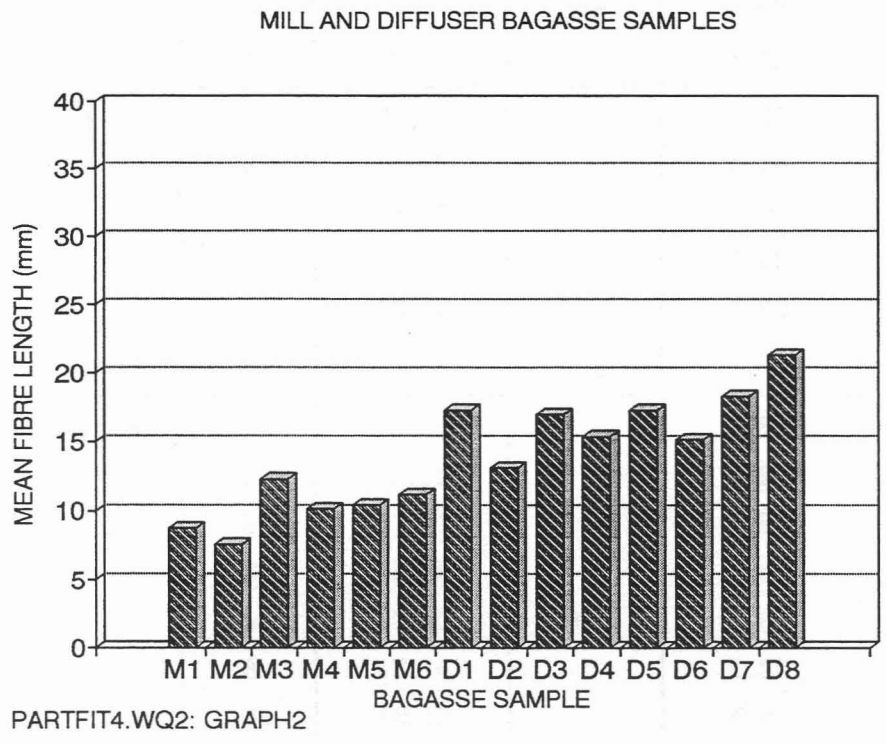

Figure 3.9 Mean fibre length of the bagasse samples used in the determination of bagasse bulk properties

TABLE 3.7

Mean fibre length, coefficient of variation and coarse-fine ratio of bagasse samples used in the determination of bulk properties

Bagasse type	Sample No	Mean fibre length mm	Average mm	Coefficient of variation	Coarse-fine ratio
Depithed fibre	1	20.36		0.74	1.49
	2	22.95		0.67	1.88
	3	18.34	22.6	0.73	1.60
	4	23.36		0.62	2.48
	5	27.93		0.46	5.63
Pith	1	4.24		0.74	0.02
	2	4.61	7.3	0.95	0.04
	3	12.20		0.78	0.90
Mill bagasse	1	8.73		0.67	0.50
	2	7.56		0.74	0.32
	3	12.27		0.59	1.26
	4	10.10	10.0	0.65	0.79
	5	10.46		0.69	0.77
	6	11.17		0.61	1.10
Diffuser bagasse	1	17.28		0.82	1.08
	2	13.06		0.91	0.63
	3	17.01		0.87	0.91
	4	15.38		0.82	0.98
	5	17.30	16.9	0.82	1.01
	6	15.14		0.95	0.70
	7	18.30		0.80	1.20
	8	21.33		0.72	1.57

A comment relating to the sensitivity of this measure may be appropriate. As shown in Table 3.6 eleven mass fractions are used and each of these is multiplied by its corresponding mean fibre length. A variation in the mass of one of the size fractions will therefore not produce a major impact on the overall mean fibre length. Since in the computation each mass fraction is multiplied by the mean length for that fraction, variations in the mass of the largest size group (the coarsest fibres) will have the greatest impact. In other words, the mean fibre length is expected to show significant value changes due to variations in the coarse range but be relatively insensitive to mass variations in the smaller particle range.

While analysing the sieving data for different bagasse types it was noted that for depithed fibre samples relatively large mass fractions were retained on the coarsest sieve, namely the one with 6.7 mm apertures. The thought arose that, if a coarser sieve was used, this might affect the value of the mean fibre length obtained. In order to determine the effect of adding a coarser sieve to the usual set of sieves, a 13.2 mm sieve was obtained.

Four different bagasse samples were analysed in duplicate: once without the 13.2 mm sieve and once with it. The bagasse samples consisted of one from a milling tandem, two from diffuser factories and one of depithed fibre. The results are shown in Table 3.8. It can be seen that the mean fibre length obtained is significantly different only for the depithed fibre sample.

It needs to be mentioned that the determination of mean fibre length as detailed in the earlier portions of this section uses the curve fitting equations 3.8 and 3.9 which were derived from sieving data where the coarsest sieve had an aperture of 6.7 mm. Application of these equations to data based on the use of the 13.2 mm sieve involves extrapolation, the validity of which may be questionable. From the graphs presented in Figure 3.8 it is, in fact, clear that the region of highest uncertainty is the coarse region. It is therefore acknowledged that extension of equations 3.8 and 3.9 to sieving

data which utilises the 13.2 mm sieve is likely to introduce errors which are difficult to quantify. It is nevertheless hoped that these are not excessive, as appears to be indicated by the data in Table 3.8. It would obviously be desirable to repeat the experimental work by which the parameters in equations 3.8 and 3.9 were obtained to include a coarser sieve having apertures close to 13 mm.

TABLE 3.8

Mean fibre length obtained with and without the 13.2 mm sieve

Bagasse Type	Mean fibre length (mm)	
	Without 13.2 mm sieve	With 13.2 mm sieve
Mill bagasse	10.8	11.2
Depithed fibre	31.5	46.1
Diffuser bagasse 1	21.8	25.2
Diffuser bagasse 2	11.6	12.3

Unfortunately the possibility of obtaining a more accurate mean fibre length by using the 13.2 mm sieve only occurred to the author near the completion of the experimental work reported in the thesis. All of the correlations in chapter 4 (with the exception of those for surface friction, for which mean fibre lengths were based on the 13.2 mm sieve) are based on fibre length data using the 6.7 mm sieve as the coarsest. Particle analyses relating to the bridging tests described in chapter 5 used the 13.2 mm sieve. The uncertainty introduced is regrettable, but it is unlikely that it will affect the overall conlusions and results to a marked degree.

In general therefore it is recommended that, particularly for coarse bagasse samples, the 13.2 mm, or similar, sieve be included in the nest of sieves and

that equations 3.8 and 3.9 be updated using fibre length data which includes this coarse range.

3.6 COARSE-FINE RATIO

The mean fibre length defined in the previous section is a representative figure for the average length of the fibres in a given sample, but it does not give an indication of the relative proportions of coarse and fine particles. It is likely that these proportions will have a significant influence on the handling characteristics and bridging behaviour of bagasse. For this reason it was considered necessary to introduce another particle measure which quantifies this aspect.

The coefficient of variation (CV) is a frequently used dimensionless measure of the degree of variability exhibited by a collection of data. Table 3.7 indicates that for bagasse samples of widely differing mean fibre lengths the CV values show little variation. Gaylord and Gaylord (1984, p. 44) state that the flowability of granular materials is largely determined by the flow properties of the fine particles. Whether this is the case for bagasse is not certain. It is conceivable, however, that the relative proportions of fibres and pith particles can influence its flow behaviour significantly. Fibre-pith ratios are defined and measured differently by different sugar technologists. The author therefore decided to define, what he terms the "***coarse-fine ratio***" c as follows:

$$c = \frac{mass\ of\ particles\ retained\ by\ 2\ mm\ and\ coarser\ sieves}{mass\ of\ particles\ that\ pass\ through\ the\ 0.85\ mm\ sieve} . \qquad (3.15)$$

The choice of 2 mm and 0.85 mm as cut-off sizes for the coarse fibre and pith fractions respectively is somewhat arbitrary, but was made after consideration of the extensive particle size measurements which are

summarised in section 3.4. The coarse-fine ratio values obtained for the different types of bagasse analysed are given in Table 3.7. It is noteworthy that this measure gives a far more discriminating set of values than the coefficient of variation and that it is a quantity which is easy to calculate from direct sieving analysis data.

While one would generally expect a strong link between the mean fibre length and the coarse-fine ratio, the two measures express different characteristics of a sample. For this reason the two measures are included as separate variables in the numerical expressions of the succeeding chapters.

CHAPTER FOUR

BULK PROPERTIES OF BAGASSE

4.1 INTRODUCTION

In view of the large diversity of shapes and sizes of bagasse particles, as described in the previous chapter, special analysis techniques and equipment may be necessary to perform bulk property measurements. For example, the determination of surface friction by measuring the inclination of a sliding plane is likely to be highly inaccurate because of the loose aggregation of the particles, the low bulk density, the limited contact area of the particles with the plane and the natural migration of the small pith particles towards the bottom of the material (particularly if dry bagasse is being used). A standard shear cell (Gaylord and Gaylord, 1984, p.41) will not yield meaningful results because the fibrous nature causes the bagasse to bunch up instead of shear and hence makes it impossible to conduct a normal shear test. For these reasons it was considered necessary to use equipment that had been specially designed, or selected, in order to obtain valid measurements of the bulk properties of bagasse.

In general terms, whatever device is used to measure a property of bagasse, this device needs to suit the large range of fibre lengths that is normally encountered. This means that it should be much larger than equipment that is used for the analysis of "normal" particulate solids. For example, the longest fibres that can be found in diffuser bagasse are of the order of 100 mm or longer, which can be considered at least 20 times as long as the diameter of the largest particle that is likely to be encountered in test samples of other particulate materials. Furthermore, the apparatus should be designed and built in a way which produces the minimum artificial change in the natural agglomeration or alignment of the particles. Objects such as spikes which penetrate the bagasse during a tensile strength test, for example, are likely to alter the bulk properties of the bagasse significantly.

The bulk properties that were measured, and are reported here, are the following:

* surface friction
* bulk density and compactibility
* shear strength
* translation of vertical pressure into lateral pressure
* tensile strength.

Each of these will be described under the headings

apparatus
method
data analysis
results.

Data acquisition for the measurements reported in this study was effected with an electronic system described in Appendix A.

The reader may be surprised that "angle of repose" is not one of the bulk properties included in the above list. The reasons for this are that, for bagasse, the angle of repose depends, apart from the particle characteristics measured in this study, on a number of additional factors such as time and temperature of storage which, in turn, influence the extent of microbiological activity causing varying degrees of degradation. The last-mentioned has a profound effect on the fibre rigidity and cohesiveness which determine the angle of repose. A further reason why this measure has not been investigated is that a very large apparatus is required for valid measurements because of the wide range of particle sizes encountered in a normal bagasse sample. The best place for doing angle of repose measurements is in an industrial bagasse store. Such measurements have been done by the author, but he found that within one bagasse pile the angle of repose varied from 45° to 60°. It was therefore decided that the angle of repose was not a useful measure for bagasse.

4.2 SURFACE FRICTION

The friction between a bulk solid and the surface on which this solid moves is clearly important in determining the handling characteristics of that solid. It affects the power required to move such a solid on horizontal or inclined surfaces with the aid of slat conveyors as well as the required angle of inclination of chutes whose function it is to perform downward transfer of the material. Furthermore it plays a significant role in the formation of transient or stable bridges within items of equipment such as bins, hoppers and chutes.

The factors that influence surface (or wall) friction are particle size distribution, particle hardness, degree of compaction, moisture content, temperature, relative speed of movement, sand content and surface roughness.

In the investigation of surface friction of bagasse the surfaces used were polished 316 stainless steel, mild steel coated with a rust-resistant etching primer PA10 and smooth polycarbonate sheeting. The stainless steel was used to simulate a typical surface on which bagasse slides in a sugar factory. Even though many such surfaces are not made from stainless steel, the scouring action of the bagasse polishes them smooth within a short time and it was assumed that polished stainless steel had very similar friction characteristics to sliding surfaces used in industry. The other two surfaces were those used in the equipment in which measurements of tensile strength and bridging characteristics were done.

Because the bagasse that was used in most of the tests reported here had been transported from sugar factories over long distances, it was not possible to control temperature. The sand content of bagasse is frequently dependent on weather conditions at harvest. If there has been excessive rainfall before harvest then the average sand content can rise from the normal 1 to 1.5% by mass to as high as 10%. Since the sand particles have diameters comparable with those of the small pith particles and normally constitute a very small fraction of the total mass, it was assumed that the effect of sand on friction was likely to be negligible. As far as particle hardness is concerned, the author could not find a method that could be used to measure this, and it has therefore not been included in the investigation.

Two different methods of measuring surface friction were investigated. The first used a cylindrical stainless steel shell whose axis was vertically orientated with an inside diameter of 0.7 m and height of 1.5 m in which a plug of bagasse was rotated by an axially mounted stirrer. The stirrer was driven by an hydraulic motor for which the rotational speed could be adjusted continuously from zero to maximum. Thus the effect of varying the relative speed of sliding of bagasse over the surface could be studied. Normal pressure was measured by three pressure transducers mounted

symmetrically on the circumference at the same vertical level flush with the inside wall of the cylindrical shell. Friction force was obtained by measuring the torque required to rotate the plug of bagasse. This was done with the aid of a load cell.

The second method utilised flat surfaces of the three different materials over which bagasse was moved and which were placed on a horizontal table. The bagasse was contained in a rectangular box with a wire mesh bottom and an open top. The box was filled with bagasse so that a layer of approximately 10 mm protruded beyond the open lip of the box and the box was inverted over the sliding surface so that only bagasse made contact with the sliding surface. Further details are given in the apparatus part of this section.

The results of the second method showed a significantly better repeatability than the first. For this reason only these results are reported here. This means, however, that the effect of the relative speed of sliding is not taken into account. Since this thesis centres on the factors that contribute to the formation of bagasse bridges, and bagasse bridges form under essentially static conditions, a lack of understanding of the influence of sliding speed is not a disadvantage.

This section on surface friction therefore deals with the influence of particle size distribution, compaction, moisture content and type of sliding surface on the magnitude of the friction.

Most theoretical analyses of bulk solids flow behaviour assume that the solid behaves as an ideal Coulomb solid. For such a solid the relationship between sliding frictional stress, τ_w, and normal stress, σ_w, is assumed to be linear (Nedderman, 1982) of the form

$$\tau_w = \mu_w \sigma_w + C_w \quad (4.1)$$

where C_w is called the cohesion and μ_w is the coefficient of wall friction which is often written as tan ϕ_w where ϕ_w is called the angle of wall friction. The aim in this section is to determine the form of the relationship between τ_w and σ_w which bagasse exhibits.

Bullock and Murry (1957) reported extensive measurements of surface friction coefficients for bagasse, but their study was undertaken at pressures normally encountered in extraction mills (between 200 kPa and 20 MPa), in other words, at pressures up to 200 times higher than those that would normally occur in ordinary bagasse chutes. These results can therefore not be considered relevant. Douglas *et al.* (1991) report measurements of wall friction on shredded cane and bagasse which were carried out on samples that were thoroughly soaked with water. The moisture content in Douglas' tests was mostly more than eight times higher than the maximum moisture content of the samples investigated in this study. Furthermore, Douglas' measurements do not result in a true value of the coefficient of friction because vertical load on bagasse is used as a measure of normal stress whereas the frictional shear stress is derived from the sliding resistance exerted on vertically positioned side walls. For determination of the normal coefficient of friction, if a vertical load is applied to a mass of material, sliding must occur over a horizontal surface.

McLean (1988) found that for coal the wall yield locus is generally not linear, but has an upward facing convexity, as shown in Figure 4.1. His measurements indicate that if angle of wall friction ϕ_w is plotted against consolidating pressure σ_w the value of ϕ_w increases as σ_w decreases. At high consolidating pressures an asymptotic value is reached whereas at very low pressures the wall friction angle in many cases exceeds the rough wall friction angle, which can be taken as the value of the internal angle of

friction, as indicated in Figure 4.2. The data of Douglas *et al.* (1991) show a similar trend.

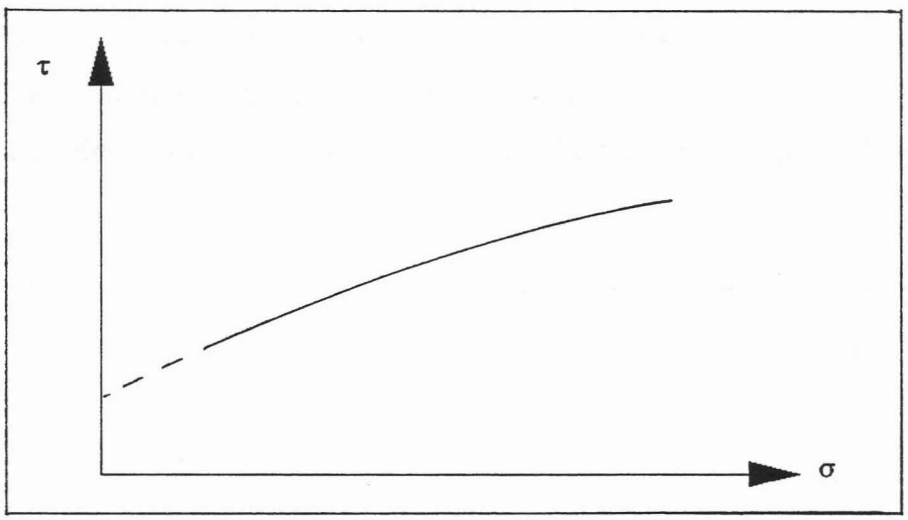

Figure 4.1 *Wall yield locus for coal sample*

The friction that is being considered is the maximum value that is recorded as motion commences. It is generally observed that dynamic friction, in other words the friction that occurs during fully developed motion, is generally less than the maximum frictional resistance that occurs at the commencement of movement. It is, of course, this maximum friction that is relevant in bridging studies.

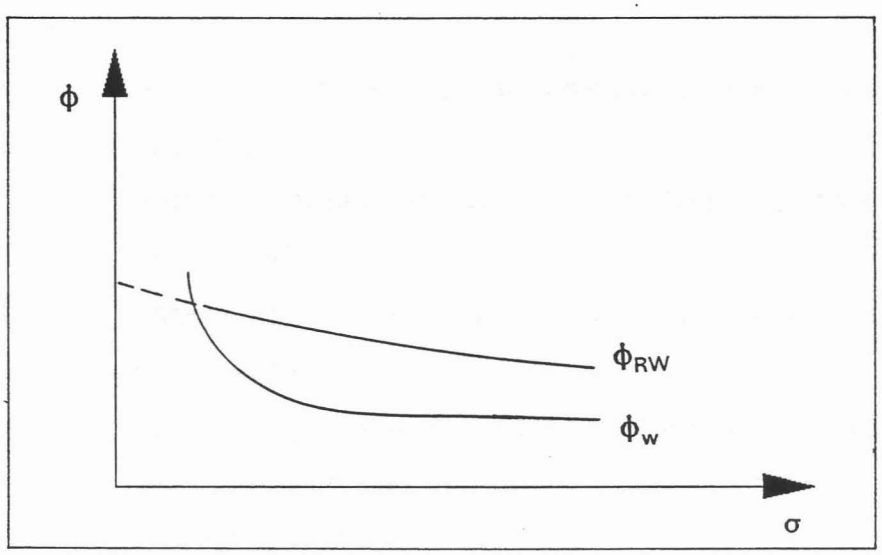

Figure 4.2 *Variation of wall friction angle with consolidating pressure*

Apparatus

The apparatus used in this study for the second method of determining the surface friction characteristics of bagasse is illustrated in Figure 4.3. A photograph depicting this apparatus in use is shown in Figure 4.4.

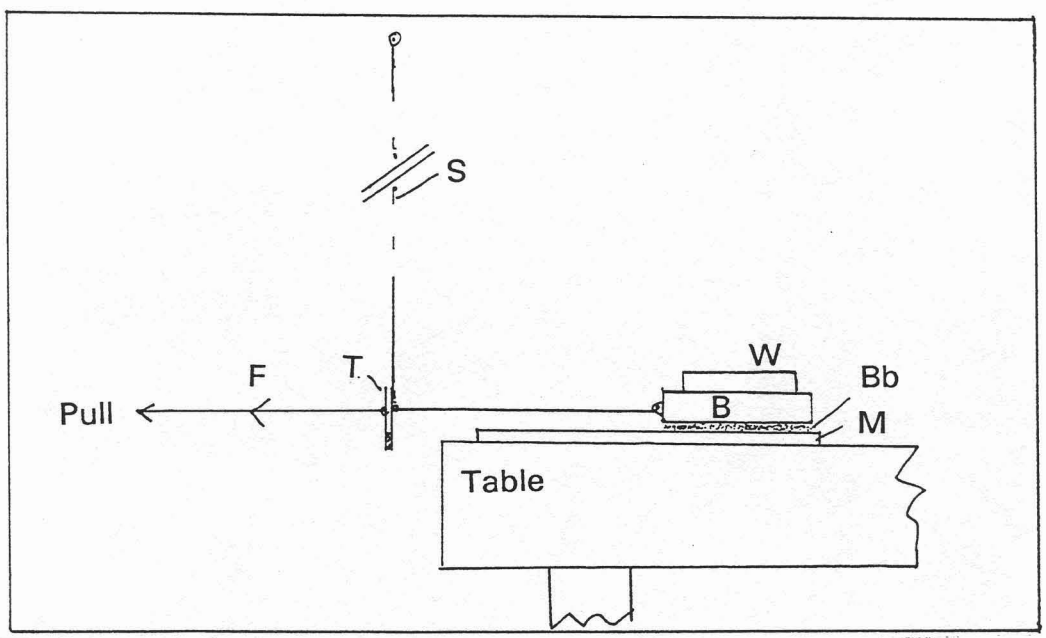

Figure 4.3 *Apparatus used to measure bagasse surface friction*

B	rectangular stainless steel box containing the bagasse
Bb	bagasse
F	horizontal frictional force required to start moving the box of bagasse
M	sheet of material whose surface friction characteristics is to be evaluated
S	suspending string to neutralise any vertical component of the weight of T affecting the friction force F
T	tension mesuring device
W	weight placed on box to vary the normal stress

As mentioned above, three different plane surfaces M, namely polished stainless steel, corrosion protected mild steel and smooth polycarbonate sheeting were used. Their thicknesses were 0.5, 4.0, and 3.0 mm respectively while the length of each surface was 400 mm and its width 300 mm.

Figure 4.4 *Photograph of surface friction apparatus*

A rectangular stainless steel box B, 210 mm wide by 260 mm long by 85 mm deep, and fitted with a 2 mm square stainless steel mesh floor, was used to contain a given mass of bagasse which was dragged horizontally across the sliding surface. The box was filled with bagasse so that a layer of about 10 mm bagasse protruded above the lip of the box. Two strings were attached to brackets fitted in the middle of two of the corners of the box and combined about 15 cm in front of the box to pull it in a controlled manner so that the pulling force F on the box was directed parallel to the surface (that is, horizontally). A tension measuring device T which measured

the force F was attached to the string pulling the box. A description of this device, as well as the calibration details are given in Appendix B. The tension readings were monitored by an electronic data collection system. In order that the friction force F was not affected by the weight of the device T a suspending string S was used. This string, the length of which was 1.95 m, was fixed vertically above the sliding surface. The sliding movement on the friction surface was less than 25 cm and the mass of T was 185g. The maximum error of the force measured by T as a result of the deviation of the angle of suspension away from the vertical, caused by pulling the bagasse across the friction surface, was estimated to be 0.2 N. The box containing the bagasse was pulled slowly over the sliding surface by hand, taking care that the string by which it was pulled always remained in a horizontal direction.

Method

The different types of bagasse that were used to measure surface friction included mill and diffuser bagasse, as well as depithed fibre and pith. Thus the influence of mean fibre length and coarse-fine ratio could be investigated. The method of their determination has been described in section 3.5. In order to obtain readings for a range of moisture contents some samples were left to dry while being spread out on the floor of an open building prior to the tests.

A sub-sample of the bagasse was removed for sieve and moisture analysis before measuring of the surface friction commenced. Bagasse was put into the rectangular box by hand but care was taken to avoid artificial alignment of the fibres. The box was filled and then weighed. From a knowledge of the weight of the empty box, that of the box with bagasse and the dimensions of the box, the bulk density of the bagasse, as well as the normal force during friction measurements, could be determined. A flat plate was placed

on the bagasse and the box was inverted over the sliding surface. Then the plate was removed carefully. The tension measuring device was then connected to the box and was carefully pulled until sliding commenced. The maximum reading of the tension, which represented the maximum static friction, was recorded. When four tension readings had been taken, a block of wood of known weight was placed centrally on the inverted box to increase the normal force. Another set of four readings was taken as before. The average of each set of four readings was converted into a pulling force (in newtons) using the calibration factors given in Appendix B. The friction forces measured were in the range 2 - 20 N, so the maximum error of 0.2 N caused by the deviation of the suspending string from the vertical can be considered negligible. This procedure was repeated until altogether five different normal forces had been used.

Further samples of bagasse from the same parent batch were used to take similar measurements for the other two surfaces. From the weights of the box, the bagasse and the added weights, as well as the contact area, the normal stress σ could be calculated and from the pulling force F and the area of contact the frictional shear stress τ was determined. A typical set of results of surface friction measurements for one type of bagasse at a given moisture content is shown in Table 4.1.

Data analysis

For each type of bagasse and the three surfaces employed the shear stress, normal stress, moisture content, mean fibre length and coarse-fine ratio were tabulated. Altogether there were 195 sets of readings of which the first 20 are shown in Table 4.2.

Table 4.1

A typical set of results of surface friction measurements

BAGASSE SAMPLE:	FX5 (DEPITHED FIBRE)
MEAN FIBRE LENGTH (mm):	23.04
COARSE-FINE RATIO:	2.36
MOISTURE CONTENT (%):	30.66
SAMPLE + TRAY MASS (kg):	1.025
BULK DENSITY (kg/m3):	80.4

MILD STEEL

SHEAR STRESS	NORMAL STRESS
82.4	184.2
106.4	232.1
135.7	283.0
156.8	329.7
320.0	590.7

STAINLESS STEEL

SHEAR STRESS	NORMAL STRESS
57.1	184.2
80.4	232.1
107.3	283.0
128.0	329.7
244.9	590.7

POLYCARBONATE

SHEAR STRESS	NORMAL STRESS
83.7	184.2
105.9	232.1
125.2	283.0
152.9	329.7
297.3	590.7

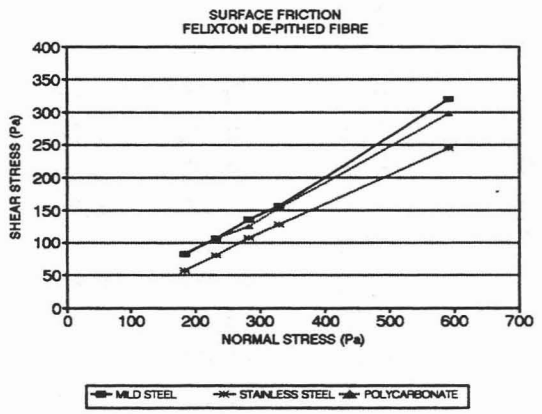

LINEAR REGRESSIONS

	GRADIENT	INTERCEPT
M/STEEL	0.590	-30.7
S/STEEL	0.459	-25.2
POLYCARB.	0.532	-19.3

The units of 'SHEAR STRESS' and 'NORMAL STRESS' are Pa

Table 4.2

Datasets representing the surface friction measurements

SUMMARY OF SURFACE FRICTION DATA FOR MODELLING

SHEAR	DENS	NORMAL	MOIST	LENGTH	COARSE	S1	S2
Pa	kg/m3	Pa	%	mm	-	-	-
86.7	123.2	221.9	56.3	20.49	2.15	0	0
119.6	123.2	269.9	56.3	20.49	2.15	0	0
156.5	123.2	320.7	56.3	20.49	2.15	0	0
175.3	123.2	367.4	56.3	20.49	2.15	0	0
329.5	123.2	628.4	56.3	20.49	2.15	0	0
91.7	123.2	221.9	56.3	20.49	2.15	0	1
119.6	123.2	269.9	56.3	20.49	2.15	0	1
136.4	123.2	320.7	56.3	20.49	2.15	0	1
166.5	123.2	367.4	56.3	20.49	2.15	0	1
281.8	123.2	628.4	56.3	20.49	2.15	0	1
91.9	123.2	221.9	56.3	20.49	2.15	1	0
139.5	123.2	269.9	56.3	20.49	2.15	1	0
167.8	123.2	320.7	56.3	20.49	2.15	1	0
187.4	123.2	367.4	56.3	20.49	2.15	1	0
363.5	123.2	628.4	56.3	20.49	2.15	1	0
82.4	80.4	184.2	30.66	23.04	2.36	0	0
106.4	80.4	232.1	30.66	23.04	2.36	0	0
135.7	80.4	283	30.66	23.04	2.36	0	0
156.8	80.4	329.7	30.66	23.04	2.36	0	0
320.0	80.4	590.7	30.66	23.04	2.36	0	0

A statistical computer package (Statgraphics 5.0, 1991) was used to determine the significant variables affecting surface friction and to find a model by which this could be predicted. Surface friction expressed in terms of shear stress τ (in Pa) as a dependent variable was regressed using a multiple linear regression model against the following independent variables:

bulk density	ρ_b	kgm^{-3}
normal stress	σ	Pa
moisture content	W	%
mean fibre length	L	mm
coarse-fine ratio	c	-
surface variables	S_1, S_2	-.

An increase in the scatter of the residuals for large values of the shear stress suggested that a logarithmic or square root transformation of τ might improve the fit. This was indeed so and two additional model structures were evaluated using the above independent variables.

The basic form of the model is shown in equation 4.2

$$\tau = \beta_0 + \beta_1\rho_b + \beta_2\sigma + \beta_3 W + \beta_4 L + \beta_5 c + \beta_6 S_1 + \beta_7 S_2 + \varepsilon \quad (4.2)$$

where ε is an error term with mean 0 and variance σ^2_ε and $ß_0$, ...$ß_7$ are regression model parameters. In order to make allowance in the statistical model for friction on the three different surfaces Murray (personal communication, 1995) suggested the use of two dummy variables S_1 and S_2. The values used to distinguish between the three surfaces are given in Table 4.3.

Table 4.3

Definitions of S1 and S2

Surface type	S1	S2
Mild steel	0	0
Stainless steel	0	1
Smooth polycarbonate	1	0

If the mild steel surface proves to have a significant effect on τ whereas the other two surface types (stainless steel and and smooth polycarbonate) do not, then this will be shown if the constant parameter β_0 is significant and S_1 and S_2 are not. If S_1 is a significant variable then smooth polycarbonate has an effect on τ and if S_2 proves to be significant then stainless steel significantly influences τ.

Results

The linear model obtained as a result of the regression is given by equation 4.2.

The transformed linear models that utilised the logarithm and square root of τ respectively have the form

$$\log_{10}\tau = \beta_0 + \beta_1\rho_b + \beta_2\sigma + \beta_3 W + \beta_4 L + \beta_5 c + \beta_6 S_1 + \beta_7 S_2 + \varepsilon \qquad (4.3)$$

and

$$\sqrt{\tau} = \beta_0 + \beta_1\rho_b + \beta_2\sigma + \beta_3 W + \beta_4 L + \beta_5 c + \beta_6 S_1 + \beta_7 S_2 + \varepsilon \; . \qquad (4.4)$$

The values of the coefficients and relevant statistical data are given in Table 4.4. When the 195 datasets were fitted to the above three models the adjusted r^2 values obtained were 0.905, 0.917 and 0.942 respectively, indicating a relatively good fit for all three models. Adjusted r^2 values are those which are adjusted according to the number of degrees of freedom applicable in the analysis. The above r^2 values also show that the square root model gives a slightly better fit than the other two.

The t-values in the three models described (see Table 4.4) show that the only variable that is not significant is S_1, which means that the friction characteristics of smooth polycarbonate are similar to those of mild steel, while stainless steel gives a different response. This is partially illustrated in

the graphs shown in Table 4.1. The individual graphs of τ vs σ (only one set is depicted in Table 4.1) showed that the gradients and positions for mild steel and polycarbonate were very similar whereas the stainless steel graph was lower than the other two. In other words, the friction against stainless steel was less than that against mild steel or polycarbonate. By implication therefore the type of surface does play a role in the sliding friction of bagasse. An in-depth study of surface roughness for the three different surfaces was not attempted because this was considered to be beyond the scope of this work.

Table 4.4

Parameters and relative statistics for models on surface friction

(a) Linear model

Variable	Coefficient	Std. error	t-Value	95% Confidence Limits	
				High	Low
Constant	75.529	12.90	5.86	50.08	100.98
Bulk density ρ_b	-1.0767	0.128	-8.39	-1.33	-0.82
Normal stress σ	0.5081	0.015	33.55	0.478	0.538
Moisture W	3.7921	0.282	13.46	3.24	4.348
Fibre length L	-10.181	1.274	-7.99	-12.70	-7.666
Coarse-fine c	41.94	10.44	4.02	21.35	62.54
S_1	-6.425	5.27	-1.22	-16.83	3.974
S_2	-33.83	5.27	-6.42	-44.23	-23.43

Table 4.4 (contd)

(b) Logarithmic model

Variable	Coefficient	Std. error	t-Value	95% Confidence Limits	
				High	Low
Constant	1.9107	0.034	55.93	1.843	1.978
Bulk density ρ_b	-0.0030	0.0003	-8.96	-0.004	-0.002
Normal stress σ	0.0013	.00004	32.67	0.001	0.001
Moisture W	0.0119	0.0007	15.96	0.010	0.013
Fibre length L	-0.0310	0.0034	-9.18	-0.038	-0.024
Coarse-fine c	0.1188	0.0276	4.30	0.064	0.173
S_1	0.0010	0.0140	0.07	-0.027	0.029
S_2	-0.0963	0.0140	-6.90	-0.124	-0.069

(c) Square root model

Variable	Coefficient	Std. error	t-Value	95% Confidence Limits	
				High	Low
Constant	8.9271	0.385	23.20	8.168	9.686
Bulk density ρ_b	-0.0413	0.004	-10.80	-0.049	-0.034
Normal stress σ	0.0189	.0005	41.82	0.018	0.020
Moisture W	0.1543	0.008	18.36	0.138	0.171
Fibre length L	-0.4094	0.038	-10.77	-0.484	-0.334
Coarse-fine c	1.6489	0.311	5.30	1.035	2.263
S_1	-0.1214	0.157	-0.77	-0.432	0.189
S_2	-1.3019	0.157	-8.28	-1.612	-0.992

In conclusion, surface friction of bagasse is very dependent on the normal stress, the bulk density and the moisture content and to a lesser extent (but still significantly, from a statistical perspective) on mean fibre length, coarse-fine ratio and type of surface. Figure 4.5 shows a plot of predicted against observed shear stress for the model fitting the best, viz. the square root model (equation 4.4).

The models presented apply to a shear stress (τ) range of 0-600 Pa or a normal stress (σ) range of 0-900 Pa. The results indicate that, over the stated range of stresses, for a given type of bagasse of a certain bulk density and mean fibre length, coarse-fine ratio and moisture content sliding on a given surface, friction for bagasse follows a linear relationship of the form

$$\tau = a + b\sigma \qquad (4.5)$$

as can be seen in the examples depicted in Table 4.1. The value of b can be considered to be the coefficient of wall friction.

4.3 BULK DENSITY AND COMPACTIBILITY

A knowledge of the bulk density is essential for the design of bagasse handling equipment such as belt conveyors. Moreover, the bulk density of a given mass of bagasse moving down a chute is one of the important factors determining whether it will bridge or not. Because of the fibrous composition of bagasse it is easily compacted resulting in large changes of its bulk density. In this section the aim is to find a correlation between the compacting stress and bagasse bulk density taking into account the influence of mean fibre length, coarse-fine ratio and moisture content.

Another factor that can affect compactibility is fibre rigidity, but this aspect

was not investigated because it was felt that a meaningful investigation of this complex topic was beyond the scope of this work.

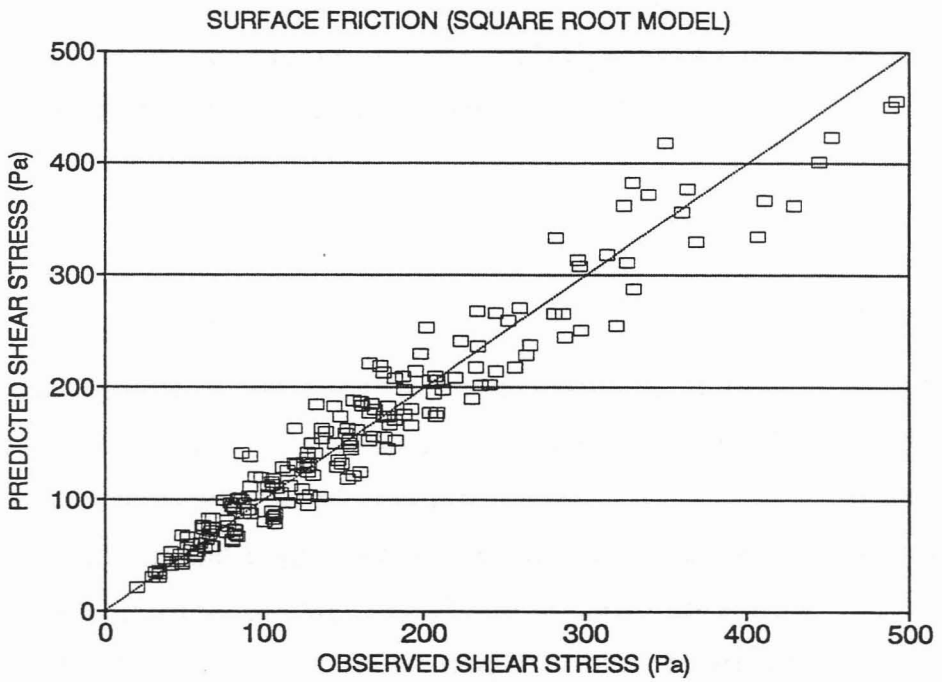

Figure 4.5 *Predicted vs. observed frictional shear stress for square root model*

A precise definition of compactibility will not be given because it is not going to be used in any quantitative expression. In qualitative terms, the greater the increase of a material's bulk density under a compacting load, the greater its compactibility. In considering compaction one can distinguish between two types of compacting stress. Hydrostatic compacting stress is a three-dimensional stress occurring when, for example, a mass of bagasse contained in a plastic bag is immersed in a liquid which exerts a uniform pressure at a given level in all directions on the bag. The other type of stress is unidirectional compacting stress where the compacting force acts only on one plane of the material. It is this type of stress situation which will be considered here and the symbol that will be used for compacting stress is σ_1.

The investigation presented here is also intended to take into account the phenomenon that when bagasse has been compressed by a load, and that load is subsequently removed, it does not return to its original volume. It is usually found that an increase in volume does occur after removal of the compacting force, but the degree to which this occurs is dependent on the particle size distribution and the moisture content.

Apparatus

The measurements of bulk density changes under different compacting loads was done in a very simple apparatus shown in Figure 4.6. A translucent plastic measuring cylinder M of 5 litre capacity was filled with bagasse B. From the mass of the bagasse and the volume indicated on the measuring cylinder the uncompacted bulk density could be determined. The compacting device consisted of a flat circular disc D which fitted into the measuring cylinder with a 5 mm clearance around the circumference. This was welded concentrically to a ring R made from a section of 100 mm diameter pipe. The function of the ring was to retain any weights W_1, W_2 that were placed on the disc D for additional compaction load and to facilitate symmetrical loading to try to ensure compaction so that the top surface remained horizontal. From the cross-sectional area of the measuring cylinder and the weight of the compacting device as well as additional weights the compacting stress was determined. The volume of the bagasse under compaction was read off at the bottom edge of the compacting disc D against the graduations of the measuring cylinder. The possible effect of the surface friction of the bagasse against the vertical wall of the measuring cylinder on the compacting load was not taken into account in the calculation of the compacting stress.

Method

Using a particular type of bagasse at a predetermined moisture content the measuring cylinder was filled to the 5 litre mark and weighed. This mass minus the tare mass of the cylinder was used for bulk density determinations. Different degrees of compaction were achieved by using the compacting device (R and D) the mass of which had previously been ascertained, as well as additional weights W_1, W_2 etc. For each weight the relevant total compacting mass as well as the corresponding bagasse volume were recorded for bulk density determinations. A time interval of 10 seconds was allocated after changing the compacting load before taking the corresponding volume reading to allow the bagasse to settle to a steady volume.

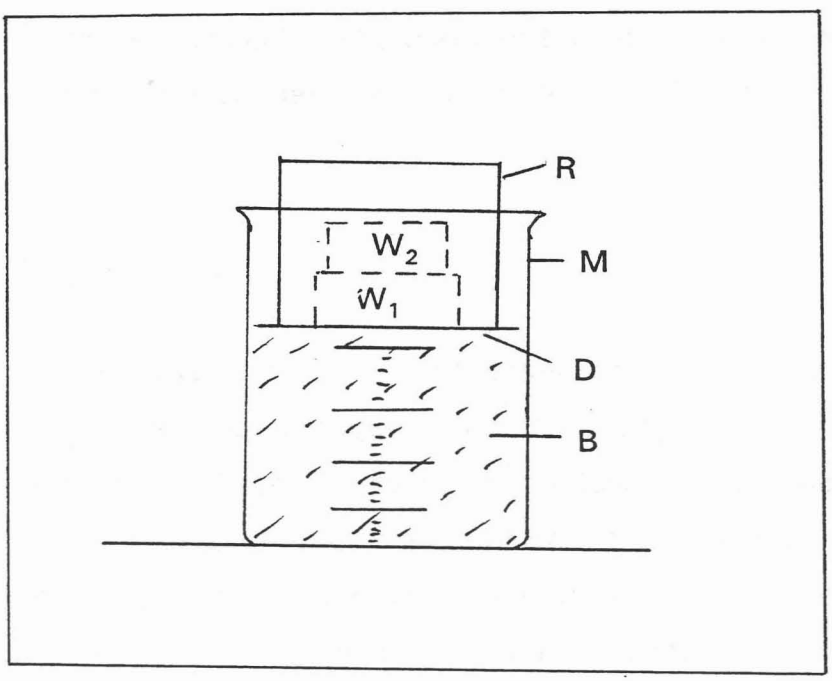

Figure 4.6 *Apparatus used for the measurements of bulk density and compactibility*

To assess the elastic properties of bagasse under compaction, after the maximum load had been used weights were taken off stepwise while monitoring the bagasse volume for every reduced load until all the weights and the compacting device had been removed. The 10 s time interval was applied on unloading as per loading. For each sample type two tests of loading and unloading were performed. In the first test five loads were added sequentially until the total compacting stress was 2033 Pa. The loads were then removed in three steps. For the second test a fresh sample from the same batch of bagasse was used. Loading was performed in the identical fashion as for the first test, but unloading was done in one step. This was done to ascertain if the behaviour of the bagasse was different for gradual as compared with sudden unloading.

The above readings were repeated for different bagasse types and a range of moisture contents. For each test a graph of bulk density vs. compacting stress was drawn. A typical set of results is shown in Table 4.5.

Data analysis

Measurements like those shown in Table 4.5 were done on thirteen samples of bagasse to accommodate a range of mean fibre length, coarse-fine ratio and moisture content. Since the response to loading was significantly different from that to unloading, as is evident from the two graphs included in Table 4.5, separate statistical analyses were done for the loading and the unloading data. For the loading case the rate of increase of bulk density at low compacting stresses was greater than at the higher stresses. In other words the graphs showed an upward convex curvature which flattened off as compacting stress increased. The graphs representing the variation of bulk density during unloading showed an essentially linear response.

Table 4.5

Bulk density and compacting stress measurements for one type of bagasse

BAGASSE SAMPLE: FXPITH2
MEAN FIBRE LENGT 5.13
COARSENESS INDE 0.04
MOISTURE CONTE 42

Cross-sectional area of beaker: 269 cm^2

TEST 1

MASS OF BAGASSE 0.430 kg

MASS ADDED kg	TOTAL MASS kg	TOTAL FORCE N	VERTICA STRESS N/m2	VOLUME ml	BULK DENSITY kg/m3
0.000	0.000	0.000	0.0	5000	86.0
1.235	1.235	12.115	450.4	4000	107.5
0.545	1.780	17.462	649.1	4000	107.5
0.535	2.315	22.710	844.2	3900	110.3
1.831	4.146	40.672	1512.0	3500	122.9
1.430	5.576	54.701	2033.5	3500	122.9
-1.430	4.146	40.672	1512.0	3500	122.9
-1.831	2.315	22.710	844.2	3500	122.9
-2.315	0.000	0.000	0.0	3600	119.4

TEST 2

MASS OF BAGASSE 0.465 kg

MASS ADDED kg	TOTAL MASS kg	TOTAL FORCE N	VERTICA STRESS N/m2	VOLUME ml	BULK DENSITY kg/m3
0.000	0.000	0.000	0.0	5000	93.0
1.235	1.235	12.115	450.4	4250	109.4
0.545	1.780	17.462	649.1	4100	113.4
0.535	2.315	22.710	844.2	4000	116.3
1.831	4.146	40.672	1512.0	3750	124.0
1.430	5.576	54.701	2033.5	3500	132.9
-5.576	0.000	0.000	0.0	3600	129.2

AVERAGES OF BULK DENSITY

BEFORE LOADING 89.5
PEAK 127.9
AFTER LOADING 124.3

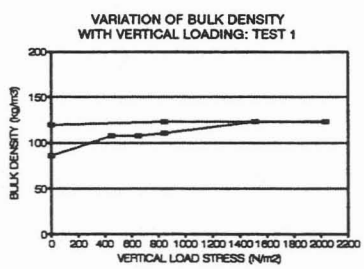

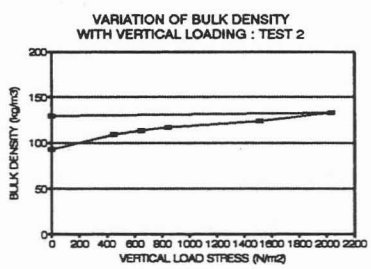

For statistical analysis the tabulated variables were: bulk density (ρ), compacting stress (σ_1), mean fibre length (L), coarse-fine ratio (c) and moisture content (W). Stepwise multilinear regression using the computer package Statgraphics 5.0 (1991) was employed to determine which variables had a significant effect on bulk density. In order to account for the

curvature of bulk density as a function of compacting stress the natural logarithm of the bulk density, ln ρ, was used as the dependent variable in the regression analysis.

Results

The model obtained by stepwise multilinear regression that fitted the tabulated data for the case where bagasse was being compacted by a unidirectional load had the form expressed in equation 4.6. It was based on 156 datasets and gave an adjusted r^2 value of 0.888. In this model bulk density was transformed by applying its natural logarithm, as mentioned above.

$$\ln\rho = \beta_0 + \beta_1\sigma_1 + \beta_2 L + \beta_3 W + \beta_4 c + \varepsilon \qquad (4.6)$$

The values of the coefficients $ß_0,..ß_4$ are stated in Table 4.6 which also lists the t-values and confidence intervals. The t-values show that all the independent variables are statistically significant. A plot of predicted vs measured bulk density using the model of equation 4.6 is shown in Figure 4.7.

Stepwise multilinear regression was also applied to determine a model describing the bulk density for unloading of bagasse that had been previously compacted. Since the relationship between compacting stress and density appeared to be linear the stress was not transformed by applying the square root as for the loading case. The model obtained using 78 datasets had the form given in equation 4.7 with an adjusted r^2 value of 0.829.

$$\rho = \beta_0 + \beta_1\sigma_1 + \beta_2 L + \beta_3 W + \varepsilon \qquad (4.7)$$

The statistical details for this model are given in Table 4.7. The stepwise multilinear regression once again showed that coarse-fine ratio was a non-significant variable. Table 4.7 also indicates that load is not a significant variable. In other words, the change in bulk density during unloading is, from a statistical viewpoint, very small. The coefficient for the compacting stress σ_1 is positive, however, indicating that for a decrease in compacting load a small decrease in bulk density can be expected. This is an indication of a small degree of elastic behaviour which can have a marked effect in bagasse bridging. A graph of expected vs measured bulk density values for this model is shown in Figure 4.8.

Table 4.6

Statistical data for compaction model of bulk density

Variable	Coeffi-cient	Std. error	t-Value	95% Confidence Limits	
				High	Low
Constant	4.1898	0.0434	96.45	4.1040	4.2757
Comp. Str. σ_1	0.00019	0.0000	12.66	0.00016	0.00021
Fibre Length L	-0.01346	0.0031	-4.38	-0.0195	-0.0074
Moisture W	0.01299	0.0006	19.86	0.0117	0.0143
Coarse-fine c	-0.0636	0.0149	-4.27	-0.0931	-0.0342

Table 4.7

Statistical data for the unloading model of bulk density

Varia-ble	Coeffi-cient	Std. error	t-Value	95% Confidence Limits	
				Low	High
Constant	77.26	7.301	10.58	62.70	91.81
Comp. Str. σ_1	0.0035	0.002	1.736	-0.0005	0.007
Fibre Length L	-1.825	0.284	-6.417	-2.392	-1.258
Moisture W	1.632	0.106	15.35	1.420	1.843

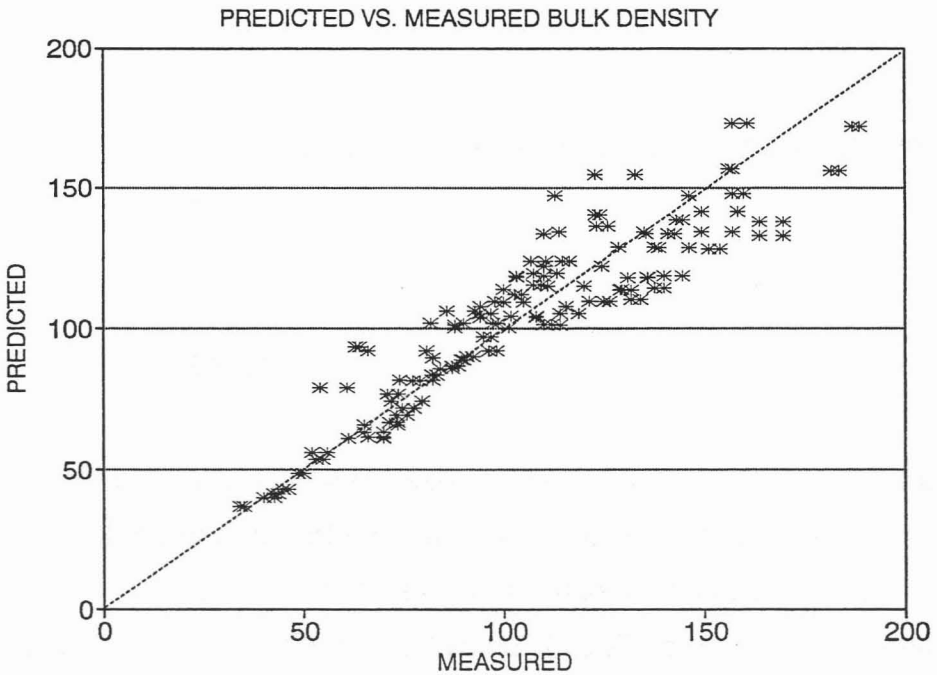

Figure 4.7 *Predicted vs. measured bulk density using equation 4.7*

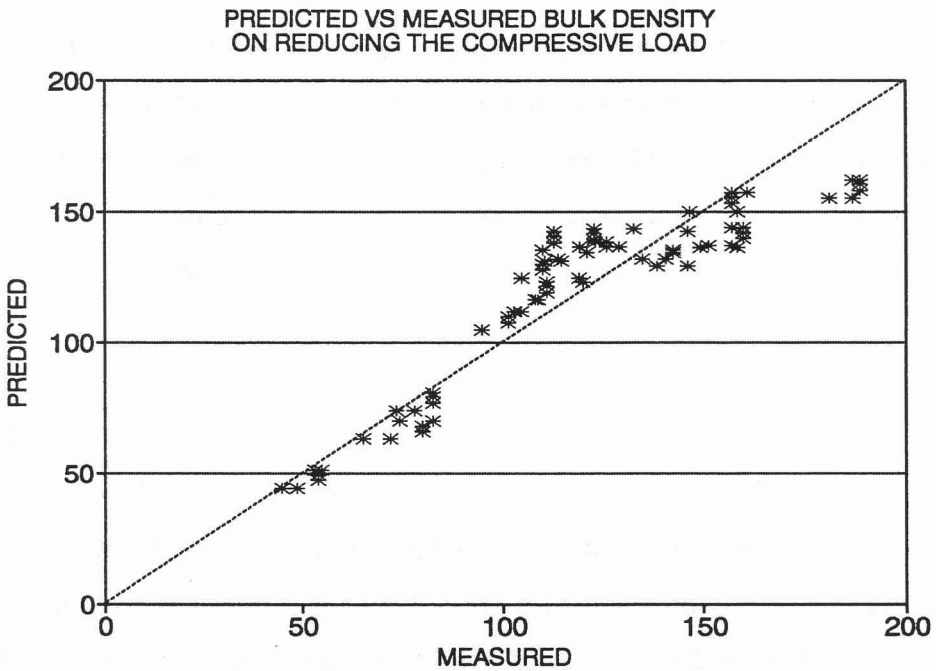

Figure 4.8 *Predicted vs. measured bulk density for the unloading case*

4.4 SHEAR STRENGTH

An important measure which is used in the prediction of the flow behaviour of a bulk solid is the angle of internal friction ϕ. It was mentioned in chapter two that for many bulk solids this can be measured with the aid of a Jenike (1960) shear tester or a Carr and Walker (1967) annular shear cell. It was also stated that these devices are not suitable for measuring the shear strength of bagasse because the bagasse fibres tend to compact and the material increases in strength as soon as an attempt is made to cause shear failure by the relative tangential movement of one surface against another.

The bagasse shear apparatus described by Plaza and Edwards (1994) which operated at the very high pressures encountered in milling does not, in the author's opinion, measure true shear strength because it produces a significant amount of particle shear, which is different from the bulk solids shear that forms the basis of the determination of the angle of internal friction. This assertion was subsequently confirmed by Edwards, one of the authors of that paper (personal communication, 1995). For these reasons it was decided to build an apparatus to investigate specifically the shear characteristics of bagasse.

Apparatus

The cylindrical stainless steel shell of 0.7 m diameter and 1.5 m height described in section 4.2 (that had been used during the initial attempts to measure surface friction) was modified for shear tests. A plan view of the modifications is shown in Figure 4.9. Eight baffles B were fixed at 45° gaps round the periphery of the shell so that their plane faces were directed towards the axis of the shell. The baffles were made from 75 mm x 50 mm x 5 mm angle iron. The framework supporting the baffles (not shown in Figure 4.9) was made from lighter gauge angle iron and was bolted to the top and bottom flanges of the cylindrical shell. Bagasse was made to shear adjacent to the baffles by a stirrer paddle P which was constructed of four 2 mm flat rectangular mild steel plates of dimensions 155 mm x 1000 mm welded to a 30 mm BMS shaft S and reinforced by angular rods also welded to the flat plates (not shown in Figure 4.9). A circular flat plate was welded to the bottom of the paddle plates to hold up the bagasse during rotation. The radial clearance between the stirrer paddle and the baffles was 8.0 cm. The assumed shear plane was a cylindrical surface situated halfway between the edges of the baffles and those of the paddle plates (indicated by a dotted circle in Figure 4.9). The area of the shear surface (for determination of shear stress) was determined from the diameter of this cylindrical surface

and the height of bagasse in the apparatus. All mild steel components were coated with PA10 etching primer to ensure a uniform contact surface. The torque, from which the shear strength was determined, was measured by means of a load cell fitted to a lever which was fixed to the hydraulic motor rotating the paddle. The motor speed could be varied continuously and a proximity device fitted to its shaft enabled its speed (as rpm) to be recorded. The Status-74 (1989) datalogging software was used to take torque and paddle speed readings at a frequency of 10 Hz. The calibration details of the torque meter and paddle speed measuring device are given in Appendix C.

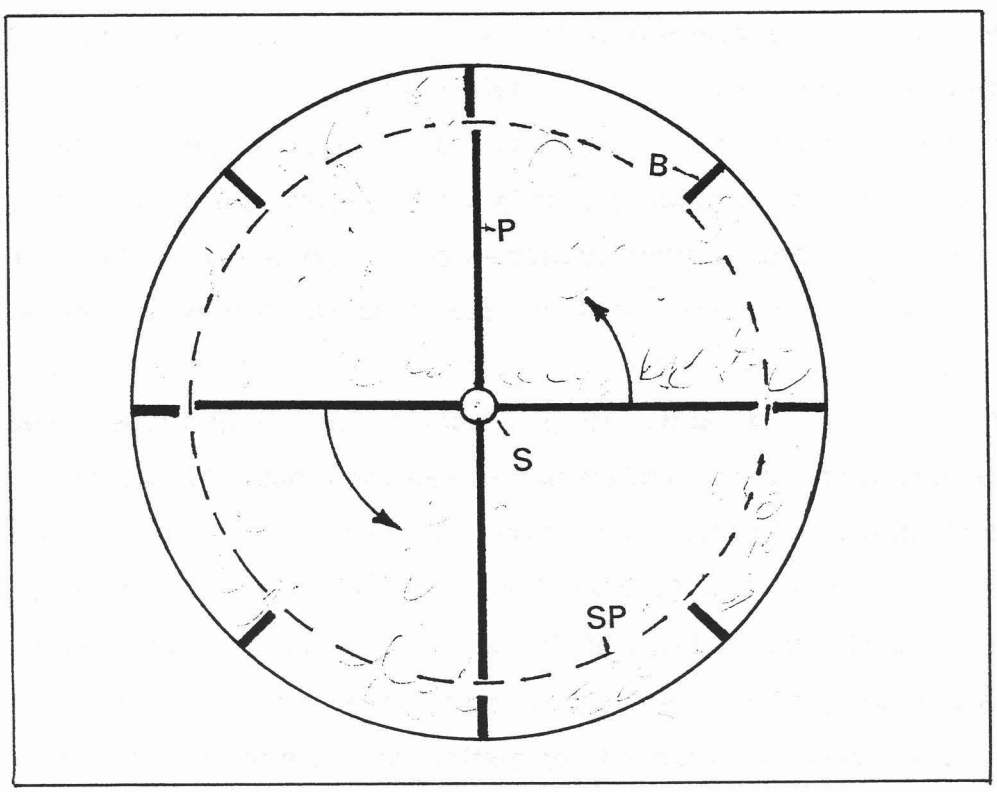

Figure 4.9 *Plan view of apparatus used for shear strength tests*

Method

The shear strength of bagasse samples of different mean fibre length, bulk density, coarse-fine ratio and moisture content was investigated. For each

sample the mass of bagasse and height of the surface in the apparatus was determined, from which an estimate of the bulk density could be made. The shear strength is the maximum stress applied as the bagasse fails in shear. Using the Status-74 (1989) software a simultaneous record of the speed and torque measurements was made. Shear stress was determined from the recorded torque divided by the surface area of the shear plane which, in this case, was assumed to be the cylindrical surface halfway between the baffle and the paddle edges, as described above. Further comment on this assumed shear surface will be made in the paragraph on results.

Speed readings were taken, not to determine the effect of speed on shear strength, but to indicate whether movement was taking place. A graph of a typical shear stress and speed record against time is shown in Figure 4.10. This graph shows that rotation of the paddle commenced at about 11 s. Initially the shear stress reading is negative, approximately -20 Nm^{-2}. The negative reading represents an offset which occurred because the loadcell used to measure torque was, of necessity, calibrated out of situ. Just before the speed recording shows an increase, the shear stress reading starts climbing rapidly. This climb represents the static increase in shear stress as the paddle takes up the slack at the commencement of rotation. The first peak (approximately 46 Nm^{-2}, at about 14.5 s) occurs as shear failure commences and it is this reading which is used to calculate the shear strength. The first trough of the shear stress trace (at 15 s) occurs as the paddle moves from one set of baffles to the next set, and then a peak occurs again when shear failure takes place once more, and so on. It can be seen that the heights of the peaks differ. This is most likely because of the anisotropy of the bagasse mass. At 23 s the speed was reduced to zero and the resultant reduction in shear stress is evident. The speed was then increased to a higher value than before giving the characteristic peaks and troughs which now occurred at greater frequency than before, as expected.

A set of readings with no bagasse in the apparatus was taken so as to

obtain a measure of the rotational frictional resistance of the apparatus. The corresponding graph for this is shown in Figure 4.11. Since there was no shear surface in this case, the shear stress could not be calculated. The maximum torque measured is approximately 2.5 Nm which, from other graphs, can be shown to be equivalent to a shear stress of approximately 10 Nm^{-2}. In other words, the frictional resistance of the apparatus causes an overcalculation of the shear stress by 10 Nm^{-2} which must therefore be subtracted.

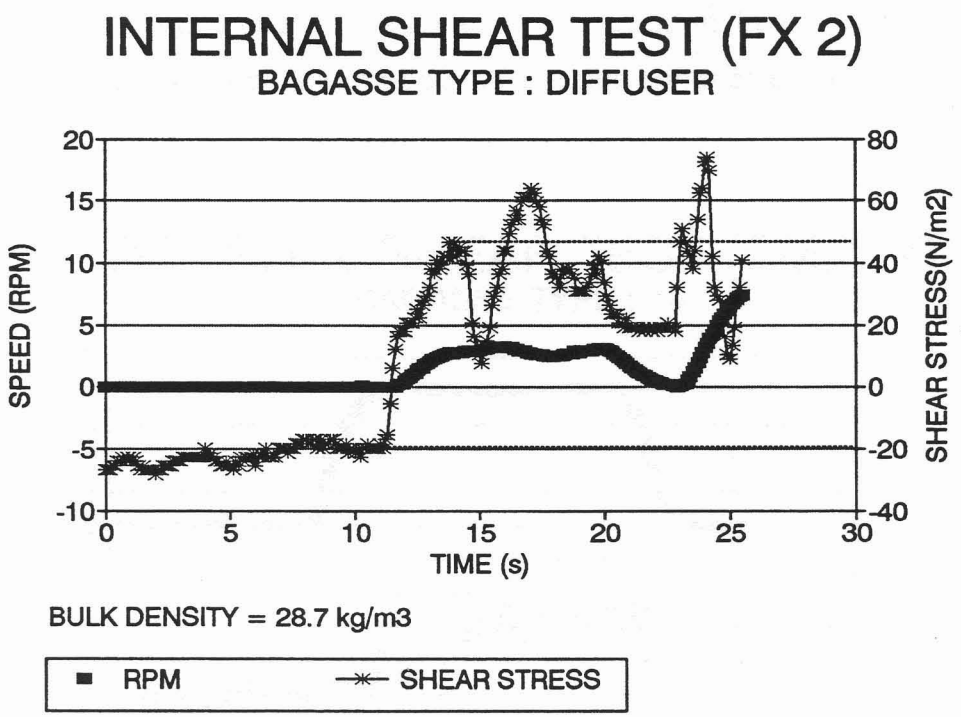

Figure 4.10 *Torque and speed measurements for a typical shear strength test*

The shear strength in a particular test was therefore obtained by subtracting the baseline reading from the reading corresponding to the first peak after commencement of rotation of the paddle (as indicated by the dotted lines in Figure 4.10) minus the shear stress equivalent to the apparatus' frictional resistance of 10 Nm^{-2}. For the example depicted it would equate to a shear strength of 56 Nm^{-2}.

On occasions the resistance of the bagasse was so high that the hydraulic motor stalled because it was not powerful enough to cause shear failure. In this case the shear stress measurement recorded a maximum but the speed sensor showed zero, as shown, for example, in Figure 4.12. This record indicates a few minor bumps on the speed trace as the hydraulic motor attempted to rotate the paddle but failed to move it sufficiently to cause the bagasse to shear. The shear stress trace does not show the typical oscillations occurring when the paddle rotates and causes bagasse shear failure every time the edge of a paddle plate moves past a baffle. Those tests in which the motor stalled were not included in the data analysis because bagasse failure did not occur and hence shear strength could not be determined.

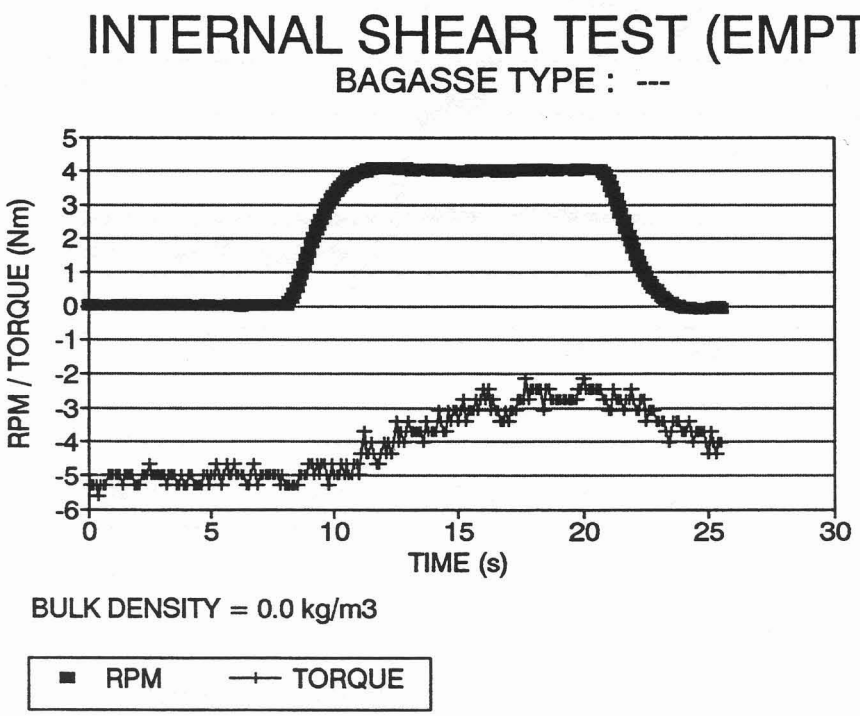

Figure 4.11 Graph used to estimate frictional resistance of apparatus

For each type of bagasse the shear strength of three different masses was measured. After the first measurement, a further amount of bagasse was added and a second set of measurements was taken. This was repeated

after an additional amount of bagasse had been added. It is likely that if shear has taken place at a particular surface, the particle alignment will have changed from the normal "pre-sheared" state and that a second attempt to shear this bagasse will tend to give a different, or artificial, shear strength. Whether this was the case or not will become evident from the results. Altogether 39 shear tests were recorded which formed the basis of the analysis which follows. The effect of storage on the shear strength of bagasse was not investigated.

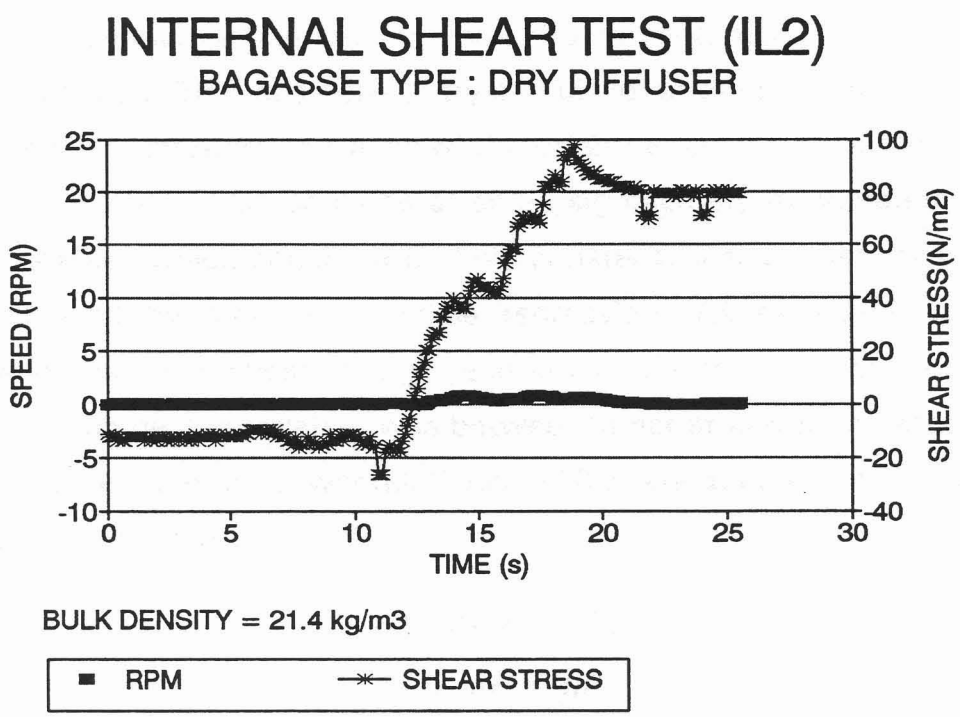

Figure 4.12 *Speed and torque recording for stalled motor*

Data analysis

For each shear test the shear strength was determined from the graph as outlined in the previous paragraph and then the adjusted shear strength was

calculated by subtracting the 10 Nm^{-2} for the frictional resistance of the apparatus. The other variables that were tabulated were bulk density, moisture content, mean fibre length, coarse-fine ratio and bagasse sample label, as shown in Table 4.8. Graphs of adjusted shear strength against the numerical variables are shown in Figure 4.13. Each of these graphs shows a considerable degree of scatter with no definite trend.

The statistical analysis involved the following. Initially linear regression was performed using the four mathematical expressions shown in equation 4.8 between adjusted shear strength as dependent variable and each of the independent variables bulk density, moisture content, mean fibre length and coarse-fine ratio. This was done to try and discover the form of relationship between shear strength and each of the other variables, while recognizing that such a relationship could be affected significantly by variation of the other variables which could not be held constant. Simple linear regression was followed by stepwise multiple regression. As expected, no high correlation between shear strength and any of the four variables could be obtained. The best correlation was between shear strength and mean fibre length according to the power relationship (ii) of equation 4.8 which yielded an adjusted r^2 value of 0.139.

$$y = ax + b \quad (i)$$

$$y = ax^b \quad (ii)$$

$$y = \exp(ax + b) \quad (iii)$$

$$1/y = ax + b \quad (iv) \qquad (4.8)$$

Results

Stepwise multilinear regression also showed that all four independent variables were statistically non-significant. Mean fibre length, however, gave an F-value of 3.39 indicating that a low correlation exists between it and

shear strength. Once fibre length had been forced into the multilinear model, the coarse-fine ratio now showed an F-value of 4.80 which is above the acceptance level. So coarse-fine ratio was also forced into the model and the result was that indicated in Table 4.9 for which an adjusted r^2 value of 0.1711 was obtained.

Table 4.8

Measurements of variables for shear strength tests

SUMMARY OF SHEAR STRENGTH DATA						
SHEAR STRENGT N/m2	ADJUST. SHR.STR N/m2	BULK DENSITY kg/m3	MOIST CONT %	FIBRE LENGTH mm	COARSE INDEX -	BAGASS SAMPLE -
48	38	50.3	54.00	8.73	0.50	MS1
85	75	50.6	54.00	8.73	0.50	MS1
81	71	52.1	54.00	8.73	0.50	MS1
85	75	41.3	42.00	7.56	0.32	MS2
117	107	35.2	44.50	13.06	0.63	PG1
58	48	37.4	44.50	13.06	0.63	PG1
65	55	42.1	44.50	13.06	0.63	PG1
51	41	29.2	32.50	17.01	0.91	PG2
70	60	33.0	32.50	17.01	0.91	PG2
94	84	37.4	32.50	17.01	0.91	PG2
63	53	28.7	53.50	20.36	1.49	FX1
86	76	25.7	53.50	20.36	1.49	FX1
91	81	31.4	53.50	20.36	1.49	FX1
86	76	22.4	42.00	22.95	1.88	FX2
82	72	25.1	42.00	22.95	1.88	FX2
83	73	25.6	42.00	22.95	1.88	FX2
106	96	20.2	10.50	17.28	1.08	IL1
91	81	22.4	10.50	17.28	1.08	IL1
75	65	11.2	11.00	27.93	5.63	MLF1
81	71	12.9	11.00	27.93	5.63	MLF1
85	75	12.8	11.00	27.93	5.63	MLF1
61	51	20.4	11.50	12.20	0.90	MLPITH1
77	67	22.1	11.50	12.20	0.90	MLPITH1
52	42	40.9	54.50	11.17	1.10	GH1
38	28	43.3	54.50	11.17	1.10	GH1
124	114	28.0	50.30	18.30	1.20	SZ7
113	103	31.0	50.30	18.30	1.20	SZ7
135	125	36.1	50.30	18.30	1.20	SZ7
140	130	28.2	48.30	21.33	1.57	SZ8
123	113	34.9	48.30	21.33	1.57	SZ8
49	39	19.6	30.50	12.27	1.26	MS3
83	73	24.2	30.50	12.27	1.26	MS3
96	86	26.2	30.50	12.27	1.26	MS3

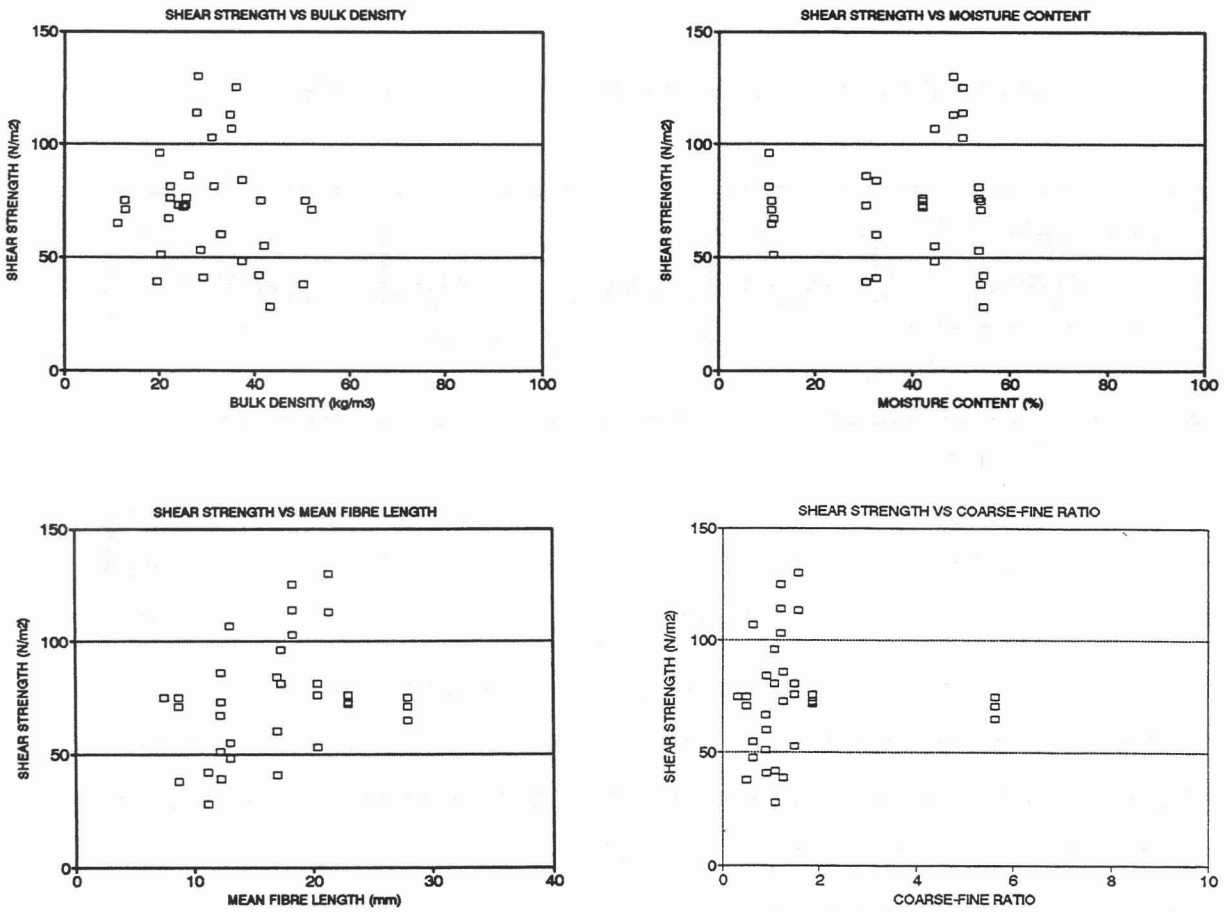

Figure 4.13 *Graphs of adjusted shear strength vs. bulk density, moisture content, mean fibre length and coarse-fine ratio*

$$\tau_s = 33.13 + 3.402L - 10.6c + \varepsilon \qquad (4.9)$$

The resulting empirical model is shown in equation 4.9 for which relevant statistical details are presented in Table 4.9. In equation 4.9 τ_s is the shear strength in Nm^{-2}, L the mean fibre length in mm and c the coarse-fine ratio which is dimensionless.

The predicted versus observed shear strength values from this relationship are shown in Figure 4.14. This graph illustrates the rather poor fit of the model to the data.

Table 4.9

Statistical data for bagasse shear strength model

Variable	Coefficient	Std. error	t-Value	95% Confidence Limits	
				Low	High
Constant	33.13	14.95	2.216	2.591	63.67
Fibre Length L	3.402	1.162	2.926	1.028	5.776
Coarse-fine c	-10.61	4.843	-2.191	-20.05	-0.716

The fact that there seemed to be no definite trend for any of the measured variables made the author suspect that, once a sample had been sheared, the alignment of the bagasse fibres at the rupture surface had changed the properties of bagasse significantly so as to affect the subsequent shearing behaviour. For this reason the statistical analysis was repeated on the datasets representing only the initial measurements, that is, on bagasse samples that had not been subjected to previous shearing. In this case there were only 13 sets of measurements. Although there was a slight improvement in the correlation between mean fibre length and shear strength, the improvement was too slight to be considered significant. No strong correlation between shear strength and the other variables - bulk density, moisture content and coarse-fine ratio - was found. For this reason the results of that analysis on the reduced dataset will not be presented.

Even when the effect of moisture on bulk density was discounted by calculating dry bulk density, no greater statistical significance was shown between shear strength and the independent variables.

Visual observation during the experiments reinforced the notion that bagasse does not shear in the sense in which bulk solids shear is normally understood. As the edge of the rotating paddle approached the baffle on the periphery of the apparatus the bagasse, instead of being sheared, compacted to an increasing extent. An attempt to illustrate this phenomenon diagrammatically is shown in Figure 4.15.

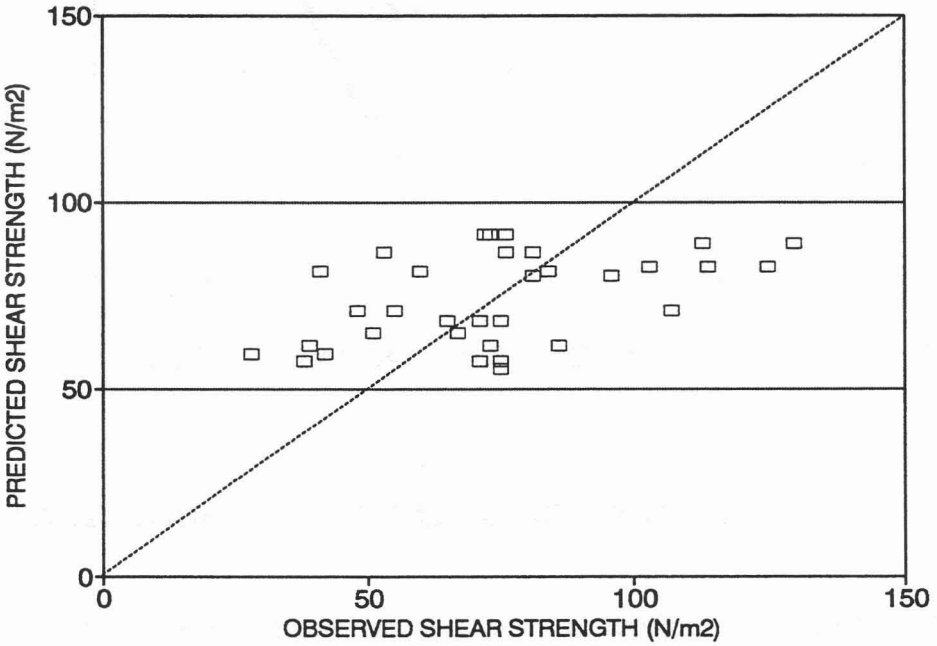

Figure 4.14 *Predicted vs. observed shear strength values*

At the obstruction the compacted bagasse seemed to mould itself into a dense ball which rolled under the influence of the moving paddle to find the path of least resistance. If the paddle motor did not stall then the compact ball rolled around the baffle, the larger volume of it trailing the paddle. Because no distinct shear surface could be seen, the calculation of shear strength, which is based on the cylindrical surface indicated by the dotted circle in Figure 4.9, is in doubt. This may be one of the main reasons why the data points plotted in Figure 4.13 show such a large scatter. It therefore seems, both from the statistical analysis as well as from the visual observation, that shear strength, as measured in the manner described above, is not a useful parameter in describing bagasse flow behaviour.

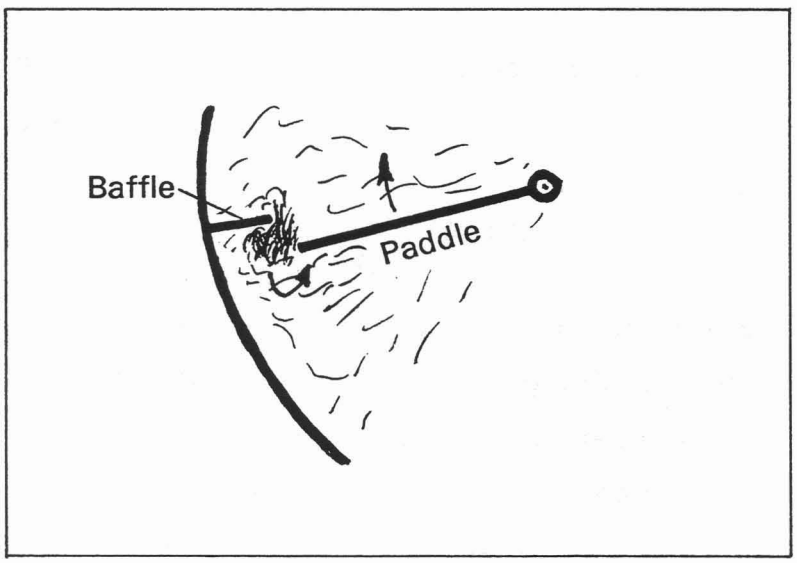

Figure 4.15 *Compaction response of bagasse during shearing tests*

4.5 TRANSLATION OF VERTICAL TO HORIZONTAL PRESSURE

In order to make predictions on the flow behaviour of a bulk solid it is necessary to have a quantitative measure of the internal friction of the solid. In the previous section it was argued that the conventional equipment used to measure this was unsuitable for bagasse. Furthermore, from the shear strength experiments reported in that section, it became clear that the direct measurement of internal friction of bagasse is very difficult. For that reason it was considered necessary to resort to an indirect technique.

The internal friction properties of a bulk solid influence the degree to which vertical pressure is translated into horizontal pressure. In a fluid the pressure at a point is the same in all directions, but for a particulate solid it is the interparticle friction, the adhesion forces as well as the interlocking properties of the particles that result in a reduced horizontal pressure compared with the local corresponding vertical pressure. In the current context the terms vertical normal stress (σ_v) and horizontal normal stress (σ_h)

are used interchangeably with vertical and horizontal pressure respectively.

Janssen (1895) assumed that for a particular bulk solid the ratio K of horizontal to vertical stress

$$K = \frac{\sigma_h}{\sigma_v} \qquad (4.10)$$

was constant. Subsequent workers (for example Jenike (1960), Walker (1966), Walters (1972), Molerus (1975) and Blight (1988)) recognised that for any bulk solid the value of this ratio was significantly affected by the state and degree of compaction. This phenomenon had been mentioned in chapter two. The aim of this section is to present the results of measurements of vertical and corresponding horizontal pressures on a variety of bagasse samples to provide an indirect quantitative representation of internal friction characteristics. An attempt will be made to express K in equation 4.10 as an empirical function of bulk density, moisture content, mean fibre length and coarse-fine ratio, plus any other variable determined during the investigation that appears to be significant.

Apparatus

The measurements that had to be taken were weight of bagasse, from which vertical stress was derived, and horizontal pressure. In addition, for bulk density determination the volume of bagasse was determined from the dimensions of the apparatus and the level of the bagasse in that apparatus. A diagrammatic representation of the apparatus used is shown in Figure 4.16.

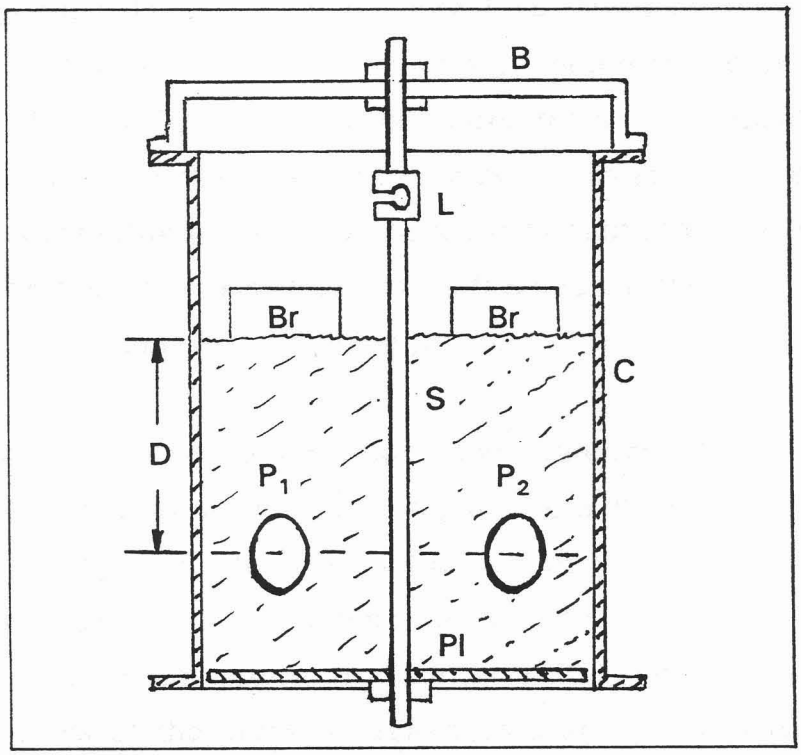

Figure 4.16 *Apparatus used to measure translation of vertical to horizontal pressure*

In this figure C is the cylindrical stainless steel shell (0.7 m in diameter and 1.5 m in height) that had also been used for the first series of surface friction tests, as well as the internal shear tests. It was bolted to a framework approximately 1.8 m from ground level to facilitate emptying it of bagasse after each set of measurements. Pl was a flat circular platform attached in a horizontal position to a shaft S. It was mounted 2.0 cm above the bottom flange of C and there was a 10 mm clearance between its periphery and the inner surface of C. Its function was to hold up bagasse in C so that horizontal pressure measurements could be taken. The shaft which was made from a 10 mm mild steel round bar was suspended along the axis of C from a bracket B that was fixed to the top flange of C. Provision was made to detach the shaft S from the bracket B so that the platform Pl supporting the bagasse could be lowered out of the shell C during emptying.

Lowering of the platform laden with bagasse was done by means of a ratchet pulley which is not shown in Figure 4.16. The shaft S was attached to a load cell L the function of which was to record the total downward force on the platform Pl. This was used to determine the vertical stress σ_v. The total downward force measured by L was the resultant of the weight of the bagasse, the platform and the vertical component of the wall friction of the bagasse on the side walls of C. The shaft S and platform Pl were coated with corrosion-resistant PA10 etching primer.

P_1 and P_2 were two pressure transducers that were mounted to the wall of C so that the pressure sensing diaphragms were flush with the internal surface of C. Altogether three pressure transducers fitted at 120° to each other around the periphery of C at the same horizontal level were used, their centres being 29.5 cm above the platform Pl. The construction and calibration details of the pressure transducers are given in Appendix D. Ideally the cylindrical shell which contained the bagasse during measurements should have been equipped with a large number of pressure transducers situated at different horizontal levels of the apparatus. For cost reasons, and because of the limitations of the datalogging system, only three pressure transducers were used. The reasons why these three transducers were all mounted at the same horizontal level, instead of three different levels, were to obtain an indication of the variability of the pressure readings at a given level, and to try to obtain an internal check on the validity of the readings. The pressure readings were in most cases extremely low, and the operation of a transducer could easily be affected by bagasse fibres wedged between the transducer housing and the sensing diaphragm, hence such a check was considered advisable.

Method

From each sample of bagasse used in these tests sub-samples were taken

for mean fibre length, coarse-fine ratio and moisture content determination. The test procedure consisted of loading a weighed amount of bagasse onto the platform Pl suspended within the apparatus shown in Figure 4.16. A reading of the bagasse level was taken. From the mass and the level reading the bulk density could be determined. The load cell and pressure transducer readings were logged electronically by the Status74 (1989) system. An additional weighed amount of bagasse was added to that already in the apparatus, and the same set of readings was recorded. To increase the vertical pressure without adding more bagasse a number of weighed bricks (Br) were added, taking care to distribute them evenly on the surface, and a new set of readings was taken. This process was repeated by adding a second set of bricks. Thus for one sample of bagasse four sets of readings were obtained. Eleven different bagasse samples were used for these tests yielding a total of 44 datasets.

Data analysis

The apparatus depicted in Figure 4.16 was used to obtain corresponding sets of readings of lateral normal stress σ_h and vertical normal stress σ_v from which the ratio K (equation 4.10) was determined. The measurements of the three pressure transducers P_1, P_2 and P_3 were used to obtain values for σ_h. For the determination of σ_v the weight of bagasse ***above the level of the pressure transducers*** and that of the bricks Br which provided additional downward force, divided by the cross-sectional area of the cylindrical shell C were used. This calculation assumes a uniform density of bagasse with depth, that the upward (or downward) force on the bagasse due to wall friction is negligible and that the tensile force exerted by bagasse below the level of the pressure transducers on the bagasse above that level is insignificant. The next section provides information on the tensile strength of bagasse. It will show that this has a small effect on the vertical stress determined as outlined. In view of the scatter of the pressure readings

obtained, as well as the relatively small depths of bagasse used, the above assumptions seemed justifiable. For each pressure transducer reading a corresponding value K, viz. K_1, K_2 and K_3, being the ratio of σ_h/σ_v, was calculated. The load cell readings did not provide useful information, largely because of the interference of the wall friction, which was affected in a complex fashion by the uneven loading of the bricks. So the load cell readings have not been used in any calculations. Wall friction is assumed to affect the stress distribution in the vicinity of the wall only. For this reason the vertical stress calculation did not take wall friction into account.

The vertical stress was calculated from the weight of bagasse above the level of the pressure transducers as well as the additional load applied to the bagasse surface. In calculating the weight of bagasse above the pressure transducers the total bagasse weight was divided according to the proportion of the total depth taken up by the bagasse above the transducers. The full dataset is listed in Table 4.10.

From each set of values of K_1, K_2 and K_3 an average K value was calculated. Table 4.10 indicates that, at times, not all three values were used for the determination of that average. The reasons for this are that during some tests one or two of the pressure transducers were not operational. In some cases the cause could be identified, such as, for example, a twisted, or disconnected, tube from the sensor to the differential pressure cell. In other instances the reason may have been bagasse fibres getting stuck in the crevices between the transducer housing and the pressure sensing diaphragm. It should also be remembered that the actual pressures measured were extremely low, of the order of 50 - 800 Pa, which requires a very sensitive instrument for accurate determination. The following code was employed in Table 4.10 to indicate how many of the three readings were used to calculate the average K value.

A <u>all</u> three values used

O only <u>one</u> value used

T <u>two</u> values used

N average obtained was <u>not</u> used for the statistical analysis.

The decisions for accepting all three, two or one of the K_i values for determining the average value of K were based on the pressure readings P_1, P_2 and P_3 which represented the σ_h values. Pressure values close to zero, or readings that remained constant for different vertical stress conditions were a sure indication that the respective pressure transducer was faulty. Where one of the three K_i values was significantly different from the other two, this reading was omitted for the determination of the average, K, unless there was strong evidence that both pressure readings for the two agreeing K values were likely to be erroneous. The latter decision was made on the basis of the trends of the respective pressure readings. All of the datasets that were excluded from the statistical analysis (marked N) were cases where the level of bagasse was only a short distance above that of the pressure transducers and hence the pressure readings were unreliable, partly as a result of instrument offset. The vertical stress σ_v calulations relied on weights that had been determined using standard weighing equipment, and were likely to be reasonably accurate.

The statistical analysis on the datasets which remained (39 altogether) after discarding those marked "N" was done in a similar fashion to that for the previous variable viz. shear strength of bagasse. The ratio K of horizontal stress σ_h to vertical stress σ_v was the dependent variable. The independent variables investigated were bed depth (above the level of the pressure transducers), vertical stress and, as before, mean fibre length, coarse-fine ratio, bulk density and moisture content. A plot of K against each of the independent variables is shown in separate graphs in Figure 4.17.

Table 4.10

Datasets for the relationship of lateral vs. vertical pressure

P1 Pa	P2 Pa	P3 Pa	DEPTH m	V.STRESS Pa	K1 -	K2 -	K3 -	K -	*	DENS. kg/m3	LENGTH mm	COARSE -	MOIST. %
97.6	72.7	86.5	0.075	27.6	3.53	2.63	3.13	3.10	N	45.9	27.93	5.63	11.0
121.4	141.2	130.5	0.385	179.8	0.68	0.79	0.73	0.73	A	50.4	27.93	5.63	11.0
191.3	244.3	177.4	0.285	778.1	0.25	0.31	0.23	0.26	A	59.5	27.93	5.63	11.0
739.9	350.0	472.4	0.225	1372.2	0.54	0.26	0.34	0.30	T	66.8	27.93	5.63	11.0
139.3	130.6	80.9	0.235	223.9	0.62	0.58	0.36	0.52	T	105.5	18.34	1.60	53.6
150.7	161.7	121.7	0.575	584.5	0.26	0.28	0.21	0.25	A	108.0	18.34	1.60	53.6
158.4	164.6	331.0	0.455	1158.1	0.14	0.14	0.29	0.29	O	126.0	18.34	1.60	53.6
438.5	433.8	511.6	0.385	1734.7	0.25	0.25	0.29	0.27	A	139.5	18.34	1.60	53.6
37.3	-5.8	56.0	0.085	55.8	0.67	-0.10	1.00	0.52	N	80.2	23.36	2.48	50.0
51.4	-2.7	71.5	0.405	307.9	0.17	-0.01	0.23	0.20	T	81.8	23.36	2.48	50.0
253.0	398.4	307.0	0.285	882.6	0.29	0.45	0.35	0.40	T	99.7	23.36	2.48	50.0
261.6	737.3	318.9	0.225	1463.6	0.18	0.50	0.22	0.20	T	111.9	23.36	2.48	50.0
107.9	79.4	88.1	0.185	109.1	0.99	0.73	0.81	0.77	T	66.4	17.28	1.08	10.5
107.9	96.4	82.7	0.455	328.0	0.33	0.29	0.25	0.29	A	77.2	17.28	1.08	10.5
218.0	215.3	350.3	0.405	935.4	0.23	0.23	0.37	0.28	A	83.0	17.28	1.08	10.5
375.6	427.1	689.8	0.335	1522.8	0.25	0.28	0.45	0.26	T	92.7	17.28	1.08	10.5
96.9	71.5	88.6	0.015	3.9	24.79	18.29	22.67	21.92	N	85.4	12.20	0.90	11.5
132.0	93.8	87.5	0.205	150.1	0.88	0.62	0.58	0.60	T	81.8	12.20	0.90	11.5
286.0	121.1	106.7	0.105	715.0	0.40	0.17	0.15	0.40	O	103.9	12.20	0.90	11.5
449.9	475.9	308.4	0.095	1321.2	0.34	0.36	0.23	0.31	A	106.8	12.20	0.90	11.5
98.4	73.7	81.7	-0.285	-	-	-	-	-		-	-	-	-
101.7	72.7	88.1	0.045	51.4	1.98	1.42	1.72	1.70	N	159.3	10.10	0.79	58.9
252.4	77.5	106.2	0.325	519.9	0.49	0.15	0.20	0.49	O	174.0	10.10	0.79	58.9
462.3	86.1	237.2	0.315	1135.0	0.41	0.08	0.21	0.41	O	177.0	10.10	0.79	58.9
550.1	137.1	331.6	0.275	1713.3	0.32	0.08	0.19	0.26	T	190.1	10.10	0.79	58.9
42.2	-3.6	43.0	0.055	56.7	0.74	-0.06	0.76	0.75	T	136.4	10.46	0.77	47.3
144.3	5.5	44.8	0.385	502.2	0.29	0.01	0.09	0.29	O	140.7	10.46	0.77	47.3
253.3	58.5	306.1	0.335	1093.5	0.23	0.05	0.28	0.26	T	152.4	10.46	0.77	47.3
460.7	381.5	498.9	0.315	1692.9	0.27	0.23	0.29	0.26	A	157.7	10.46	0.77	47.3
139.0	72.5	115.3	0.315	452.2	0.31	0.16	0.25	0.28	T	156.4	15.38	0.98	53.7
372.3	82.3	129.7	0.625	954.4	0.39	0.09	0.14	0.39	O	161.7	15.38	0.98	53.7
605.3	121.5	144.6	0.585	1556.5	0.39	0.08	0.09	0.39	O	169.4	15.38	0.98	53.7
789.3	135.6	274.5	0.505	2121.7	0.37	0.06	0.13	0.37	O	187.0	15.38	0.98	53.7
30.9	-4.5	37.5	0.085	74.4	0.42	-0.06	0.50	0.46	T	106.9	17.30	1.01	48.5
75.8	32.3	42.7	0.385	442.3	0.17	0.07	0.10	0.17	O	123.9	17.30	1.01	48.5
219.4	185.8	97.8	0.285	1004.4	0.22	0.18	0.10	0.20	T	146.5	17.30	1.01	48.5
564.6	408.4	117.6	0.245	1587.2	0.36	0.26	0.07	0.31	T	157.9	17.30	1.01	48.5
27.9	-1.7	40.5	0.065	74.5	0.37	-0.02	0.54	0.46	T	146.5	4.24	0.02	49.8
107.6	47.3	43.3	0.325	447.6	0.24	0.11	0.10	0.24	O	149.7	4.24	0.02	49.8
241.1	129.4	155.1	0.245	1007.4	0.24	0.13	0.15	0.17	A	173.2	4.24	0.02	49.8
345.6	247.3	273.1	0.215	1592.2	0.22	0.16	0.17	0.18	A	184.1	4.24	0.02	49.8
28.5	-0.8	35.7	0.005	-5.9	-4.80	0.13	-6.02	-3.56	N	129.9	4.61	0.04	42.0
61.2	38.2	43.0	0.275	305.2	0.20	0.13	0.14	0.16	A	121.7	4.61	0.04	42.0
195.0	308.8	187.0	0.205	879.8	0.22	0.35	0.21	0.26	A	139.9	4.61	0.04	42.0
436.0	755.8	493.2	0.155	1449.3	0.30	0.52	0.34	0.32	T	156.5	4.61	0.04	42.0

* A : ALL THREE VALUES USED TO DETERMINE AVERAGE K VALUE
N : NOT USED FOR STATISTICAL ANALYSIS
T : K VALUE BASED ON AVERAGE OF CLOSEST TWO VALUES
O : K VALUE TAKEN AS THE MOST PLAUSIBLE ONE READING

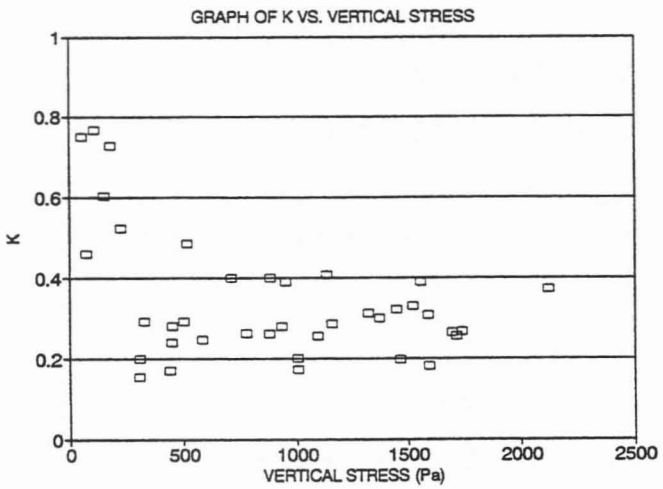

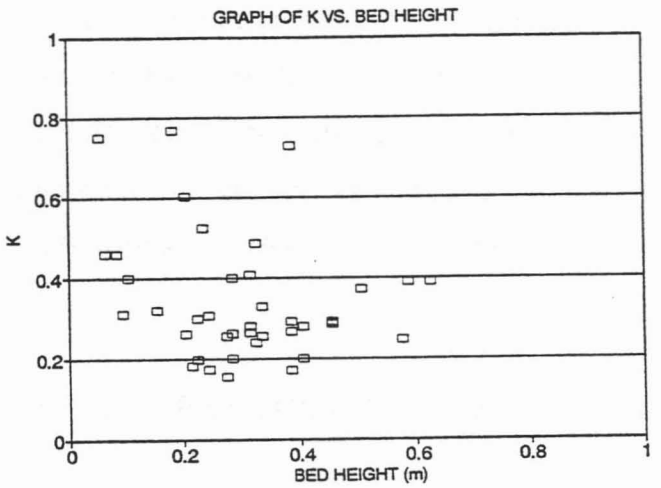

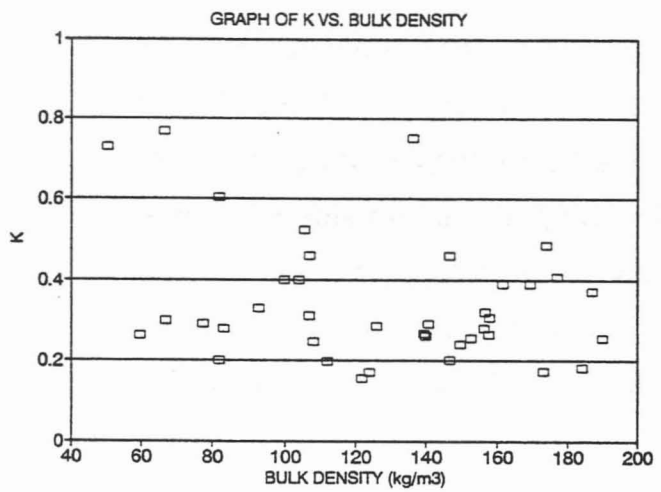

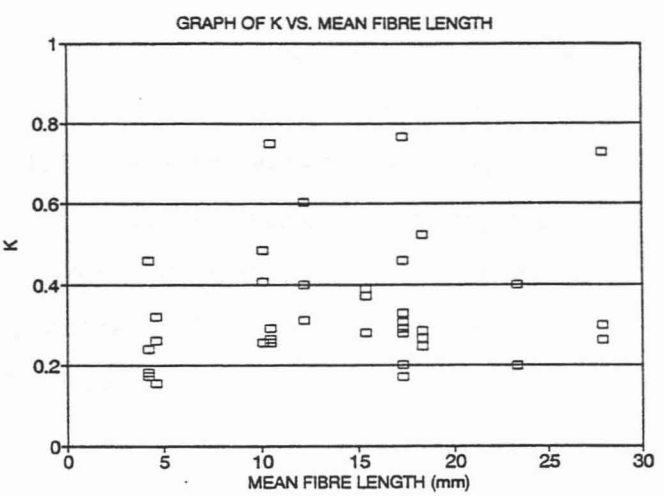

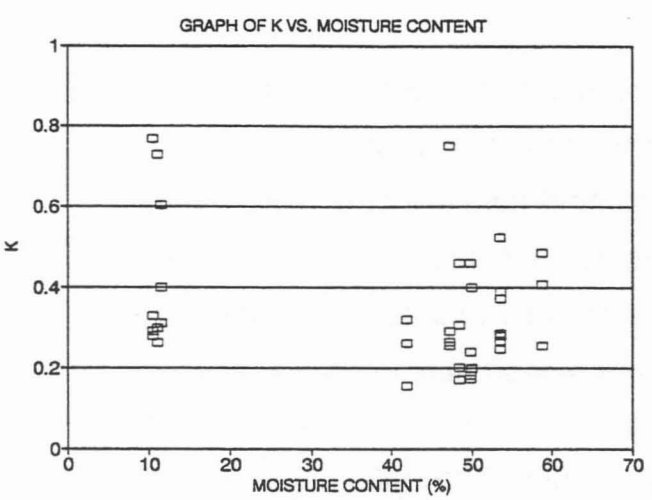

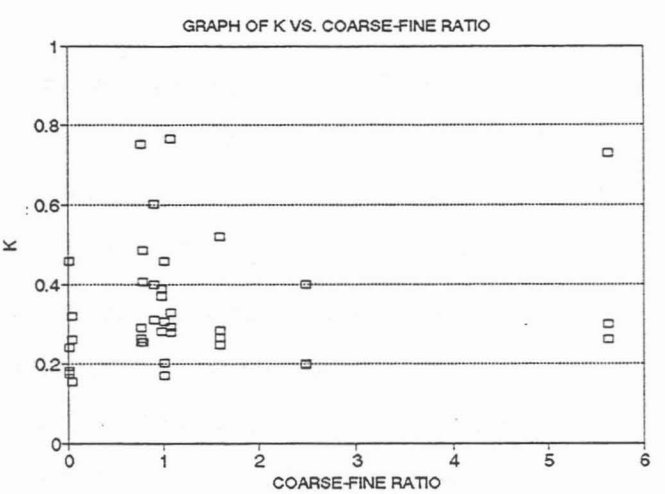

Figure 4.17 *Graphs of K vs. each of the respective independent variables*

A considerable degree of scatter of the datapoints is evident for all the variables, the scatter probably aggravated by the fact that the other variables not being plotted were not held constant. The only graph showing some discernible trend was the one between K and vertical stress, the trend being that of an exponential decay with an approximate asymptotic value of 0.2.

With the help of the programme "Precision curve fitter (1994)" the following relationship was fitted

$$K = 0.2 + a \exp(-b\sigma_v) \qquad (4.11)$$

and the parameters calculated by the programme were a = 0.459 and b = 0.00236. Since simple regression did not produce any significant relationships for any of the other variables an attempt was made to establish a multivariable model using stepwise multilinear regression which used the exponential transformation of vertical stress suggested by equation 4.11 instead of the unmodified values. An acceptance F limit of 4.0 for inclusion of a variable in a model was applied initially.

Results

The exponential transformation of vertical stress (exp (-0.00236σ_v)) proved to be an obvious significant variable with an F entry value of 25.7. The variable showing the next highest F value (2.93) was moisture content W. Since this was below the acceptance value of 4.0, moisture content had to be artificially entered into the model. A similar procedure led to the inclusion of density ρ and mean fibre length L. The form of the empirical multivariate model (equation 4.12) that was finally selected with the help of Statgraphics 5.0 (1991) had an adjusted r^2 value of 0.535. The statistical parameters in Table 4.11 indicate that all the variables included do have a significant effect on the ratio K. Bed height h and coarse-fine ratio c proved

to be non-significant. A plot of observed versus predicted K values is shown in Figure 4.18.

$$K = \beta_0 + \beta_1 \exp(-0.00236\sigma_v) + \beta_2 \rho + \beta_3 L + \beta_4 W + \varepsilon \qquad (4.12)$$

Table 4.11

Statistical data on empirical model for ratio of lateral pressure to vertical pressure

Variable	Coefficient	Std. error	t-Value	95% Confidence Limits	
				Low	High
Constant	-0.2582	0.176	-1.468	-0.616	0.099
$e^{-0.00236\sigma v}$	0.534	0.084	6.339	0.363	0.705
Density ρ	0.0041	0.001	3.311	0.002	0.007
Fibre Length L	0.01345	0.004	3.111	0.005	0.022
Moisture W	-0.0063	0.002	-3.435	-0.010	-0.003

It may be argued that vertical stress and bulk density are linked variables and should therefore be represented by a single variable. However, the relationship between these is not a simple direct one, and furthermore each of these variables is shown separately to be significant in Table 4.11 by their respective t-values. It is therefore considered appropriate that they appear as separate variables in the model. It is also clear that moisture content affects bulk density. In order to separate the effect of moisture content from bulk density the statistical analysis was repeated using dry bulk density instead of bulk density as measured (i.e. with included moisture). This

analysis did not, however, provide a better fit (the adjusted r^2 value was 0.485, which is inferior to 0.535 obtained with measured bulk density).

From Figure 4.18 it appears that the model given in equation 4.12 and Table 4.11 represents an acceptable description of the relation between horizontal and vertical pressures in bagasse. The model indicates that this relation depends significantly on the vertical stress operating at the level of interest, that lateral pressure tends to increase with increased bulk density and mean fibre length and decrease with increased moisture content. From the above it appears that the measurement of lateral pressure as a function of vertical pressure is a valid technique for determining indirectly the internal friction characteristics of bagasse.

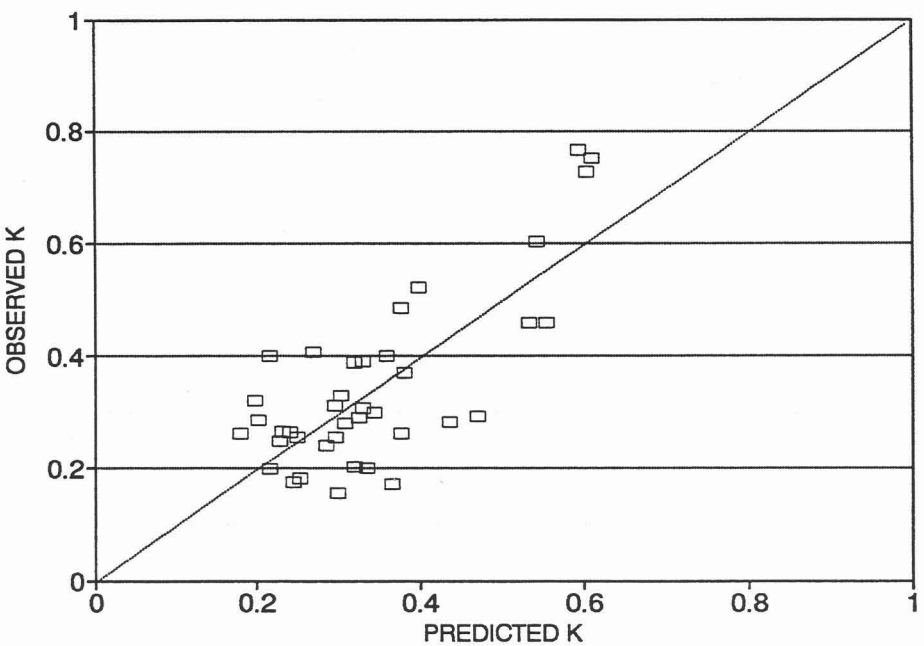

Figure 4.18 *Observed vs. predicted K values*

4.6 TENSILE STRENGTH

In traditional theory of the flow behaviour of bulk solids tensile strength does

not play a prominent role. Walker (1966) specifically states that his analysis only considers compacting stresses because "the tensile strength of the powders concerned is very small". Some authors have, however, emphasised that the tensile strength exhibited by a particulate material does play a part in attempts to predict its flow properties.

The tensile strength σ_T of a material can be determined from the yield locus, as indicated in Figure 4.19, by the intercept of the locus on the σ axis. On the same diagram the cohesion C is indicated as the shear stress τ at zero normal stress σ.

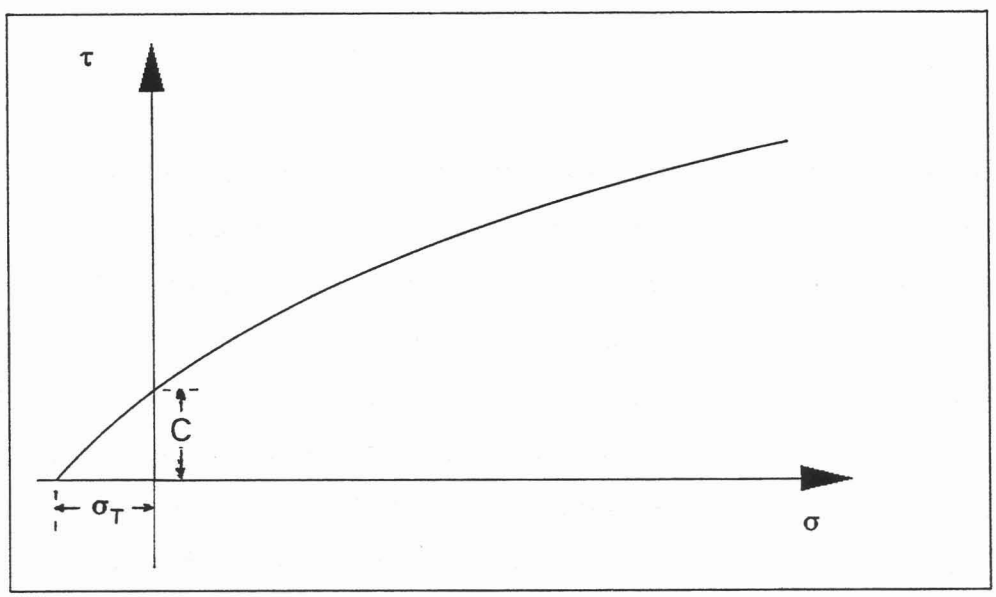

Figure 4.19 *Generalised yield locus of a bulk solid*

Williams and Birks (1967) discuss the consequences of the fact that industrial powders may have appreciable tensile strength. They advocate the inclusion of tensile strength in the determination of the internal friction characteristics of a powder. Farley and Valentin (1968) present a correlation (equation 4.13) for tensile strength σ_T in terms of the bulk density ρ and the particle density ρ_p of the material

$$\sigma_T = A\left(\frac{\rho}{\rho_p}\right)^m \qquad (4.13)$$

in which A and m are different constants for different powders. They furthermore propose the following mathematical model (equation 4.14) for the yield locus where n is called the shear index. Molerus (1985) highlights the importance of adhesion forces between small particles (100 μm or less) which are considered to be van der Waals forces. For powders which consist predominantly of such small particles the tensile strength is the result of these adhesion forces.

$$\left(\frac{\tau}{C}\right)^n = \frac{\sigma}{\sigma_T} + 1 \qquad (4.14)$$

It is not possible to construct a yield locus for bagasse for, as was shown in the section on shear strength (section 4.4), shear failure cannot be measured. The mechanism contributing to tensile strength proposed by Molerus (1985) does not operate in bagasse since most of the particles are much larger than those for which adhesion forces are significant. The tensile strength for bagasse is undoubtedly a structural phenomenon caused by the interlocking tendency of the fibres. For this reason it is expected that tensile strength plays a far more dominant role in the flow behaviour of bagasse than in granular bulk solids.

Apparatus

The basic principle on which the design of the tensile strength apparatus was based is shown in Figure 4.20. The concept is borrowed from mechanical engineering tensile strength testing equipment which clamps a rod of material of standard diameter at its two ends and measures the tensile force required to cause the rod to fail in tension. The tensile strength is

determined from the maximum tensile force applied divided by the cross-sectional area.

The apparatus that was used to measure the tensile strength of a "bar" of bagasse is shown in Figure 4.21 and a photograph of it is shown in Figure 4.22. It consisted of two identical trolleys with rectangular cross-section 50 cm long, 20 cm wide and 26 cm high. The bottom of each trolley was made of a section of U-beam, for rigidity, with the legs of the U turned downwards and the "back" of the U serving as floor on which the bagasse rested. The side plates consisted of 2 mm thick mild steel plate fixed securely to each side of the U-beam. For each trolley the two side plates were secured at the top by two strips of flat mild steel plate 20 mm wide and 3 mm thick so that the rectangular compartments were totally rigid. One end of each trolley was closed off with 2 mm mild steel plate while the other end remained open. During a tensile test the two open ends were placed adjacent to each other and this is where tensile failure of the bar of bagasse contained within the two trolleys occurred. The top of each trolley was open so that the trolleys could be filled with bagasse.

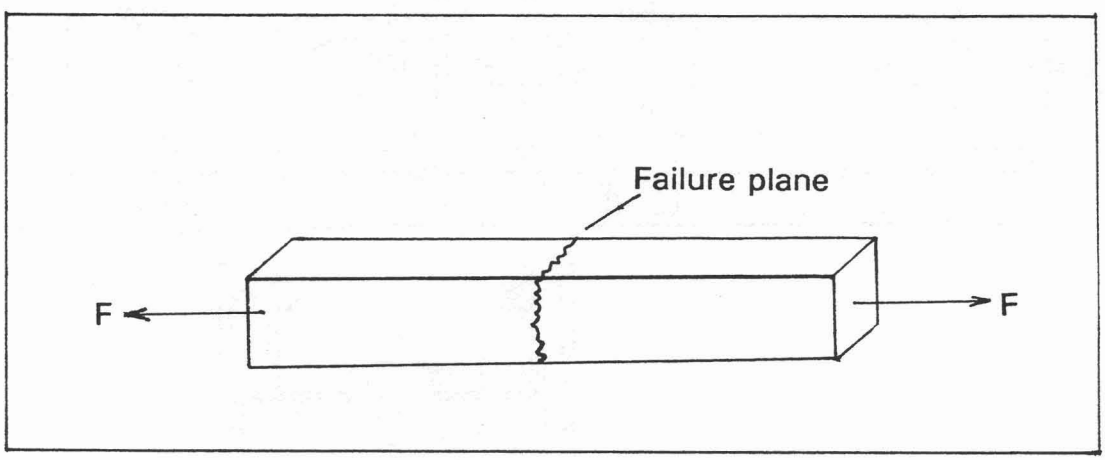

Figure 4.20 *Tensile failure of a "bar" of bagasse*

Once the trolleys had been filled with bagasse a top plate T was placed on

top of the bagasse in each trolley. The plates, the dimensions of which were slightly smaller than the internal perimeter of each trolley, could be pressed down on the bagasse to produce any desired degree of compaction of the bagasse within the apparatus. The plates were reinforced round the periphery to resist distortion. Each plate was equipped with four threaded rods R welded to vertical bars which straddled the sides of the trolleys. The threaded rods passed through holes in brackets B welded on the outside of the side walls to hold the top plates in position with the help of crocodile clips. Both trolleys were coated with PA10 anti-corrosion etching primer. Measuring scales S were fixed on the outside of each side wall by which the level of the top plates could be ascertained. These scales assisted in achieving more or less uniform packing density, and were used to take level readings from which the bulk density of the bagasse in the apparatus could be determined.

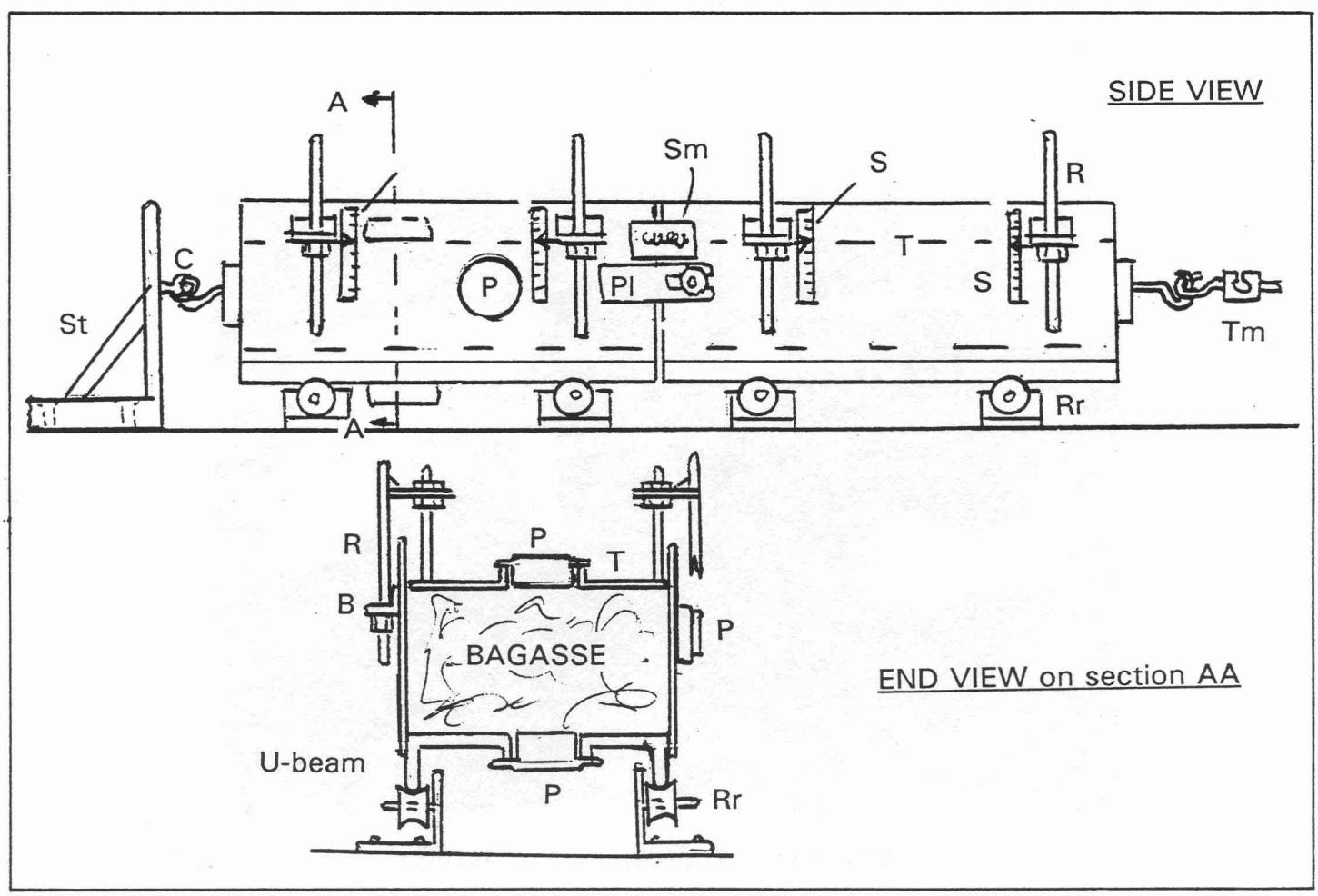

Figure 4.21 *Apparatus used to measure tensile strength of bagasse*

Three pressure transducers P (shown in end-view of Figure 4.21) were fitted to the apparatus - one on the floor, one on a side wall and one on a top plate to take readings of compacting stress, but it was subsequently found that these readings were of no benefit because of the interference of surface friction, and because of the different readings obtained for bottom, side and top pressures.

Both trolleys could run on sets of rollers Rr fitted on two parallel, horizontal rails. The lips of the U-beam sections by which the trolleys moved on the rollers had been machined smooth so that the movement would occur with the minimum of friction. To one end of the rails was fixed a vertical stay St to which one trolley could be coupled by means of a chain link C and hook. At the other end of the rails a pulley which operated through a worm gear (visible in Figure 4.22) was fitted to facilitate slow, controlled pulling of the second trolley away from the stationary one anchored to the vertical stay.

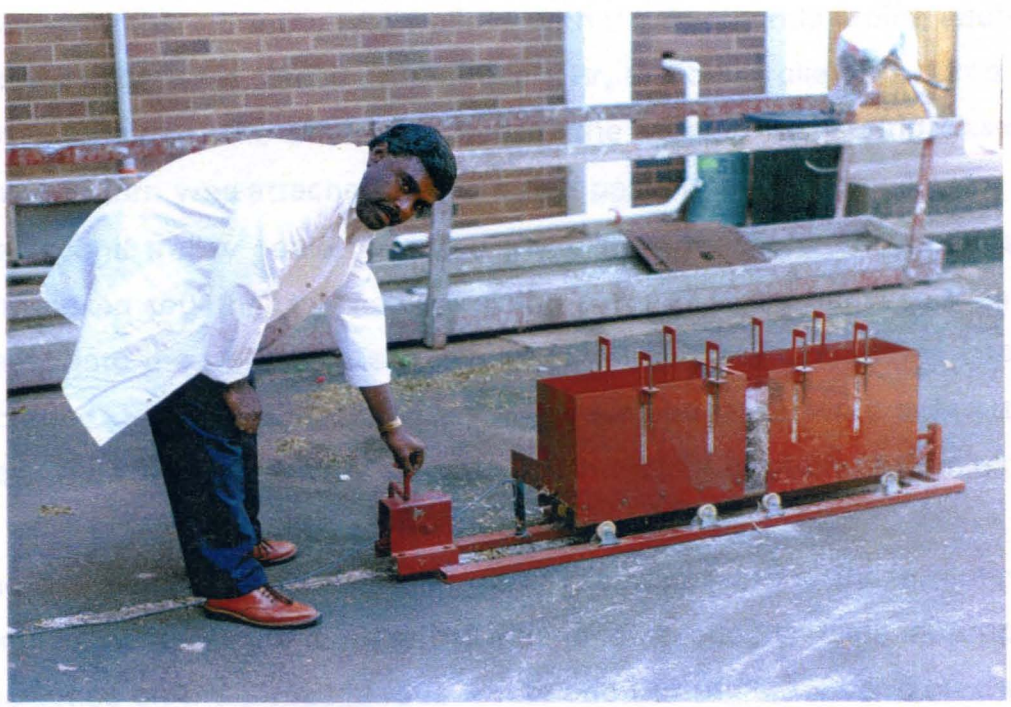

Figure 4.22 *Photograph of tensile strength apparatus*

A tension measuring device Tm (the same one that had been used for surface friction measurements described in section 4.2, the technical details of which are given in Appendix B) was fixed between the end of the second trolley and the non-elastic string attached to the pulley by which the second trolley was slowly pulled away from the first. It was judged that the surface friction between the bagasse and the internal walls of the two trolleys would be sufficient to hold the bagasse within them while rupture of the bagasse occurred at the gap between the two trolleys. This assumption proved correct. The second trolley was also equipped with a strain measuring device Sm to indicate the distance moved away from the first. While the two trolleys were being filled with bagasse a small metal plate Pl fastened to both trolleys at the middle held them together so that no pulling force was exerted on the "bar" of bagasse prior to a tensile strength test. This plate was removed just before the commencement of a test.

Method

In essence therefore the two trolleys with the open ends facing each other in the middle were placed on the rollers Rr, the one trolley anchored to the vertical stay St, the other attached to the tension measuring device Tm which in turn was attached to the string passing over the pulley by which the second trolley could be pulled away from the first. The trolleys were both linked together by the restraining plate Pl while bagasse was being loaded into the trolleys to an even height. The mass of bagasse used was recorded. Sub-samples of the same type of bagasse were submitted for mean fibre length, coarse-fine ratio and moisture content determination.

The top plates T were then placed on the bagasse and these plates were secured at a constant level by means of crocodile clips appropriately positioned on the threaded rods R in relation to the brackets B on the sides of the trolleys. The level of the plates was read from the measuring scales

S. The bulk density of the bagasse was determined from the level and the mass. Just before the commencement of a tensile strength test the restraining plate PI holding the two trolleys together was removed.

The electronic data acquisition procedure (using the Status-74 system, 1989), which took readings of tensile force and strain at a frequency of 10 Hz, was activated. The handle of the pulley at the far end of the track on which the second trolley moved was turned at constant speed, gradually pulling the second trolley away from the first which was anchored in position to the vertical stay by the chain link C and hook. A typical set of graphs obtained during a tensile strength test is shown in Figure 4.23.

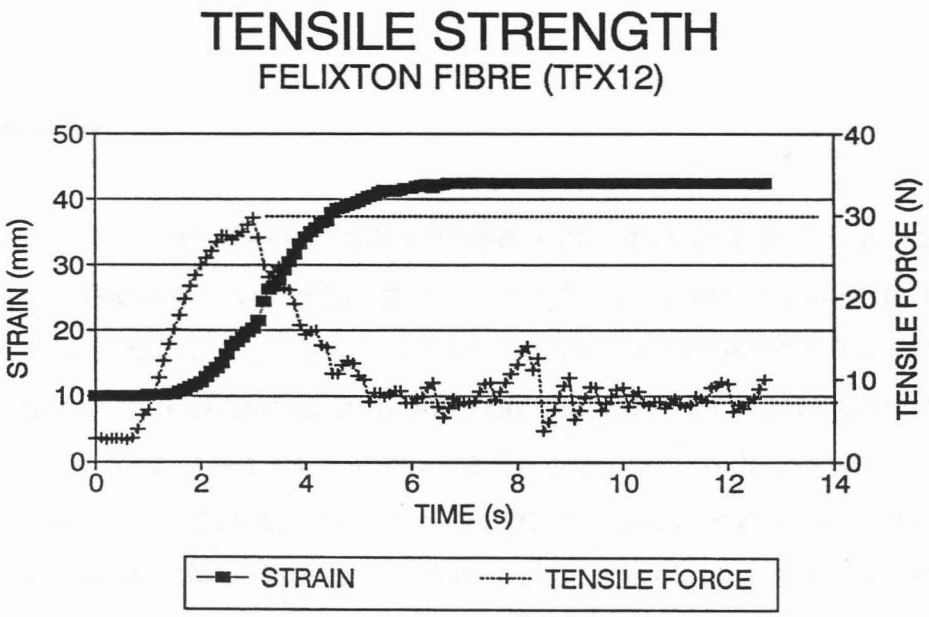

Figure 4.23 *Graphs of a typical data record of a tensile strength test*

The tensile strength of a sample of bagasse was determined from the peak of the tensile force curve minus the average baseline reading of the same curve after the peak had been reached, as illustrated by the dotted horizontal lines in Figure 4.23, divided by the cross-sectional area of the bagasse "bar" contained in the two trolleys. The baseline reading after attainment of the peak includes the frictional resistance of the moving trolley, therefore the

difference between the peak and the baseline represents the tensile resistance due to the bagasse only. The oscillations on that baseline are due to the jerky response of the trolley while being pulled by the string attached to the tensile force measuring device, which was made from two sections of a hack saw blade and inevitably had some inherent elasticity. The cross-sectional area was calculated from the width of the internal space of the trolleys and the height of bagasse, which was read off using the measuring scales on the outside walls of the trolleys.

For each bagasse sample three tensile strength tests were conducted, each at a different degree of compaction. For each test a new amount of bagasse was loaded into the trolleys. Altogether 60 tests were performed.

Data analysis

For each test the tensile strength was determined as outlined in the previous paragraph. The other variables that were tabulated were mean fibre length L, coarse-fine ratio c, bulk density ρ and moisture content W. The degree of compaction had an obvious influence on the value of the tensile strength. Bulk density was used as a measure of compaction because it was not possible to find a logical means of using pressure readings to derive the degree of compaction . However, bulk density is also affected by moisture content. In order to separate moisture content from bulk density, so that these could be used as independent variables, it was decided to calculate the dry bulk density ρ_d from the wet bulk density ρ_w by the formula in equation 4.15

$$\rho_d = \rho_w \left(1 - \frac{W}{100}\right) \qquad (4.15)$$

where W is the percentage moisture content. The full dataset which formed the basis of the analysis is shown in Table 4.12.

Table 4.12

Complete dataset for tensile strength statistical analysis

SUMMARY OF TENSILE STRENGTH RESULTS					
TENSILE STRENGT N/m2	FIBRE LENGTH mm	COARSE INDEX -	MOIST %	WET B.DENS kg/m3	DRY B.DENS kg/m3
859	16.67	0.91	46.5	217.8	116.5
980	16.67	0.91	46.5	219.0	117.2
448	16.67	0.91	46.5	170.5	91.2
944	15.14	0.70	48.5	192.3	99.0
372	15.14	0.70	48.5	162.2	83.5
2148	15.14	0.70	48.5	218.5	112.5
376	18.30	1.20	50.3	127.2	63.2
608	18.30	1.20	50.3	152.0	75.5
1617	18.30	1.20	50.3	195.5	97.2
245	8.73	0.50	54.0	208.6	96.0
717	8.73	0.50	54.0	269.2	123.8
327	8.73	0.50	54.0	241.8	111.2
131	7.56	0.32	42.0	136.9	79.4
327	7.56	0.32	42.0	173.2	100.5
996	7.56	0.32	42.0	223.6	129.7
273	12.27	1.26	30.5	98.4	68.4
347	12.27	1.26	30.5	112.7	78.3
699	12.27	1.26	30.5	136.4	94.8
230	10.46	0.77	47.3	150.3	79.2
612	10.46	0.77	47.3	178.3	94.0
1301	10.46	0.77	47.3	207.3	109.2
225	13.06	0.63	44.5	157.3	87.3
507	13.06	0.63	44.5	179.7	99.7
902	13.06	0.63	44.5	206.8	114.8
291	17.00	0.91	32.5	144.2	97.3
1184	17.00	0.91	32.5	184.2	124.3
407	17.00	0.91	32.5	170.7	115.2
322	17.30	1.01	48.5	128.8	66.3
647	17.30	1.01	48.5	171.3	88.2
1829	17.30	1.01	48.5	203.3	104.7
332	20.36	1.49	53.5	112.7	52.4
577	20.36	1.49	53.5	129.4	60.2
1328	20.36	1.49	53.5	175.8	81.7
283	22.95	1.88	42.0	100.0	58.0
732	22.95	1.88	42.0	134.1	77.8
1729	22.95	1.88	42.0	157.9	91.6
307	23.36	2.48	50.0	92.0	46.0
245	23.36	2.48	50.0	101.4	50.7
935	23.36	2.48	50.0	138.2	69.1
180	4.61	0.04	42.0	124.2	72.0
280	4.61	0.04	42.0	153.8	89.2
569	4.61	0.04	42.0	182.9	106.1
233	17.28	1.08	10.5	82.9	74.2
462	17.28	1.08	10.5	95.4	85.4
703	17.28	1.08	10.5	111.1	99.4
169	17.28	1.08	10.5	76.7	68.6
559	17.28	1.08	10.5	101.4	90.8
1429	17.28	1.08	10.5	105.3	94.2
219	27.93	5.63	11.0	51.9	46.2
690	27.93	5.63	11.0	42.9	38.2
786	27.93	5.63	11.0	68.8	61.2
353	27.93	5.63	11.0	61.3	54.6
507	27.93	5.63	11.0	62.9	56.0
2236	27.93	5.63	11.0	89.4	79.6
236	9.58	0.90	11.5	81.1	71.8
445	9.58	0.90	11.5	98.2	86.9
527	9.58	0.90	11.5	109.4	96.8
245	9.58	0.90	11.5	92.0	81.4
355	9.58	0.90	11.5	94.6	83.7
942	9.58	0.90	11.5	115.9	102.6

A statistical analysis procedure similar to that adopted for the other bagasse properties was employed. Using tensile strength σ_T as the dependent variable simple linear regression was performed with each of the other variables as independent ones using again the four transformations listed in equation 4.8. This was then followed by stepwise multilinear regression. It is emphasised that the technique of initially regressing one independent variable at a time against the dependent variable has limitations, since it had not been possible to keep the other variables constant. This technique was done simply to obtain the approximate form of the relationship applicable to the individual independent variables. Bulk density, and in particular, dry bulk density, proved to be a highly significant variable. The equation (4.16) that gave the best fit between σ_T and dry bulk density ρ_d is:

$$\sigma_T = \exp(a + b\rho_d) \qquad (4.16)$$

where a and b are constants. It was therefore decided to use ln σ_T as dependent variable in the subsequent stepwise multilinear regression.

The stepwise multilinear regression analysis using ln σ_T as dependent variable and dry bulk density ρ_d, mean fibre length L, coarse-fine ratio c and moisture content W as independent variables showed that dry bulk density and mean fibre length were significant variables while coarse-fine ratio and moisture content were non-significant. An adjusted r^2 value of 0.555 was obtained and the relevant statistical information is given in Table 4.13.

This analysis therefore gives the following empirical relationship

$$\ln\sigma_T = 2.631 + 0.0277\rho_d + 0.078L + \varepsilon \qquad (4.17)$$

for which the correlation between observed and calculated ln σ_T values is shown in the graph of Figure 4.24.

Table 4.13

Statistical data for stepwise multilinear regression on tensile strength

Variable	Coefficient	Std. error	t-Value	95% Confidence Limits	
				Low	High
Constant	2.631	0.421	6.25	1.788	3.473
Dry Bulk Dens. ρ_d	0.0277	0.003	8.24	0.021	0.034
Fibre Length L	0.0785	0.011	6.95	0.056	0.101

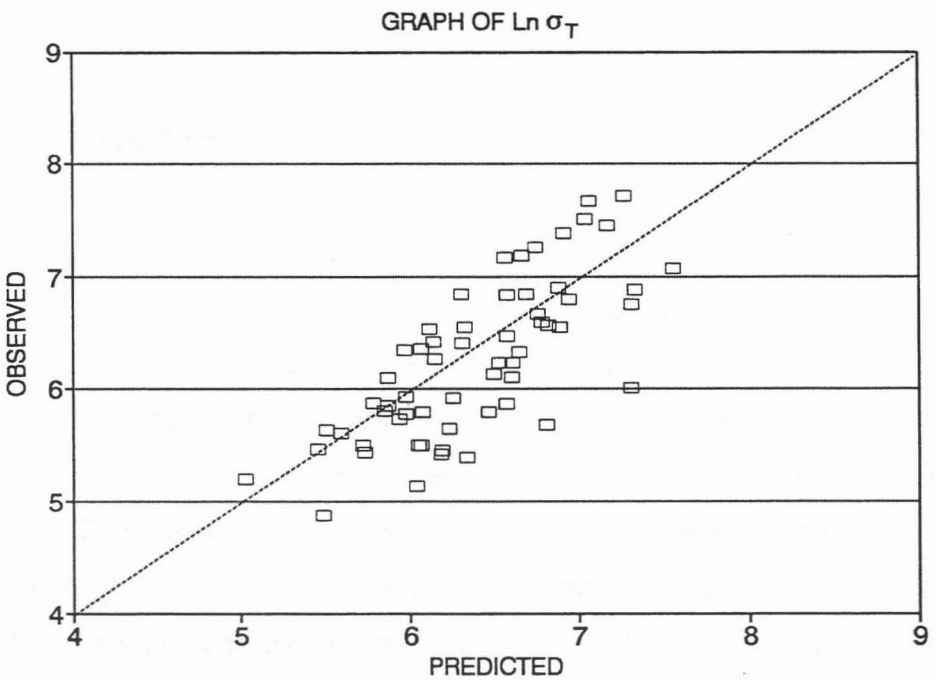

Figure 4.24 *Observed vs. calculated ln σ_T values*

CHAPTER FIVE

BRIDGING OF BAGASSE: EXPERIMENTAL INVESTIGATION AND EMPIRICAL MODEL

5.1 INTRODUCTION

The aim in this chapter is to present, and validate, an approximate model by which, for a given hardware configuration, it is possible to predict whether or not stable bagasse bridges are likely to form for a given range of mean fibre length, coarse-fine ratio and moisture content. The model will use some of the empirical relations that were developed for relevant variables in chapter 4. Due to the complexity of the bridging phenomenon no attempt has been made to give a coherent mechanistic theory. The model that is offered is purely empirical and uses as basis the results of bridging experiments performed in an apparatus specifically designed for the purpose.

The apparatus that was designed for this purpose is described in section 5.2 and the experimental procedure in section 5.3. The results of the bridging tests are given in section 5.4. The empirical model is described in section 5.5, as well as a comparison of measured results from the bridging

experiments with values predicted by the model. Some applications of the bridging model will be described in section 5.6.

5.2 BRIDGING APPARATUS

The apparatus that was used to investigate bagasse bridging consisted, in essence, of two vertical, parallel rigid plates held in position by a sturdy framework. A diagrammatic representation of the apparatus is shown in Figure 5.1 and a photograph in Figure 5.2.

The plates Pℓ were intended to represent sections of two opposing walls of a bagasse chute with rectangular cross-section. The other two walls which complete the rectangular form of the chute consisted of clear polycarbonate sheeting Po that permitted observation of the bridging behaviour and facilitated measurement of bagasse levels. The two rigid plates were made of 4 mm thick mild steel 0.7 m wide by 1.48 m high. To ensure rigidity, 3 cm of the edge of each plate was bent backwards at right angles to the plane of the plate at the top and the two sides. A pressure transducer Pr that had been specially developed for bagasse pressure measurements (see description in Appendix D) was fitted in the centre of each plate, 30 cm from the bottom edge, so that the transducer diaphragm was flush with the inner surface of the plates and there was no protrusion of any studs or bolts which secured the pressure tranducers to the rigid plates beyond the plate surface. In order to ensure that the contact surface of the plates had the same surface roughness throughout the experimental programme, a coat of PA10 etch primer was applied to the plates. Care was exercised that there were no points of surface roughness beyond the natural surface finish. The inner surfaces of the plates which contacted the bagasse were plain and devoid of any ridges. The inclination of the plates to the vertical, and to each other, could be changed from one test to another, or during a test, but all the experiments were conducted with the plates

positioned vertically and parallel to each other so as to simplify the analysis. The distance between the plates could be altered for different tests, the three distances used in the experiments were 0.20, 0,32 and 0,44 m respectively. The width of the plates was, of course, fixed at 0.70 m. The opening between the plates at the bottom always had a rectangular shape in which the shorter dimension was variable while the longer dimension was constant (0.70 m).

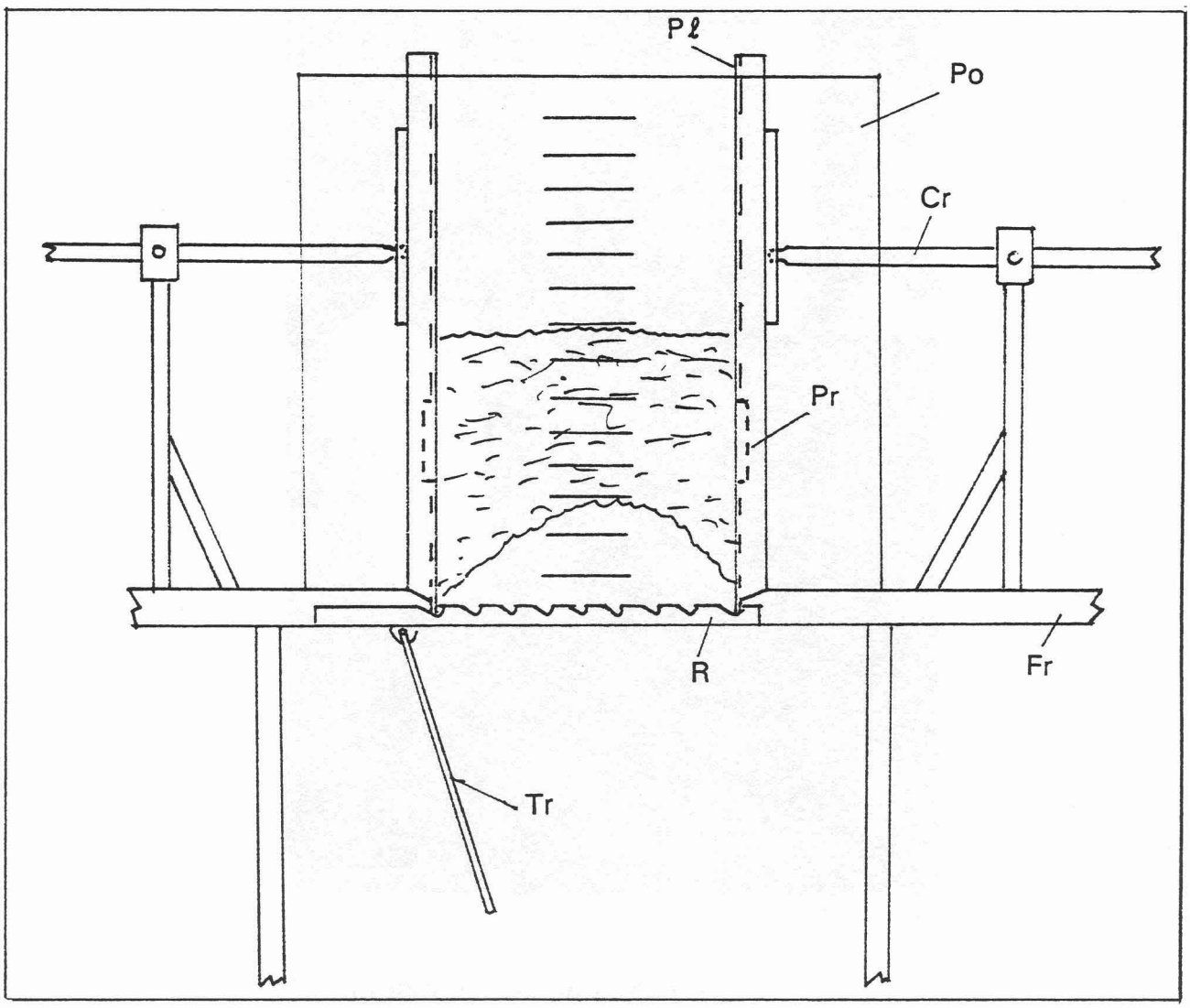

Figure 5.1 Bridging apparatus

Two conditions of bridging were investigated. The first condition concerned

the formation of a bridge of bagasse in a parallel sided chute the walls of which contained no objects that could obstruct the flow of bagasse. In this situation a bridge tended to collapse by sliding downwards in the chute. The second condition related to a bridge forming as a result of some physical obstruction protruding from the chute wall. Such a bridge failed as a result of internal collapse of the bagasse.

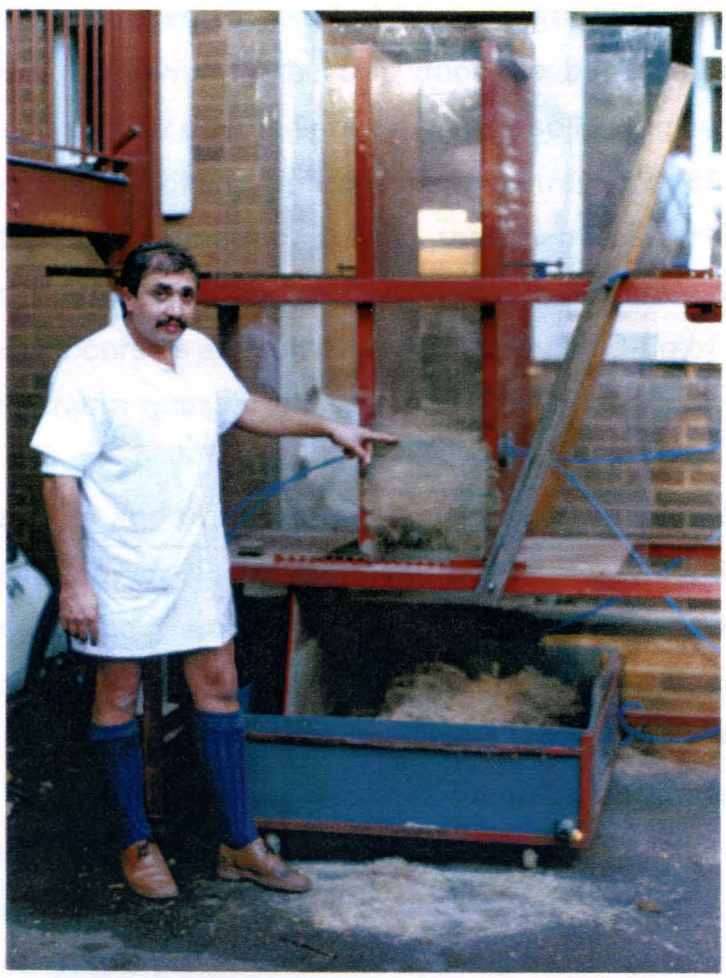

Figure 5.2 Photograph of bridging apparatus

To simulate the first condition special care was taken in designing the apparatus that nothing protruded into the parallel-sided opening between the plates. The second bridging condition was created by bolting pieces of angle

iron (not shown in the diagram) which stretched the full width of the rigid plates Pℓ to the inside of the bottom edges of the plates. In this way two parallel ridges were formed by the horizontal portions of the angle iron. Additional lateral obstructions were created by fixing pieces of flat bar to the ends of the horizontal portions of the angle iron parallel to the bottom edges of the polycarbonate sheets. These pieces of flat bar then completed a rectangular obstruction around the periphery of the bottom of the chute.

A trap door Tr was used to hold up the bagasse while the apparatus was being charged. On lowering the trap door the bagasse would either fall through the rectangular opening or be held as a solid plug by a bridge formed within the bagasse. Holding up bagasse by a trap door simulates a static condition of bridge formation. It was reasoned that, although bagasse conveying is a dynamic operation involving motion, bridging of bagasse in chutes usually occurs as a result of a momentary hold-up of bagasse, which can be considered a quasi-static situation.

The rigid plates Pℓ and transparent polycarbonate sheets Po were mounted within a rigid framework Fr constructed from 60 mm wide, 8 mm thick angle iron. Rigidity of the framework and the vertical plates was considered important to avoid any vibration which could cause artificial failure in the bridges. A spirit level was used to position the framework so that the bottoms of the bridge measuring plates were horizontal and their vertical edges in vertical planes. Two sets of positioning rails R with accurately machined slots were fixed on either side of the frame to ensure that the bottom edges of the plates were always separated by the same distance, and formed a rectangular opening. Two carpenters' sash cramps Cr were modified and fitted to the frame to adjust the distance between the rigid plates and fix them firmly in a vertical position.

5.3 EXPERIMENTAL PROCEDURE

The bridging experiments were aimed at determininig the "critical bridge dimensions", in other words, the dimensions of stable bridges which would collapse as a result of the slightest disturbance. The two modes of bridge formation referred to earlier were investigated separately. First the method of formation of a bridge held up solely by surface friction will be described and then bridge formation due to the presence of a lateral obstruction.

With the trapdoor Tr closed (refer to Figure 5.1) and ***no ridges fitted to the bottom edges of the vertical plates Pℓ*** a weighed amount of bagasse of known mean fibre length L, coarse-fine ratio c and moisture content W was charged to the apparatus, compacted with a small garden fork and levelled off. Compaction was performed because it was reasoned that bridging was unlikely to occur when the bagasse was in a loose uncompacted state. All charging of the apparatus with bagasse was done by one person to try to achieve uniform compacting forces. This method of compacting the bagasse sounds rather imprecise, but bulk density determinations carried out on the same type of bagasse at a given moisture content using equal masses of bagasse showed that the repeatability of the technique was acceptable. The bagasse level was read off from graduations painted on the polycarbonate sheets. From the mass and the level the average bulk density of the bagasse could be determined.

The trapdoor was then opened very carefully, taking care not to induce any vibration in the apparatus that could precipitate the collapse of a bagasse bridge. If all, or a portion of, the bagasse charged to the apparatus was held up between the vertical plates for a period longer than 30 seconds a stable bagasse bridge (recorded as P for "persists") was registered, otherwise a condition of "no bridging" (C for "collapse") was noted.

The experimental procedure consisted of starting out with a relatively large volume of bagasse that was charged to the bridging apparatus while keeping the gap between the vertical plates constant. If the bagasse formed a stable bridge then the apparatus was emptied and a smaller weighed amount was charged to determine if again a stable bridge formed. By continually reducing the amount of bagasse, until bridge failure occurred, the minimum or ***critical height*** h_c of a stable bridge was determined. This procedure was repeated with different types of bagasse. The gap between the vertical plates was then altered and the whole process repeated. The system could be considered a one-dimensional case where the width of the rectangular gap between the metal plates was variable while the plate width (the other dimension of the rectangle) was constant.

In this way the first manner of stable bridge formation was investigated, namely when a bridge is held up ***solely by the surface friction on the chute walls***. To determine the influence of bagasse moisture the samples of bagasse used for the tests were air-dried for different lengths of time to different moisture contents.

For the second method of bridge formation, namely that ***due to obstructions along the wall***, the artificial ridges described in the previous section were fitted to the bottom edges of the mild steel plates. Two sets of ridges were investigated, namely a set of two ***parallel*** ridges (recorded as PR) fitted at the bottom of the mild steel plates, and a ***rectangular*** closed ridge (RR) formed by adding the two flat bars described above. Apart from using the ridges at the bottom of the rectangular opening the experimental procedure for this second type of bridge formation was identical to that for the first type.

For each test the following information was recorded:

mean fibre length L (mm)

coarse-fine ratio c (-)
moisture content W (%)
parallel ridges (PR), rectangular ridge (RR) or no ridge (N) (-)
the distance l between the vertical plates (m)
the height h of the bagasse plug before lowering of the trapdoor (m)
the mass m of bagasse charged to the bridging apparatus (kg)
the bulk density ρ_b of the bagasse (kg/m^3).
bridge persisting (P) or bridge collapse (C) (-)
the thickness t was kept constant at 0.7 m for all tests (since this was the width of the apparatus).

The intention of monitoring pressure had been to determine if there was a noticeable change of pressure during bridge formation or collapse. Unfortunately only one set of pressure tranducers, which were situated 30 cm above the bottom edges of the vertical plates, was fitted to the bridging apparatus. In a number of instances the critical bridge height h_c was either below the level of the pressure transducer or slightly above it, so that the pressure reading was not representative of all the bagasse in the apparatus.

Another possible use of pressure readings was to compare these with the calculated lateral pressures on which the determination of surface friction are based. This comparison was not performed because the pressure transducers provided an indication of pressure at one specific level only and its reading could not be considered to represent that of the whole mass of bagasse. The data from the pressure transducers therefore only provided inferred information and therefore pressure is not listed as one of the recorded variables.

The types of bagasse used for the tests included diffuser bagasse from three factories and mill bagasse from two factories, as well as depithed fibre and

pith from a depithing station of one factory. Depithed fibre and pith were included to provide data on the widest possible mean fibre length range. Mean fibre lengths ranged from 3.9 mm to 23.0 mm, coarse-fine ratios from 0.02 to 2.36 and moisture contents from 9.70% to 63.50%. The distances between the vertical plates that were investigated were 0.20 m, 0.32 m and 0.44 m, the last mentioned being the upper limit of the apparatus.

5.4 RESULTS OF BRIDGING EXPERIMENTS

Altogether 79 datasets on bridge stability were accumulated. These are tabulated in Table 5.1. From these sets, for each distance l, the critical height h_c was determined, i.e. the height of bagasse which was just sufficient to support a stable bridge. A typical set of results from which the critical height for one type of bagasse was obtained is shown in Table 5.2.

For this set of tests the critical height was recorded as 0.45 m. At a height of 0.36 m the bridge collapsed (C) whereas at the next height investigated (0.45 m) it persisted (P). Of course, it is possible that the critical height lies between 0.36 and 0.45 m, but it was considered that an error of 0.09 m was acceptable. It is noteworthy that for the first row of data in Table 5.2 the density (107.6 kgm^{-3}) was much less than in the next two tests. This was the first bridging test undertaken and no effort had been made to compact the bagasse. The technique of compacting the bagasse, as stated in the experimental procedure of section 5.3, was adopted after that first test.

Table 5.1

Full set of bridging experiment results

L	c	W	RIDGE	P or C	l	h	DENS
mm	-	%	-	-	m	m	kg/m3
23.0	2.36	47.10	N	P	0.20	0.77	107.6
23.0	2.36	47.10	N	C	0.20	0.36	134.9
23.0	2.36	47.10	N	P	0.20	0.45	142.9
3.9	0.02	46.10	N	P	0.20	0.53	155.0
3.9	0.02	46.10	N	P	0.20	0.39	166.7
3.9	0.02	46.10	N	P	0.20	0.28	178.6
3.9	0.02	46.10	N	P	0.20	0.20	178.6
3.9	0.02	46.10	N	P	0.20	0.12	178.6
8.1	0.47	29.80	N	P	0.20	0.28	127.6
8.1	0.47	29.80	N	C	0.20	0.16	133.9
8.1	0.47	29.80	N	C	0.20	0.22	129.9
23.0	2.36	47.10	N	P	0.32	0.29	140.7
23.0	2.36	47.10	N	C	0.32	0.30	151.2
23.0	2.36	47.10	N	P	0.32	0.30	166.3
23.0	2.36	47.10	N	C	0.32	0.25	145.1
3.9	0.02	46.10	N	P	0.32	0.45	134.9
3.9	0.02	46.10	N	P	0.32	0.20	181.4
3.9	0.02	46.10	N	C	0.32	0.16	175.6
8.1	0.47	29.80	N	C	0.32	0.31	142.7
8.1	0.47	29.80	N	P	0.32	0.43	146.6
8.1	0.47	29.80	N	C	0.32	0.61	146.9
23.0	2.36	47.10	N	C	0.44	0.30	151.5
23.0	2.36	47.10	N	P	0.44	0.45	157.3
23.0	2.36	47.10	N	P	0.44	0.36	153.3
3.9	0.02	46.10	N	P	0.44	0.45	181.8
3.9	0.02	46.10	N	P	0.44	0.18	180.4
3.9	0.02	46.10	N	C	0.44	0.15	179.1
8.1	0.47	29.80	N	C	0.44	0.48	133.3
8.1	0.47	29.80	N	P	0.44	0.52	141.2
23.0	2.36	30.70	N	C	0.44	0.38	109.4
23.0	2.36	30.70	N	P	0.44	0.52	116.8
23.0	2.36	30.70	N	P	0.44	0.43	119.3
3.9	0.02	27.70	N	P	0.44	0.27	141.9
3.9	0.02	27.70	N	P	0.44	0.24	146.4
3.9	0.02	27.70	N	C	0.44	0.19	140.4
3.9	0.02	17.00	N	C	0.44	0.61	128.8
3.9	0.02	16.34	N	C	0.44	0.58	125.4
8.1	0.47	18.33	N	P	0.44	0.43	120.7
8.1	0.47	18.33	N	C	0.44	0.48	125.8
8.1	0.47	18.33	N	P	0.44	0.50	126.6
8.1	0.47	16.34	N	C	0.32	0.54	123.5
8.1	0.47	16.34	N	P	0.32	0.79	128.8
3.9	0.02	26.07	N	P	0.32	0.21	137.2
3.9	0.02	26.07	N	P	0.20	0.27	134.8
3.9	0.02	26.07	N	P	0.20	0.16	147.5
3.9	0.02	26.07	N	P	0.20	0.10	135.3
23.0	2.36	17.90	N	P	0.20	0.39	83.5
23.0	2.36	17.90	N	P	0.20	0.54	79.4
23.0	2.36	17.90	N	P	0.20	0.29	86.2
23.0	2.36	17.90	N	C	0.20	0.23	77.6

Table 5.1 (continued)

L	c	W	RIDGE	P or C	l	h	DENS
mm	-	%	-	-	m	m	kg/m3
8.1	0.47	16.30	N	C	0.20	0.39	113.6
8.1	0.47	16.30	N	P	0.20	0.47	120.1
3.9	0.02	9.70	N	C	0.20	0.30	109.5
3.9	0.02	9.70	N	C	0.20	0.53	111.9
3.9	0.02	9.70	N	C	0.20	0.77	117.8
23.0	2.36	15.10	N	C	0.32	0.34	71.6
23.0	2.36	15.10	N	C	0.32	0.90	85.1
16.3	0.97	63.50	N	C	0.32	0.29	180.3
16.3	0.97	63.50	N	C	0.32	0.43	197.0
16.3	0.97	63.50	N	P	0.32	0.69	133.6
16.3	0.97	63.50	N	P	0.44	0.48	204.4
16.3	0.97	63.50	N	P	0.44	0.60	205.6
16.3	0.97	63.50	N	P	0.20	0.35	183.7
16.3	0.97	63.50	N	P	0.20	0.25	200.0
16.3	0.97	63.50	N	P	0.20	0.18	198.4
16.3	0.97	63.50	N	C	0.20	0.16	178.6
16.3	0.97	24.45	N	C	0.44	0.21	102.0
16.3	0.97	24.45	N	C	0.44	0.41	100.6
16.3	0.97	24.45	N	C	0.44	0.61	100.9
21.8	1.84	47.32	PR	P	0.44	0.22	178.0
21.8	1.84	47.32	PR	C	0.44	0.13	153.6
21.8	1.84	47.32	PR	C	0.44	0.16	189.9
21.8	1.84	47.32	PR	P	0.44	0.16	204.3
21.8	1.84	47.32	RR	P	0.44	0.16	190.0
21.8	1.84	47.32	N	C	0.44	0.23	191.9
21.8	1.84	47.32	N	P	0.44	0.35	206.9
21.8	1.84	47.32	N	C	0.44	0.41	205.9
21.8	1.84	47.32	N	C	0.44	0.60	209.5
21.8	1.84	46.70	PR	P	0.32	0.22	171.5
21.8	1.84	46.70	PR	P	0.32	0.11	172.5
21.8	1.84	46.70	RR	C	0.32	0.10	154.3
21.8	1.84	46.70	RR	P	0.32	0.11	172.8
21.8	1.84	46.70	N	C	0.32	0.27	188.5
21.8	1.84	46.70	N	P	0.32	0.52	201.1
16.3	0.97	14.16	N	C	0.32	0.51	104.3
16.3	0.97	14.16	N	C	0.32	0.75	106.0
16.3	0.97	14.16	PR	P	0.32	0.22	94.0
16.3	0.97	14.16	PR	P	0.32	0.14	80.6
16.3	0.97	14.16	PR	C	0.32	0.11	82.3
16.3	0.97	14.16	RR	P	0.32	0.11	77.7
16.3	0.97	14.16	RR	P	0.32	0.10	63.5
23.0	2.36	15.10	RR	P	0.32	0.10	36.3
23.0	2.36	15.10	RR	C	0.32	0.07	42.3
8.1	0.47	16.30	RR	C	0.32	0.09	80.8
8.1	0.47	16.30	RR	P	0.32	0.12	86.6
3.9	0.02	9.70	RR	P	0.32	0.11	95.0
3.9	0.02	9.70	RR	C	0.32	0.09	90.9
3.9	0.02	9.70	PR	P	0.32	0.11	103.5
3.9	0.02	9.70	PR	C	0.32	0.10	95.5
8.1	0.47	16.30	PR	P	0.32	0.13	83.4

Table 5.1 (continued)

L	c	W	RIDGE	P or C	l	h	DENS
mm	-	%	-	-	m	m	kg/m3
8.1	0.47	16.30	PR	P	0.32	0.11	82.3
8.1	0.47	16.30	PR	C	0.32	0.10	72.5
23.0	2.36	15.10	PR	P	0.32	0.11	34.5
23.0	2.36	15.10	PR	C	0.32	0.08	34.1
16.3	0.97	14.16	N	C	0.20	0.48	99.7
16.3	0.97	14.16	N	C	0.20	0.86	105.5
23.0	2.36	15.10	PR	P	0.44	0.16	55.2
23.0	2.36	15.10	PR	C	0.44	0.13	50.4
23.0	2.36	15.10	RR	P	0.44	0.14	46.8
23.0	2.36	15.10	PR	C	0.44	0.13	45.3
8.1	0.47	16.30	PR	C	0.44	0.13	89.1
8.1	0.47	16.30	PR	P	0.44	0.16	91.9
8.1	0.47	16.30	RR	P	0.44	0.15	93.8
8.1	0.47	16.30	RR	C	0.44	0.14	88.9
3.9	0.02	9.70	PR	C	0.44	0.15	98.1
3.9	0.02	9.70	PR	P	0.44	0.16	102.2
3.9	0.02	9.70	RR	P	0.44	0.16	105.6
3.9	0.02	9.70	RR	P	0.44	0.14	106.8
3.9	0.02	9.70	RR	C	0.44	0.13	100.9

Table 5.2

Determination of critical height

L mm	c -	W %	Ridge -	P or C -	*l* m	h m	ρ_b kg/m^3
23.0	2.36	47.10	N	P	0.20	0.77	107.6
23.0	2.36	47.10	N	C	0.20	0.36	134.9
23.0	2.36	47.10	N	P	0.20	0.45	142.9

The full list of results detailing ***critical heights*** of stable bridges due to surface fricion for different bagasse types at different moisture contents is given in Table 5.3. Included in the same table is a set of measurements which represented tests in which the author could not produce stable bagasse bridges. It is interesting to note that all of the latter tests, with the

exception of two, were done with bagasse samples that had a low moisture content (less than 24.5%).

Table 5.3

Critical height h_c for bridge stability by surface friction

L	c	W	RIDGE	P or C	l	MEAS. h_c	PREDICTED HEIGHT Low	High	MASS	DENS
mm	-	%	-	-	m	m	m	m	kg	kg/m3
23.0	2.36	47.10	N	P	0.20	0.45	0.20	1.00	9.0	142.9
3.9	0.02	46.10	N	P	0.20	0.12	0.04	0.84	3.0	178.6
8.1	0.47	29.80	N	P	0.20	0.28	0.10	1.40	5.0	127.6
23.0	2.36	47.10	N	P	0.32	0.29	0.30	1.60	9.0	140.7
3.9	0.02	46.10	N	P	0.32	0.20	-	1.60	8.0	181.4
8.1	0.47	29.80	N	P	0.32	0.43	-	2.00	13.9	146.6
23.0	2.36	47.10	N	P	0.44	0.36	0.32	1.70	17.0	153.3
3.9	0.02	46.10	N	P	0.44	0.18	0.20	2.10	10.0	180.4
8.1	0.47	29.80	N	P	0.44	0.52	0.25	2.70	22.4	141.2
23.0	2.36	30.70	N	P	0.44	0.43	0.40	2.30	15.8	119.3
3.9	0.02	27.70	N	P	0.44	0.24	0.26	2.80	10.6	146.4
8.1	0.47	18.33	N	P	0.44	0.43	0.35	3.20	15.8	120.7
8.1	0.47	16.34	N	P	0.32	0.79	0.60	2.40	22.3	128.8
3.9	0.02	26.07	N	P	0.32	0.21	0.26	2.60	6.3	137.2
3.9	0.02	26.07	N	P	0.20	0.10	0.15	1.60	1.8	135.3
23.0	2.36	17.90	N	P	0.20	0.29	0.34	-	3.5	86.2
8.1	0.47	16.30	N	P	0.20	0.47	0.30	1.80	7.9	120.1
16.3	0.97	63.50	N	P	0.32	0.69	-	2.70	20.3	133.6
16.3	0.97	63.50	N	P	0.44	0.48	0.20	1.50	29.9	204.4
16.3	0.97	63.50	N	P	0.20	0.18	0.10	0.90	5.0	198.4
21.8	1.84	47.32	N	P	0.44	0.35	0.42	1.30	22.3	206.9
21.8	1.84	46.70	N	P	0.32	0.52	0.42	1.15	23.2	201.1
For the following datasets no critical heights could be obtained										
3.9	0.02	17.00	N	C	0.44	0.61	0.36	3.30	24.2	128.8
3.9	0.02	16.34	N	C	0.44	0.58	0.32	3.40	22.2	125.4
3.9	0.02	9.70	N	C	0.20	0.30	0.23	2.30	4.6	109.5
3.9	0.02	9.70	N	C	0.20	0.53	0.25	2.20	8.3	111.9
3.9	0.02	9.70	N	C	0.20	0.77	0.32	2.00	12.7	117.8
23.0	2.36	15.10	N	C	0.32	0.34	0.38	-	5.4	71.6
23.0	2.36	15.10	N	C	0.32	0.90	0.50	-	17.0	85.1
16.3	0.97	24.45	N	C	0.44	0.21	0.35	-	6.6	102.0
16.3	0.97	24.45	N	C	0.44	0.41	0.33	-	12.7	100.6
16.3	0.97	24.45	N	C	0.44	0.61	0.32	-	18.8	100.9
21.8	1.84	47.32	N	C	0.44	0.41	0.42	1.30	26.0	205.9
21.8	1.84	47.32	N	C	0.44	0.60	0.42	1.25	38.4	209.5
16.3	0.97	14.16	N	C	0.32	0.51	0.60	-	11.8	104.3
16.3	0.97	14.16	N	C	0.32	0.75	0.62	-	17.8	106.0
16.3	0.97	14.16	N	C	0.20	0.48	0.44	-	6.7	99.7
16.3	0.97	14.16	N	C	0.20	0.86	0.48	-	12.7	105.5

Bridging due to lateral obstructions

Altogether 40 experiments were performed to investigate the internal collapse of bridges held up by obstructions at the walls. The pertinent data is shown in Table 5.4. The determination of critical heights was done in a similar fashion as with bridges held up by surface friction only. In Table 5.4 the critical heights are underlined. There are thus 18 datasets representing critical heights.

A cursory glance at the 'h' column of Table 5.4 reveals that the critical heights for bridges held up by wall obstructions are between 0.1 and 0.2 m, which is a much narrower range than that obtained for surface friction bridging (0.1 - 0.8 m). This illustrates the strong tendency of bagasse to form a matted medium, even for pith which had a relatively small mean fibre length (3,9 mm). As a general rule of thumb the critical height for bridges held up by lateral obstructions is approximately one third of that for those supported by surface friction.

The repeatability of the results is indicated by the fact that there is often a very small difference between the critical height (i.e. a height at which a bridge just persists) and the height at which it collapses, as shown, for example, in the results higlighted in Table 5.5 (0.11 and 0.10 m resp.).

It is also noticeable that the critical height for parallel ridges (PR) is in most cases very close to that for the corresponding rectangular ridges (RR). Although rectangular ridges tend to give rise to critical heights that are generally slightly smaller than the corresponding values for parallel ridges, because a rectangular ridge provides more support than only two ridges, the difference is insignificant. In general, the shorter the span (variable l) the lower the critical height. Therefore in a rectangular chute of unequal horizontal dimensions it is the ***shorter*** of the two that will determine whether

a stable bridge will form (as a result of a wall obstruction as well as surface friction).

Table 5.4

Results for bridge formation due to lateral obstructions

L	c	W	RIDGE	P or C	l	h	DENS
mm	-	%	-	-	m	m	kg/m3
21.8	1.84	47.32	PR	P	0.44	0.22	178.0
21.8	1.84	47.32	PR	C	0.44	0.13	153.6
21.8	1.84	47.32	PR	C	0.44	0.16	189.9
21.8	1.84	47.32	PR	P	0.44	0.16	204.3
21.8	1.84	47.32	RR	P	0.44	0.16	190.0
21.8	1.84	46.70	PR	P	0.32	0.22	171.5
21.8	1.84	46.70	PR	P	0.32	0.11	172.5
21.8	1.84	46.70	RR	C	0.32	0.10	154.3
21.8	1.84	46.70	RR	P	0.32	0.11	172.8
16.3	0.97	14.16	PR	P	0.32	0.22	94.0
16.3	0.97	14.16	PR	P	0.32	0.14	80.6
16.3	0.97	14.16	PR	C	0.32	0.11	82.3
16.3	0.97	14.16	RR	P	0.32	0.11	77.7
16.3	0.97	14.16	RR	P	0.32	0.10	63.5
23.0	2.36	15.10	RR	P	0.32	0.10	36.3
23.0	2.36	15.10	RR	C	0.32	0.07	42.3
8.1	0.47	16.30	RR	C	0.32	0.09	80.8
8.1	0.47	16.30	RR	P	0.32	0.12	86.6
3.9	0.02	9.70	RR	P	0.32	0.11	95.0
3.9	0.02	9.70	RR	C	0.32	0.09	90.9
3.9	0.02	9.70	PR	P	0.32	0.11	103.5
3.9	0.02	9.70	PR	C	0.32	0.10	95.5
8.1	0.47	16.30	PR	P	0.32	0.13	83.4
8.1	0.47	16.30	PR	P	0.32	0.11	82.3
8.1	0.47	16.30	PR	C	0.32	0.10	72.5
23.0	2.36	15.10	PR	P	0.32	0.11	34.5
23.0	2.36	15.10	PR	C	0.32	0.08	34.1
23.0	2.36	15.10	PR	P	0.44	0.16	55.2
23.0	2.36	15.10	PR	C	0.44	0.13	50.4
23.0	2.36	15.10	RR	P	0.44	0.14	46.8
23.0	2.36	15.10	PR	C	0.44	0.13	45.3
8.1	0.47	16.30	PR	C	0.44	0.13	89.1
8.1	0.47	16.30	PR	P	0.44	0.16	91.9
8.1	0.47	16.30	RR	P	0.44	0.15	93.8
8.1	0.47	16.30	RR	C	0.44	0.14	88.9
3.9	0.02	9.70	PR	C	0.44	0.15	98.1
3.9	0.02	9.70	PR	P	0.44	0.16	102.2
3.9	0.02	9.70	RR	P	0.44	0.16	105.6
3.9	0.02	9.70	RR	P	0.44	0.14	106.8
3.9	0.02	9.70	RR	C	0.44	0.13	100.9

Table 5.5

Datasets illustrating the repeatability of bridging caused by wall obstructions

L mm	c -	W %	Ridge -	P or C -	l m	h m	ρ_b kg/m^3
21.8	1.84	46.70	RR	C	0.32	0.10	154.3
21.8	1.84	46.70	RR	P	0.32	0.11	172.8

Some general observations made during the experiments will be appropriate.

1. When a stable bagasse bridge forms between vertical, parallel walls a cross-section through the centre of the bridge has a shape similar to that shown in Figure 5.3. The bottom is generally dome-shaped as a result of some bagasse falling down because the interparticle forces are too small to maintain the integrity of the whole mass. The amount of material that falls down varies with the type of bagasse, the plate separation, the moisture content and the degree of compaction. The steepness of the sides of the dome is generally determined by the packing density - the greater this density the flatter the dome. When the trapdoor is lowered after charging a weighed amount of bagasse to the apparatus, a small degree of sagging of the bagasse is often observed during formation of a stable bridge. The top surface is often slightly concave, while the bottom surface is normally convex upwards.

2. The critical height h_c recorded for bridges held up by ***unobstructed walls*** was generally considerably greater than that measured for bridges held up by ***lateral obstructions***. For the lateral obstruction

tests there was little difference between the critical heights recorded for ***parallel*** as opposed to ***rectangular*** ridges. Furthermore, in all cases the critical height h_c was dependent on the separation of the plates l. For all bridges at the critical height the ratio h_c/l was determined and plotted against l. No definite pattern was observed for those bridges held up by surface friction only, as can be seen in Figure 5.4. The relevant data for these bridging tests is given in Table 5.3 on page 147. For the bridges held up by lateral obstructions ***this ratio had an almost constant value of 0.34***, as indicated in Figure 5.5. For both sets of bridging tests bagasse types of widely differing mean fibre length (3.9 - 23.0 mm), coarse-fine ratio (0.02 - 2.36) and moisture content (9.7 - 47.3% for lateral obstruction and 16.3 - 63.5% for unobstructed wall bridging tests) were employed.

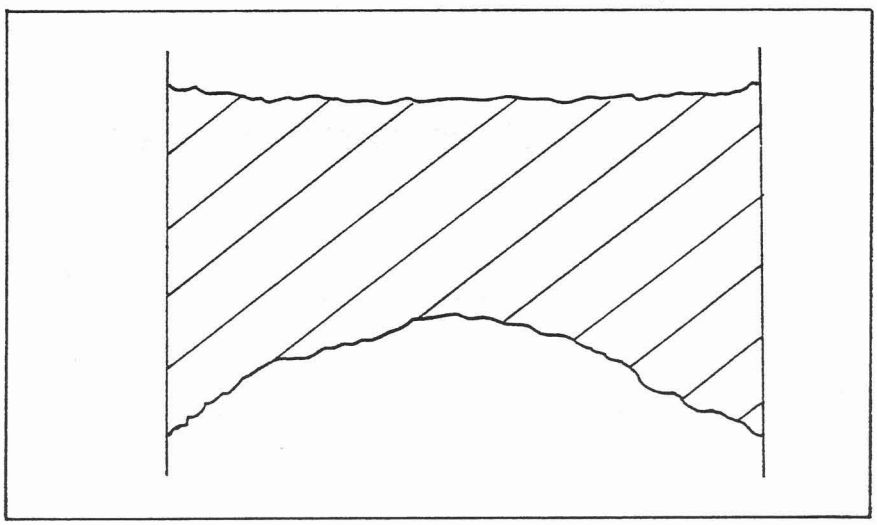

Figure 5.3 *Cross-section of a typical bagasse bridge*

3. The pressure transducers usually registered little or no change in pressure during stable bridge formation when they were positioned towards the top or middle portion of a bridge. However, in cases where the bottom of a bridge just covered the transducer, a significant increase in pressure (sometimes as much as three times the original pressure recorded prior to release of the trapdoor) was observed during stable bridge formation.

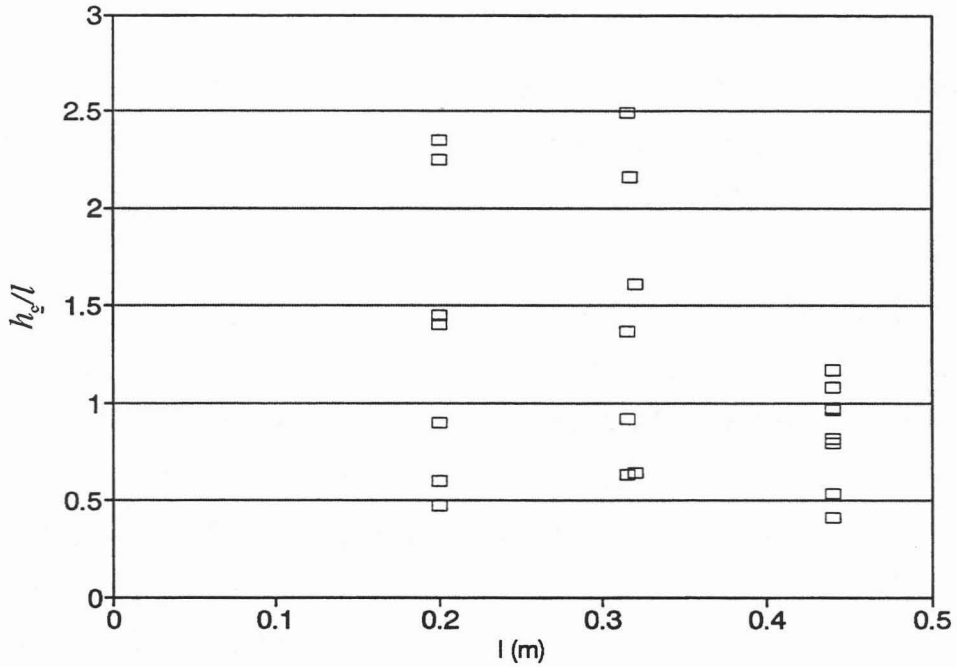

Figure 5.4 *Ratio h_e/l for surface friction bridging*

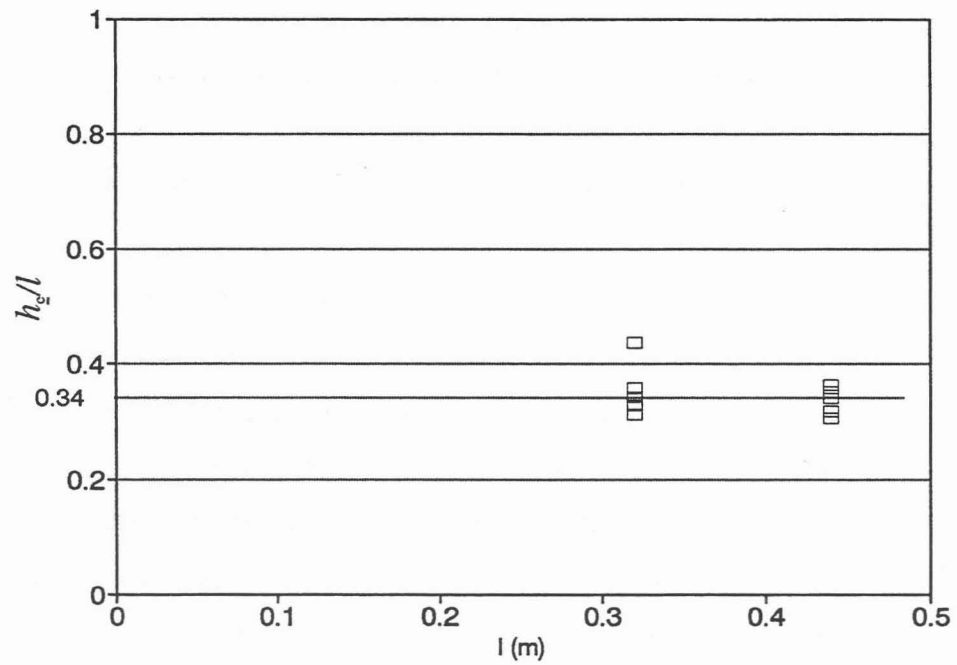

Figure 5.5 *Ratio h_e/l for lateral obstruction bridging*

5.5 APPROXIMATE BRIDGING MODEL

The aim of a bridging model is to provide a method whereby it is possible to determine whether, for a chute of given dimensions, stable bagasse bridges are likely to form for a given type of bagasse when flow is temporarily interrupted.

It is common knowledge that lateral obstructions cause severe problems in transfer of bagasse in chutes, hence no bagasse transfer equipment is designed such that there are lateral obstructions. For this reason a model for bridging as a result of lateral obstructions has no practical value. The model that is presented here applies to bridges supported by surface friction only. As will be seen, the bridging experiments with lateral obstructions were used to provide some insight into the mechanism of bridging only.

The concepts underlying the bridging model detailed here have been formed largely as a result of observations made during the bridging experiments that were described in the previous section. Some experiments were deliberately designed to test particular aspects of the model, whereas some aspects could not be confirmed due to the limitations of the hardware. It is emphasised again that, due to the complexity of the bridging phenomenon, the model that is presented is purely empirical. The author does not feel confident to advance a plausible mechanistic theory.

If a stable bridge is formed when there are no lateral obstructions then the friction between the bagasse and the containing walls must be sufficient to support the weight of the bagasse. Using the correlations of surface friction developed in chapter 4 together with bulk density determinations it became clear that the surface friction derived from the original measurements of the bagasse in the bridging apparatus while supported by the trapdoor was usually ***insufficient to sustain the weight of the bagasse***, once the trapdoor had been lowered. Additional forces must somehow be generated within the bagasse that increase the frictional wall resistance to the extent that it is now sufficient to support the bagasse weight.

It is postulated that these additional forces are generated as a result of the formation of invisible ***ARCHES*** within the material. The phenomenon of arching is frequently given as the reason for hold-up of bulk solids in silos, and an approximate theory has been published by Walker (1966). The reason why this theory cannot be applied to bagasse is that it has not been possible to devise a workable method for measuring the angle of internal friction, on which this theory depends, as has been indicated in chapter 4. It is concluded therefore that ***arching must play a significant part in increasing the surface friction to the extent that it is large enough to hold up the weight of the bagasse.*** Furthermore, it is reasoned that ***bridges of critical height held up by wall obstructions resist internal collapse mainly due to internal arching.*** The fact that the ratio h_c/l for critical bridges was nearly constant was used in formulating the conceptual model described below.

In the light of the observations described above a ***stable bagasse bridge held up by surface friction only is visualised as consisting of two regions, viz. an upper region, termed the "passive zone", in which arching plays no part (as indicated by a virtual zero pressure increase in this zone) and a bottom "arching zone" (in which there is a significant increase in lateral pressure, presumably due to arching) which results in a considerable increase in surface friction.*** Figure 5.6 gives a pictorial representation of these concepts.

According to the assumption that bridges of critical height held up by wall obstructions resist internal collapse mainly due to internal arching, the depth of the arching zone h_{arch} can be equated to h_c and can therefore be determined from the constant value 0.34 for the ratio h_c/l for these bridges according to equation 5.1.

$$h_{arch} = h_c = 0.34\ l\ . \qquad (5.1)$$

The constant value of 0.34 for h_c/l furthermore seems to suggest that the form of arch is that of two inclined linear regions meeting at the centre (as intimated in Figure 5.6) rather than a curved shape (parabolic, elliptical or

circular) for which the ratio of height to horizontal span would vary according to the magnitude of the horizontal span. An attempt was made to establish the thickness $h_{arch,eff}$ of the effective arching region in relation to the height of the arching zone h_{arch} by endeavouring to measure the height over which a significant increase in pressure occurs. This was unsuccessful, however, probably because of the relatively large diameter of the pressure transducer diaphragm (6.5 cm) compared to the estimated value of h_{arch} which, for the bridging tests performed, never exceeded 15 cm. For valid pressure measurements the pressure diaphragm must be completely covered by bagasse. Furthermore, the size of the diaphragm precluded the accurate definition of the boundaries of the effective arching zone.

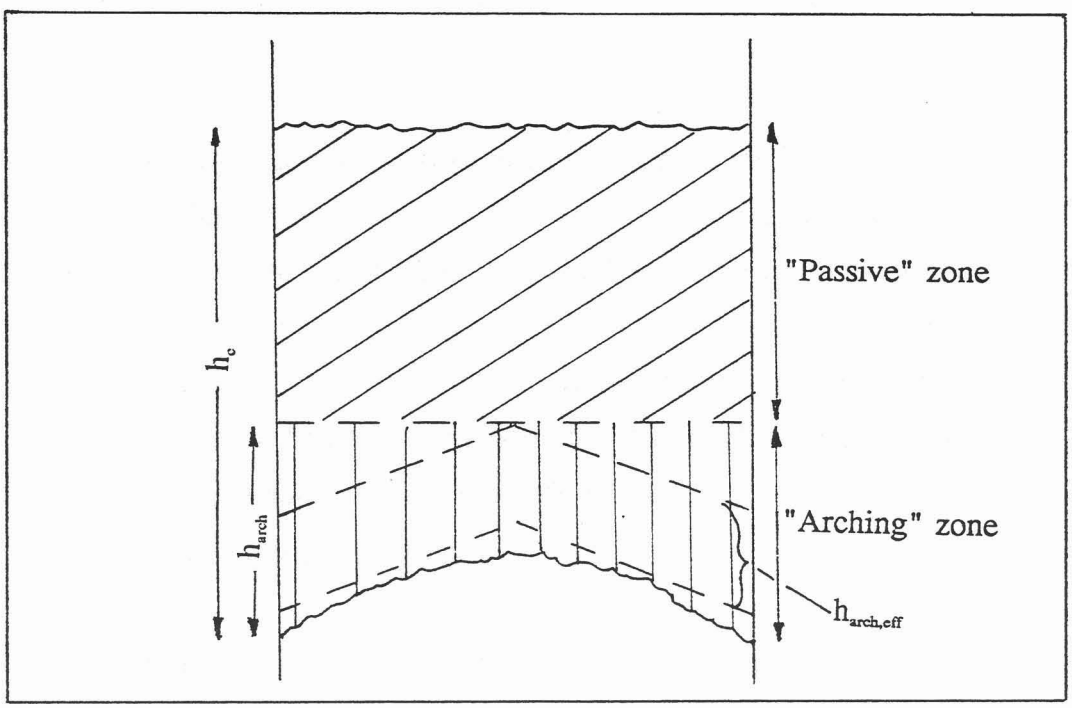

Figure 5.6 Passive and arching zones of a bagasse bridge

The conversion of the conceptual model described above into a useful quantitative form required the application of some approximations which are described below.

Arching tends to increase the lateral pressure of the bagasse against the chute walls. This increase results in an increase in surface friction. Initially an attempt was made to calculate the increased lateral pressure from the difference between the weight of material in the bagasse bridge and the surface friction calculated from bagasse measurements. However, the estimation of the increase in lateral pressure due to arching requires a knowledge of the area over which the increased pressure acts. It was stated above that it had not been possible to measure this. Several attempts were made to evaluate the increase in lateral pressure by assuming different values for the ratio of the effective arching depth $h_{arch,eff}$ compared with the total arching depth h_{arch} calculated by equation 5.1. When the resultant values were used to calculate predicted critical heights and these were compared with those actually obtained, the discrepancy was excessively large.

A more direct approach was then adopted, using the following reasoning. The ultimate effect of arching is to increase the frictional force between the bagasse and the chute walls. This increase in the frictional force must be the difference between the weight of the bagasse and the frictional force that would apply if no arching took place. ***In essence, the quantitative model calculates the normal surface friction without arching and then applies a correction factor which takes the effect of arching into account.*** The calculation details are given below.

In order to calculate the surface friction for the case where the effect of arching is omitted it is assumed that during the formation of the bridge the original dimensions that the bagasse had when it was loaded into the apparatus with the trapdoor in the horizontal position are retained by the bridge. The following information is used:

the bulk density ρ_b of the bagasse obtained from the mass of bagasse charged to the bridging apparatus, the dimensions l and t of the

apparatus and the critical depth h_c of the bagasse bridge, as well as the relevant bagasse properties like mean fibre length L, coarse-fine ratio c and the moisture content W.

The equations used are detailed below.

For surface frictional shear stress τ the following relationship (equation 4.4 with constants listed in Table 4.4)

$$\sqrt{\tau} = 8.9271 - 0.0413\rho_b + 0.0189\sigma + 0.1543W - 0.4094L + 1.6489c - 0.1214S_1 - 1.3019S_2 \quad (5.2)$$

was employed. This equation shows that surface friction is a function of bulk density ρ_b, normal stress σ, moisture content W, mean fibre length L, coarse-fine ratio c and surface characteristics (S_1, S_2). The normal stress σ is the pressure at right angles to the wall, in other words the horizontal pressure σ_h.

To calculate the normal stress σ it is necessary to use another relationship, namely the translation of vertical pressure σ_v to horizontal pressure σ_h, which is reported in section 4.5. Equation 4.12 (for which the relevant coefficients are stated in Table 4.11) gives the form of the relationship in terms of K, the ratio σ_h/σ_v:

$$K = -0.2582 + 0.534\exp(-0.00236\sigma_v) + 0.0041\rho_b + 0.01345L - 0.0063W . \quad (5.3)$$

The vertical stress σ_v in the bagasse is that due to the weight of the material and it increases from zero at the top surface to a maximum value at the bottom surface of the mass of material constituting a bridge. In this analysis the arithmetic mean value between these two extremes is used which appears justified according to the nearly linear increase in lateral pressure (which depends on vertical pressure) with depth observed when lateral pressure readings were taken for different depths of material (results shown in Appendix E).

The expression for computing the relevant vertical stress σ_v is therefore:

$$\sigma_v = 0.5 g \rho_b h \qquad (5.4)$$

where g is the acceleration due to gravity, ρ_b the bulk density of the bagasse and h the vertical height of the bagasse bridge. Using equations 5.2 to 5.4 it is possible to determine the surface frictional stress τ from a knowledge of the bulk density ρ_b, the mean fibre length L, the coarse-fine ratio c, the moisture content W and the appropriate values of S_1 and S_2 for the particular contacting surface. The total normal frictional force F_{norm} (i.e. frictional force without arching effect) is obtained by multiplying the frictional shear stress τ by the contact surface area. Thus for a rectangular bridge of uniform height h and thickness t held in a bridging apparatus in which two sides are made of mild steel and two of smooth polycarbonate the total normal frictional force F_{norm} is

$$F_{norm} = 2ht\tau_1 + 2hl\tau_2 \qquad (5.5)$$

where τ_1 is the frictional shear stress on the mild steel and τ_2 that on the polycarbonate.

The weight G of material constituting the bagasse bridge is computed from the bulk density and the volume of material which, for a rectangular bridge becomes

$$G = ghtl\rho_b \, . \qquad (5.6)$$

The total normal surface friction force F_{norm} calculated from the shear stress τ_1 and τ_2, and the total contact area, as outlined above, was in every case significantly less than the weight G of bagasse constituting the bridge. The difference between the two must be the frictional force F_{arch} generated as a result of arching. For each of the datasets representing critical bridge dimensions the value of the friction attributable to arching F_{arch} was determined according to this difference, i.e.

$$F_{arch} = G - F_{norm} . \qquad (5.7)$$

Hence, for a bridge of critical height h_c the sum $F_{arch} + F_{norm}$ should be equal to the weight G of the bagasse. If the height of bagasse exceeds h_c then the total frictional force should be greater than G. The total friction F_{tot} applicable to a plug of bagasse in a chute is therefore

$$F_{tot} = F_{norm} + F_{arch} . \qquad (5.8)$$

F_{norm} is calculated using equations 5.2 to 5.5.

The relative effect of arching compared to the normal frictional force is indicated by the ratio F_{arch} / F_{norm}. The value of this ratio was determined for each of the critical height datasets as shown in Table 5.6. The ratio F_{arch} / F_{norm} is likely to vary according to the bagasse type, its moisture content, degree of compaction and the chute dimensions. In order to obtain a formula by which this ratio can be determined for predictive purposes the actual values obtained were submitted to stepwise multilinear regression. The result of this is given in Table 5.7. The adjusted r^2 value for the regression was 0.913 and the significant variables are vertical stress σ_v, bulk density ρ_b, bridge height h, bridge span l, moisture content W, coarse-fine ratio c and mean fibre length L. In other words, the factor by which the normal surface friction should be multiplied to take the effect of arching into account can be estimated according to the following formula

$$F_{arch}/F_{norm} = -2.7025 - 0.0097\sigma_v + 0.0267\rho_b + 3.433h + 6.473l - 0.0676W - 1.7889c + 0.3115L . \qquad (5.9)$$

This equation is used to calculate F_{arch}.

The reason why the arching frictional force F_{arch} was evaluated separately, instead of trying to correlate the total frictional force F_{tot} to relevant variables such as σ_v, ρ_b, h, l, W, c, and L, is that this makes it possible to estimate the total frictional force for any depth of bagasse plug, irrespective of

whether it is close to the critical height or not.

Table 5.6

Datasets used for stepwise multilinear regression of F_{arch} / F_{norm}

L	c	W	l	h_c	DENS	VERT STRESS	F arch/ F norm
mm	-	%	m	m	kg/m3	N/m2	-
23.0	2.36	47.10	0.20	0.45	142.9	315.3	0.59
3.9	0.02	46.10	0.20	0.12	178.6	105.1	0.94
8.1	0.47	29.80	0.20	0.28	127.6	175.2	0.74
23.0	2.36	47.10	0.32	0.29	140.7	200.2	1.80
3.9	0.02	46.10	0.32	0.20	181.4	178.0	1.41
8.1	0.47	29.80	0.32	0.43	146.6	309.2	1.48
23.0	2.36	47.10	0.44	0.36	153.3	270.7	2.45
3.9	0.02	46.10	0.44	0.18	180.4	159.3	2.08
8.1	0.47	29.80	0.44	0.52	141.2	356.7	1.73
23.0	2.36	30.70	0.44	0.43	119.3	251.6	3.11
3.9	0.02	27.70	0.44	0.24	146.4	168.8	2.55
8.1	0.47	18.33	0.44	0.43	120.7	251.6	2.59
8.1	0.47	16.34	0.32	0.79	128.8	496.1	1.32
3.9	0.02	26.07	0.32	0.21	137.2	138.0	1.86
3.9	0.02	26.07	0.20	0.10	135.3	63.1	1.42
23.0	2.36	17.90	0.20	0.29	86.2	122.6	2.79
8.1	0.47	16.30	0.20	0.47	120.1	276.8	1.09
16.3	0.97	63.50	0.32	0.69	133.6	448.7	0.28
16.3	0.97	63.50	0.44	0.48	204.4	476.2	1.55
16.3	0.97	63.50	0.20	0.18	198.4	175.2	1.47
21.8	1.84	47.32	0.44	0.35	206.9	355.1	4.23
21.8	1.84	46.70	0.32	0.52	201.1	508.0	1.74

A spreadsheet model which calculates the total friction for height increments of 0.1 m of bagasse was developed using these equations. A sample printout is shown in Table 5.8. The critical height h_c is that value (0.50 m) for which the total friction begins to exceed the weight of bagasse, as indicated in Table 5.8.

whether it is close to the critical height or not.

Table 5.6

Datasets used for stepwise multilinear regression of F_{arch} / F_{norm}

L	c	W	l	h_c	DENS	VERT STRESS	F arch/ F norm
mm	-	%	m	m	kg/m3	N/m2	-
23.0	2.36	47.10	0.20	0.45	142.9	315.3	0.59
3.9	0.02	46.10	0.20	0.12	178.6	105.1	0.94
8.1	0.47	29.80	0.20	0.28	127.6	175.2	0.74
23.0	2.36	47.10	0.32	0.29	140.7	200.2	1.80
3.9	0.02	46.10	0.32	0.20	181.4	178.0	1.41
8.1	0.47	29.80	0.32	0.43	146.6	309.2	1.48
23.0	2.36	47.10	0.44	0.36	153.3	270.7	2.45
3.9	0.02	46.10	0.44	0.18	180.4	159.3	2.08
8.1	0.47	29.80	0.44	0.52	141.2	356.7	1.73
23.0	2.36	30.70	0.44	0.43	119.3	251.6	3.11
3.9	0.02	27.70	0.44	0.24	146.4	168.8	2.55
8.1	0.47	18.33	0.44	0.43	120.7	251.6	2.59
8.1	0.47	16.34	0.32	0.79	128.8	496.1	1.32
3.9	0.02	26.07	0.32	0.21	137.2	138.0	1.86
3.9	0.02	26.07	0.20	0.10	135.3	63.1	1.42
23.0	2.36	17.90	0.20	0.29	86.2	122.6	2.79
8.1	0.47	16.30	0.20	0.47	120.1	276.8	1.09
16.3	0.97	63.50	0.32	0.69	133.6	448.7	0.28
16.3	0.97	63.50	0.44	0.48	204.4	476.2	1.55
16.3	0.97	63.50	0.20	0.18	198.4	175.2	1.47
21.8	1.84	47.32	0.44	0.35	206.9	355.1	4.23
21.8	1.84	46.70	0.32	0.52	201.1	508.0	1.74

A spreadsheet model which calculates the total friction for height increments of 0.1 m of bagasse was developed using these equations. A sample printout is shown in Table 5.8. The critical height h_c is that value (0.50 m) for which the total friction begins to exceed the weight of bagasse, as indicated in Table 5.8.

Table 5.7

Statistical data for the regression model of F_{arch} /F_{norm}

Varia-ble	Coeffi-cient	Std. error	t-Value	95% Confidence Limits	
				Low	High
Constant	-2.7025	0.921	-2.93	-4.679	-0.726
Vert.stress σ_v (N)	-0.0097	0.003	-3.20	-0.016	-0.003
Density ρ_b (kgm^{-3})	0.0267	0.006	4.17	0.013	0.040
Height h (m)	3.4327	2.135	1.61	-1.149	8.014
Span l (m)	6.4726	0.646	10.02	5.086	7.859
Moisture W (%)	-0.0676	0.008	-8.90	-0.084	-0.051
Coarse-fine c (-)	-1.7889	0.417	-3.80	-2.799	-0.778
Fibre length L (mm)	0.3115	0.059	5.26	0.184	0.439

In order to ***predict*** the critical height h_c for the formation of stable bagasse bridges due to surface friction the total surface friction F_{tot} (equation 5.8) must be equated to the bagasse weight G (equation 5.6). It is not possible to obtain an explicit solution for h from these two expressions because h appears as a factor on both sides of this equation. The spreadsheet model referred to above (see sample printout in Table 5.8) calculates the weight G and total friction for height increments of 0.1 m. The ratio F_{arch} / F_{norm} was determined by using equation 5.9. The weight of material was calculated from the measured density and the corresponding values of h, l and t. The normal friction F_{norm} was calculated using equations 5.4, 5.3, 5.2 and 5.5 (in that order). The ***critical height was taken as the value of h for which the friction was equal, or just exceeded, the weight of the material.*** A typical determination of the critical height is presented in Table 5.8.

Table 5.8

Sample printout of spreadsheet bridging model

h	l	t	meas. dens	L	c	W	weight	total friction	normal friction	arch friction
m	m	m	kg/m3	mm	-	%	N	N	N	N
0.10	0.32	0.7	85.1	23.0	2.36	15.10	18.7	7.21	1.60	5.61
0.20	0.32	0.7	85.1	23.0	2.36	15.10	37.4	20.37	4.59	15.77
0.30	0.32	0.7	85.1	23.0	2.36	15.10	56.0	39.55	9.05	30.51
0.40	0.32	0.7	85.1	23.0	2.36	15.10	74.7	64.48	14.96	49.52
0.50	0.32	0.7	85.1	23.0	2.36	15.10	93.4	94.63	22.28	72.36
0.60	0.32	0.7	85.1	23.0	2.36	15.10	112.1	129.46	30.93	98.53
0.70	0.32	0.7	85.1	23.0	2.36	15.10	130.8	168.40	40.84	127.55
0.80	0.32	0.7	85.1	23.0	2.36	15.10	149.4	210.93	51.95	158.98
0.90	0.32	0.7	85.1	23.0	2.36	15.10	168.1	256.61	64.19	192.43
1.00	0.32	0.7	85.1	23.0	2.36	15.10	186.8	305.07	77.52	227.55
1.10	0.32	0.7	85.1	23.0	2.36	15.10	205.5	356.01	91.92	264.09
1.20	0.32	0.7	85.1	23.0	2.36	15.10	224.2	409.20	107.38	301.81
1.30	0.32	0.7	85.1	23.0	2.36	15.10	242.9	464.46	123.92	340.54
1.40	0.32	0.7	85.1	23.0	2.36	15.10	261.5	521.67	141.54	380.13
1.50	0.32	0.7	85.1	23.0	2.36	15.10	280.2	580.75	160.28	420.47
1.60	0.32	0.7	85.1	23.0	2.36	15.10	298.9	641.63	180.19	461.44
1.70	0.32	0.7	85.1	23.0	2.36	15.10	317.6	704.29	201.32	502.97

Figure 5.7 is a plot of the predicted total friction F_{tot} and weight G against bagasse height h for a particular type of bagasse of mean fibre length L = 16.3 mm, moisture content W = 63.5 %, bulk density ρ_b = 204.4 kgm^{-3} and coarse-fine ratio c of 0.97 at a plate separation l of 0.44 m and t = 0.7 m.

The concept of ***bridge stability*** is illustrated graphically in Figure 5.7. A bagasse bridge is considered stable when the total friction F_{tot} exceeds the weight G of bagasse. Conversely, when F_{tot} is less than G then the bridge must be considered unstable, i.e. likely to collapse or slide down. It is interesting to note that the model may predict more than one region of

bridge stability, and hence more than one critical height. This is also illustrated in the printout of Table 5.9. On comparing the values in the weight and the total friction columns, it is observed that initially the total friction value is less than the weight. At the critical height (0.2 m) the friction becomes greater than the weight. However, at a height of 0.6 m the friction becomes less than the weight again, until a height of 1.5 m is reached where the friction begins to exceed the weight again. This would suggest that if the height of the plug of bagasse is between 0.6 m and 1.5 m this plug is not expected to be held up in the chute. In other words, the two possible values for the critical height are 0.2 m and 1.5 m.

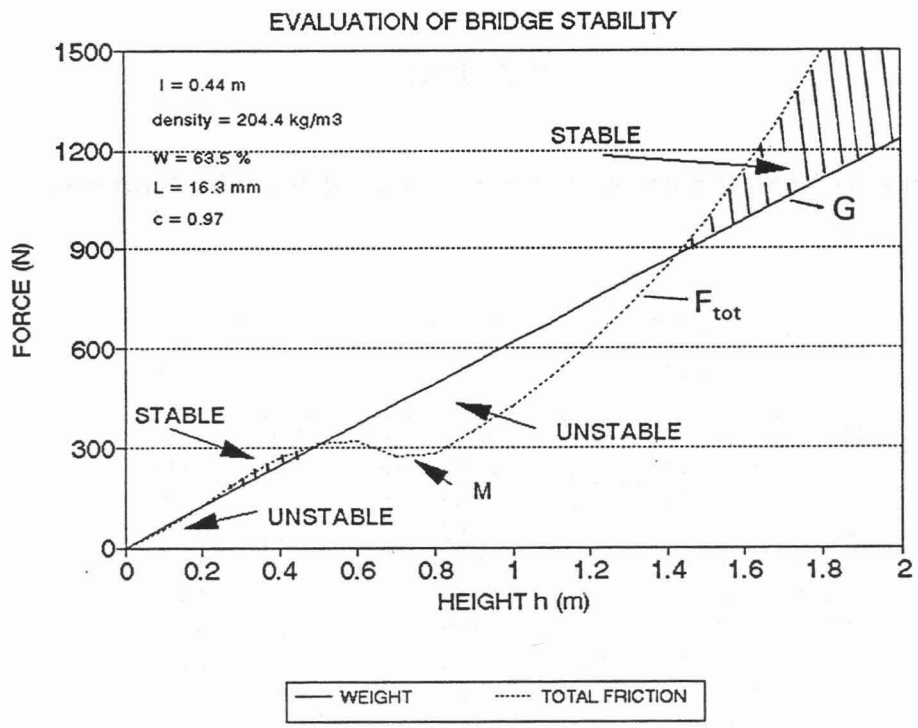

Figure 5.7 Plot of predicted total friction and bagasse weight against height

The reason for this apparent anomaly is the influence of arching. The regression model (equation 5.9) attributes the greatest impact of arching at low heights. As the height increases so the arching effect diminishes. As can be seen in the last column of Table 5.9 the friction due to arching eventually

becomes zero. Application of equation 5.9 would yield negative values beyond a certain height. The minimum value of the arching friction is obviously zero (indicated as point M in Figure 5.7), which is the value entered in the spreadsheet model when application of equation 5.9 calculates negative values. It needs to be emphasised, however, that the model described above is based on bridging measurements in which the maximum height of bagasse was 1.5 m (because of equipment limitations). For this reason it is not valid to extend the concept of multiple regions of bridge stability much beyond that limit. A larger apparatus than the one that was used in this study would be required to confirm that multiple regions of bridge stability exist beyond a height of 1.5 m.

Table 5.9

Spreadsheet model printout for case where two critical heights are predicted

h	l	t	meas. dens	L	c	W	weight	total friction	normal friction	arch friction
m	m	m	kg/m3	mm	-	%	N	N	N	N
0.10	0.44	0.7	204.4	16.3	0.97	63.50	61.7	51.62	10.30	41.32
0.20	0.44	0.7	204.4	16.3	0.97	63.50	123.4	125.98	28.75	97.23
0.30	0.44	0.7	204.4	16.3	0.97	63.50	185.1	204.57	54.53	150.04
0.40	0.44	0.7	204.4	16.3	0.97	63.50	246.8	271.30	86.95	184.34
0.50	0.44	0.7	204.4	16.3	0.97	63.50	308.5	312.83	125.69	187.14
0.60	0.44	0.7	204.4	16.3	0.97	63.50	370.2	317.37	170.85	146.52
0.70	0.44	0.7	204.4	16.3	0.97	63.50	431.9	273.28	222.84	50.44
0.80	0.44	0.7	204.4	16.3	0.97	63.50	493.6	282.30	282.30	0.00
0.90	0.44	0.7	204.4	16.3	0.97	63.50	555.3	350.05	350.05	0.00
1.00	0.44	0.7	204.4	16.3	0.97	63.50	617.0	426.98	426.98	0.00
1.10	0.44	0.7	204.4	16.3	0.97	63.50	678.7	514.04	514.04	0.00
1.20	0.44	0.7	204.4	16.3	0.97	63.50	740.4	612.23	612.23	0.00
1.30	0.44	0.7	204.4	16.3	0.97	63.50	802.0	722.51	722.51	0.00
1.40	0.44	0.7	204.4	16.3	0.97	63.50	863.7	845.88	845.88	0.00
1.50	0.44	0.7	204.4	16.3	0.97	63.50	925.4	983.29	983.29	0.00
1.60	0.44	0.7	204.4	16.3	0.97	63.50	987.1	1135.68	1135.68	0.00
1.70	0.44	0.7	204.4	16.3	0.97	63.50	1048.8	1303.99	1303.99	0.00

A series of bridging tests were done to investigate the phenomenon of two critical heights which are sometimes predicted by the model. Using bagasse from a diffuser factory with mean fibre length L of 20.7 mm, a coarse-fine ratio c of 1.63 and moisture content W measurements of 46.5, 53.5 and 47.8% for three samples taken from the same batch, the first series of tests were done for a plate separation l of 0.32 m. A bulk density ρ_b of 155 kgm^{-3} was used which was based on trial measurements with this material. The model predictions are indicated in Table 5.10.

Table 5.10

Model predictions for critical heights on diffuser bagasse

h	l	t	meas. dens	L	c	W	weight	total friction	normal friction	arch friction
m	m	m	kg/m3	mm	-	%	N	N	N	N
0.10	0.32	0.7	155	20.7	1.63	47.10	34.0	23.89	5.36	18.52
0.20	0.32	0.7	155	20.7	1.63	47.10	68.1	61.11	15.06	46.05
0.30	0.32	0.7	155	20.7	1.63	47.10	102.1	105.60	28.83	76.77
0.40	0.32	0.7	155	20.7	1.63	47.10	136.1	151.33	46.32	105.00
0.50	0.32	0.7	155	20.7	1.63	47.10	170.1	192.99	67.22	125.78
0.60	0.32	0.7	155	20.7	1.63	47.10	204.2	226.13	91.35	134.78
0.70	0.32	0.7	155	20.7	1.63	47.10	238.2	246.82	118.68	128.14
0.80	0.32	0.7	155	20.7	1.63	47.10	272.2	251.40	149.29	102.11
0.90	0.32	0.7	155	20.7	1.63	47.10	306.2	236.22	183.36	52.86
1.00	0.32	0.7	155	20.7	1.63	47.10	340.3	221.14	221.14	0.00
1.10	0.32	0.7	155	20.7	1.63	47.10	374.3	262.96	262.96	0.00
1.20	0.32	0.7	155	20.7	1.63	47.10	408.3	309.17	309.17	0.00
1.30	0.32	0.7	155	20.7	1.63	47.10	442.3	360.15	360.15	0.00
1.40	0.32	0.7	155	20.7	1.63	47.10	476.4	416.29	416.29	0.00
1.50	0.32	0.7	155	20.7	1.63	47.10	510.4	478.00	478.00	0.00
1.60	0.32	0.7	155	20.7	1.63	47.10	544.4	545.71	545.71	0.00
1.70	0.32	0.7	155	20.7	1.63	47.10	578.4	619.81	619.81	0.00

This table shows that for this type of bagasse two critical heights are predicted, namely 0.3 m and 1.6 m. Furthermore, the model predicts that a stable bridge should form at depths between 0.3 - 0.7 m. It is noteworthy that the friction calculations at those depths are relatively close to the weight values. In other words, the predicted surface friction appears to be

just sufficient to support a stable bridge, but the stability is likely to be rather tenuous.

The measured results obtained are summarised in Table 5.11.

Table 5.11

Bridging results on a sample of diffuser bagasse

Depth of bagasse when loaded (m)	Result
0.39	Slid down
0.70	Bottom half of the material fell down immediately, top half persisted as a bridge for 70s.
1.29	Bottom 2/3 of material slid down. Top 1/3 persisted as a bridge for more than 22 min.
0.30	Slid down
0.19	Slid down
0.70	Slid down

This test showed some evidence of incipient bridging at a depth of 0.34 to 0.43 m. The predicted lower bridging height range was 0.3 - 0.7 m. The fact that only 0.35 m of material remained for 70 s may be partial support for this prediction. The only other instance of stable bridging occurred when the original bagasse depth was 1.29 m, even though two thirds of the material slid down while the remainder formed a stable bridge. Whether this lends support to the concept of a second critical height (of 1.6 m) is debatable.

Table 5.3 lists the predicted critical heights obtained by applying the spreadsheet model. Both the lower and the higher predictions are shown. The spreadsheet model did not predict stable bridge formation (lower value) for three cases for which bridging had actually been observed, as indicated in Table 5.3. A graph of the predicted (lower) critical depth compared with the measured critical depth for the data for which stable bridges (P) were obtained is shown in Figure 5.8. The agreement between measured and predicted critical heights appears acceptable although the bridging model does tend to underestimate the critical bridging height. This is of course advantageous from a design perpective. The correlation coefficient between predicted and measured critical height for the 19 datasets plotted in Figure 5.8 was 0.74.

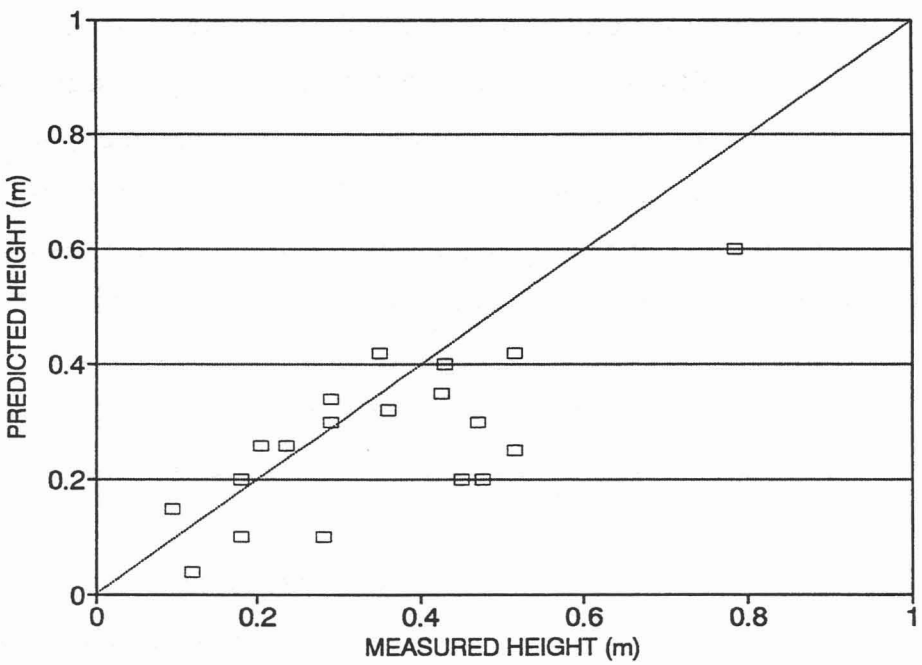

Figure 5.8 *Graph of predicted vs. measured critical depths for surface friction bridging results*

The spreadsheet surface friction bridging model was also applied to the data given at the bottom of Table 5.3 for which no stable bridges could be obtained (indicated by "C" for collapse). The measured height represents the

height of the bagasse that was measured before release of the trapdoor whereas the predicted height represents the critical height for which a stable bridge should be formed, as calculated by the proposed model. The model does predict stable bridge formation, but the error is again on the conservative side. It would be worse if the theory predicted conditions of no bridging and bridging did in fact take place. It is interesting that for nine out of sixteen of these datasets no higher critical height bridges were predicted.

5.6 APPLICATION

In this section the aim is to demonstrate how the different bagasse properties like mean fibre length, coarse-fine ratio, moisture content, and bulk density influence bridging behaviour and to indicate how the span between opposing walls of a rectangular chute affects the tendency for stable bridges to form. The results reported in the previous section showed a relatively good agreement between measured critical heights of bagasse bridges held up by surface friction and those predicted by the proposed theory. Since lateral obstructions should not be present in properly designed bagasse transfer equipment, bridging by internal collapse will not be considered. Application of the bridging model described in the previous section will be considered under the following headings.

Effect of significant variables
A design example
Bridging characteristics
Diverging chutes

Effect of significant variables

It was stated in the first chapter that, from a handling point of view, mill

bagasse has been found to behave different to diffuser bagasse. For this reason it has been decided to perform separate evaluations for the two types of bagasse. For purposes of comparison the following base properties were used. For mill bagasse a mean fibre length L of 8.0 mm with a coarse-fine ratio of 0.8 were assumed and for diffuser bagasse the corresponding values were 20 mm and 2.0 respectively. The bulk density ρ_b was assumed constant at 150 kgm^{-3}, the moisture content W at 48%, the distance l between opposite sides of the chute at 0.3 m and the width of the chute at 1.0 m. These values were kept fixed, except for the variable being investigated. The spreadsheet model that had been used in the previous section for predicting critical heights was again employed.

In the previous section it was pointed out that for surface friction there were frequently two possible critical depths at which bagasse forms stable bridges. Since the lower value is usually followed by a region of instability, in other words, if more bagasse was added the bridge would most likely slide down, only the higher value was used in the following description.

The effect of ***mean fibre length L*** on the critical height of bridges held up by surface friction is indicated in Figure 5.9. For the graph of Figure 5.9 the coarse-fine ratio c was held constant at 1.0. Normally the value of the coarse-fine ratio varies with the fibre length. The trend indicated in Figure 5.9 is contrary to what one would expect, because for longer fibres one expects a greater tendency towards bridging and therefore a lower critical height. The graph, however, is drawn for constant bulk density and an increase in fibre length is normally accompanied by a decrease in bulk density. This is the most likely reason for the anomalous curvature.

To determine the effect of variation of the ***coarse-fine ratio c*** on the critical height the mean fibre length L was kept constant at 10.0 mm, the result being shown in Figure 5.10. It is clear that the higher the coarse-fine ratio value the lower the predicted critical height.

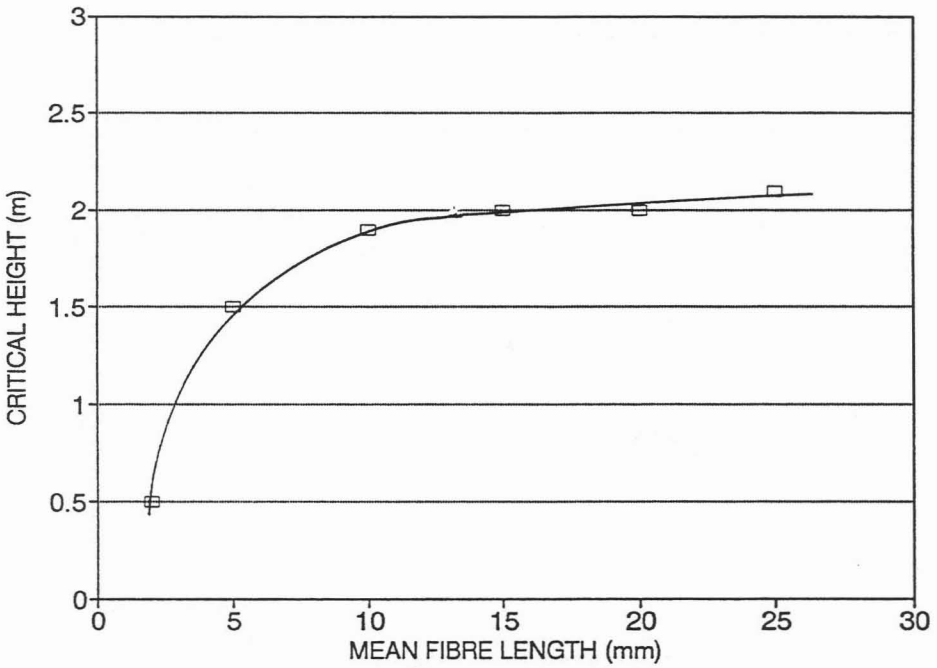

Figure 5.9 Influence of mean fibre length on critical height

The influence of ***bulk density*** ρ_b is shown in Figure 5.11. As with mean fibre length the critical height decreases with increasing bulk density. The effect is more pronounced with mill bagasse than with diffuser bagasse.

The influence of ***moisture content W*** on critical height is shown in Figure 5.12. In this case the difference between diffuser and mill bagasse is small. Both graphs show that moisture content does not significantly affect the critical height of bagasse bridges.

Figure 5.13 demonstrates how the ***span l*** between opposing walls of a chute affects the critical bridging height. Note, once again, the more marked effect on mill bagasse. As expected, the greater the span the larger the critical bridging height.

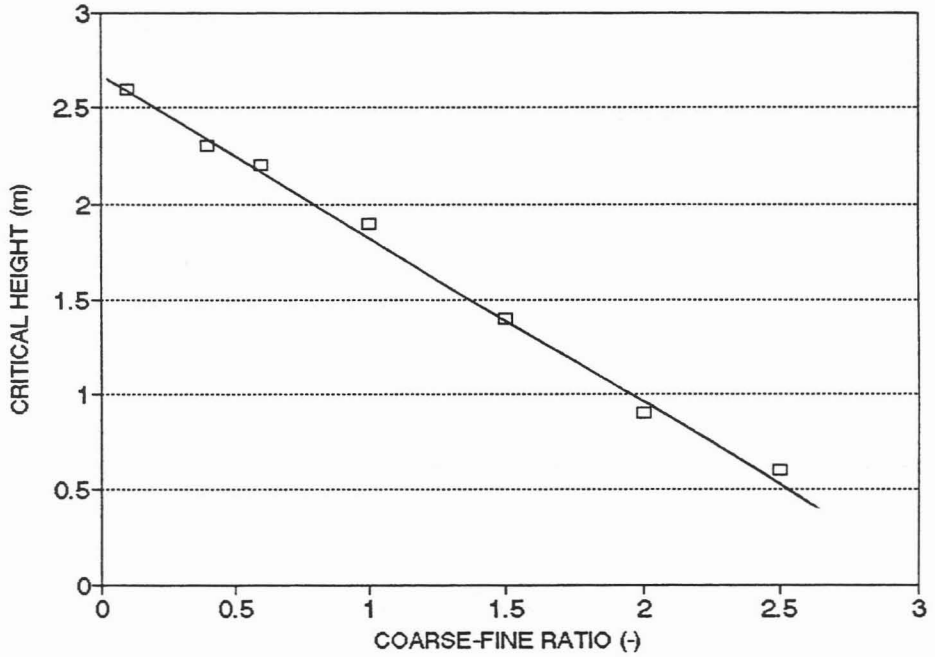

Figure 5.10 Variation of critical height with coarse-fine ratio

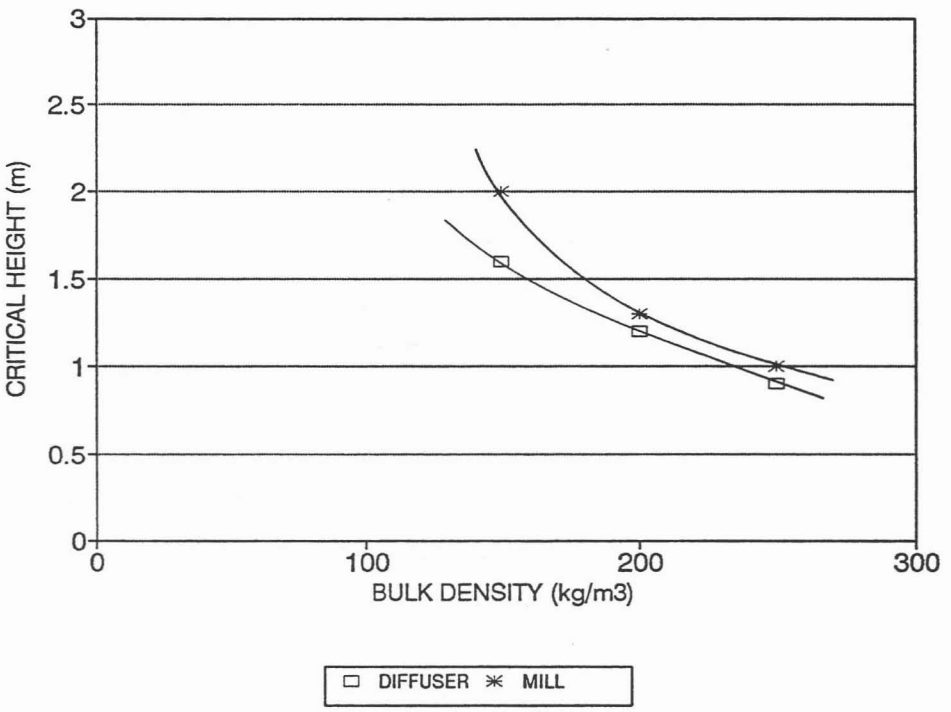

Figure 5.11 The effect of bulk density on critical bridging height

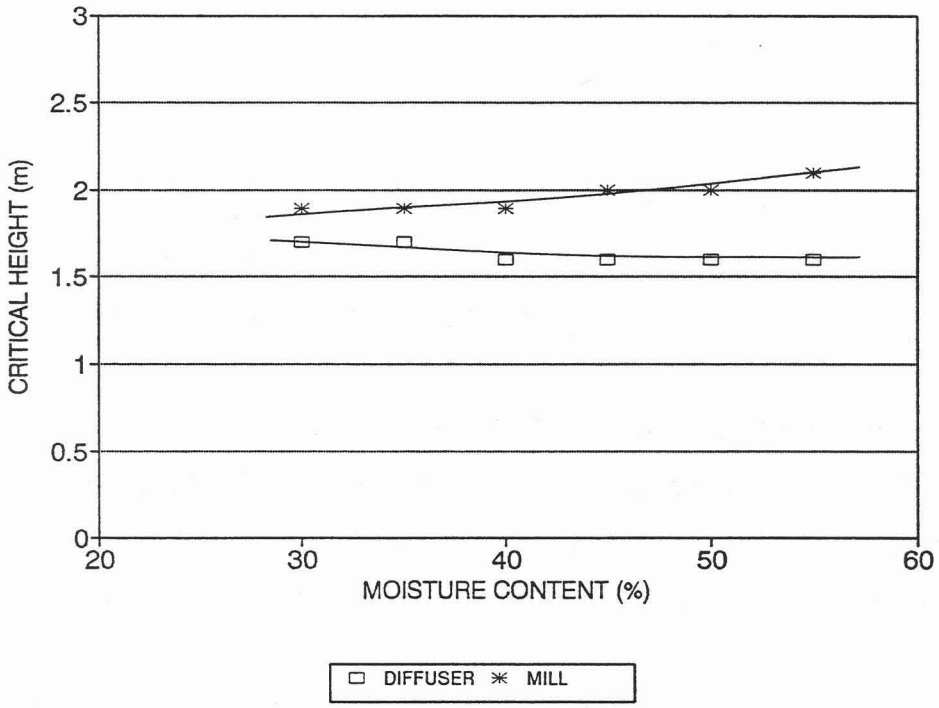

Figure 5.12 The effect of moisture content on critical height

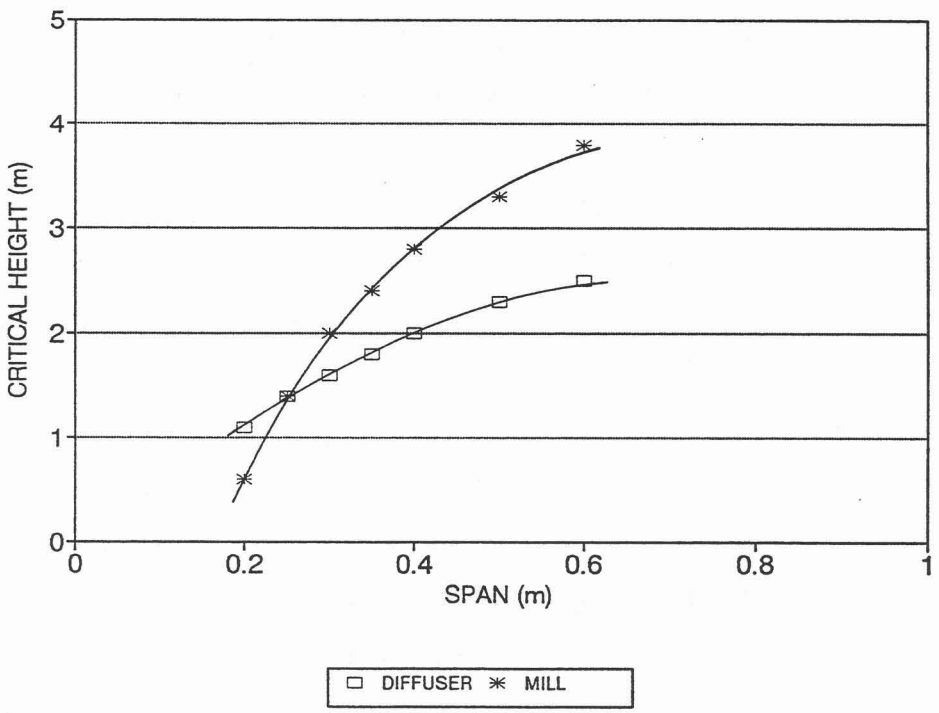

Figure 5.13 The influence of horizontal span on critical height

Design example

In order to demonstrate how the information that has been accumulated in this work can be used for design purposes the steps taken to solve the following design problem will be outlined.

> **It is required to determine the span l (horizontal distance between chute walls) in a vertical chute of rectangular cross-section to be fabricated from polished 316 stainless steel so as to ensure that bridging will not take place. The height of the chute is fixed at 2.0 m.**
>
> **The width of the chute is fixed at 1.8 m and it is to be used to transfer diffuser bagasse of which the bulk density range is 100-200 kgm^{-3} and the expected moisture content range 45-55%.**

For diffuser bagasse a mean fibre length range of 10-25 mm and a coarse-fine ratio range of 0.8-2.5 will be used. For calculation purposes the moisture content range will be slightly extended to 40-55%.

It is assumed that bridging due to surface friction is the only appropriate mode because if the chute is properly manufactured it should not have any surface obstructions or rough spots.

In order to ensure that bridging is not likely to occur it will be necessary to determine the span l which, for the type of bagasse to be transferred, will give a critical height of 2.0 m or greater. If the critical height is less than 2 m the possibility exists that a stable bridge will form in the chute which will in all probability lead to a choke. The spreadsheet model referred to in the previous section will be used for the calculations.

For stainless steel the value of S_1 in equation 5.2 is zero and for S_2 it is unity. These values therefore have to be entered in the spreadsheet model.

Since many of the variables cover a considerable range it would be a monumental task to find the optimal solution by entering a number of discrete values for each variable. The graphs (Figures 5.9 - 5.13) which show the trends of the critical height as functions of L, c, W, ρ_b and l can be used to determine the appropriate values to be entered in the spreadsheet model. Since all the trends depicted in the above figures are either monotone increasing or decreasing it will suffice to use the values at the extreme ends of each range. The task is further simplified by considering the direction of the trend.

An example will illustrate this better than a general description. The mean fibre length range L for diffuser bagasse was assumed to be 10 - 25 mm. Figure 5.9 indicates that the critical height tends to increase as fibre length increases. If one uses as basis for the calculations the higher value of the range, viz. 25 mm then this will tend to give a higher answer for the critical height than the lower value of 10 mm. Since the minimum value that the critical value must attain is 2.0 m this cut-off is more easily reached by using the high L value of 25 mm. However if the bagasse that passes through the chute has a lower L value (i.e. close to 10 mm) then the actual critical height may be less than 2 m. In other words there is a strong likelihood that bridging may occur in the chute, which is undesirable. In general therefore it is safest to use that extreme value of a variable that gives the smallest value for the critical height.

Applying this reasoning and considering the trends of the graphs depicted in Figures 5.9 - 5.12, to obtain a conservative design one would use

the shortest L value (10 mm)
the highest c value (2.5)

the highest ρ_b value (200 kgm^{-3})
and the lowest W value (40%).

With these values fixed one now determines the critical height for different l. If the model predicts two different critical heights then it is the larger value that is used because the smaller will only produce stable bridges within a narrow height range which will tend to collapse if more material is added. The results obtained are shown graphically in Figure 5.14. The required span is that corresponding to the point where the curve crosses the 2.0 m critical height. The author suggests applying a safety factor of 1.1 to this value. And the answer which is obtained by this technique is therefore (0.68 x 1.1) = 0.75 m.

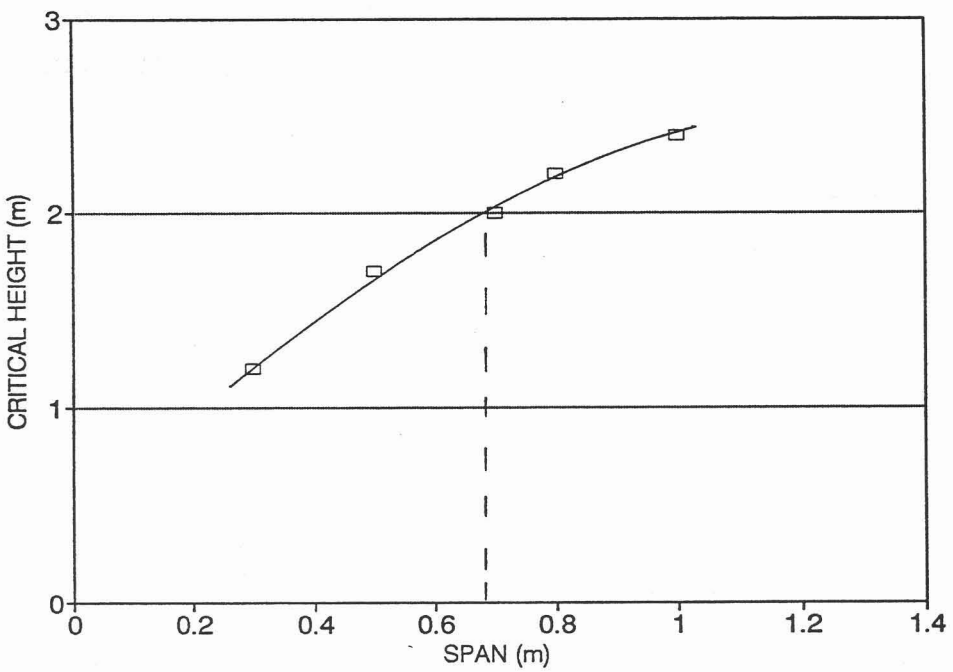

Figure 5.14 Critical heights determined by spreadsheet model for different spans

If this procedure were repeated for mill bagasse with a range of L values of 6 - 15 mm and c values of 0.8 - 1.5 the answer would be 0.61 m. Once

again the difference between mill and diffuser bagasse is evident.

Bridging characteristics

It would, from an engineering design point of view, be desirable to have a simple mathematical expresssion which could be used to determine if, for a given span, bridging is likely to take place or not. A brief reflection of the complexity of the model presented in the previous section shows that, at the current state of knowledge, this is not possible. What has been done, however, is to use the spreadsheet model to generate graphs depicting bridging characteristics for "typical" mill and diffuser bagasse. These graphs could be used to estimate roughly whether, for a given span, bridging is likely to occur or not.

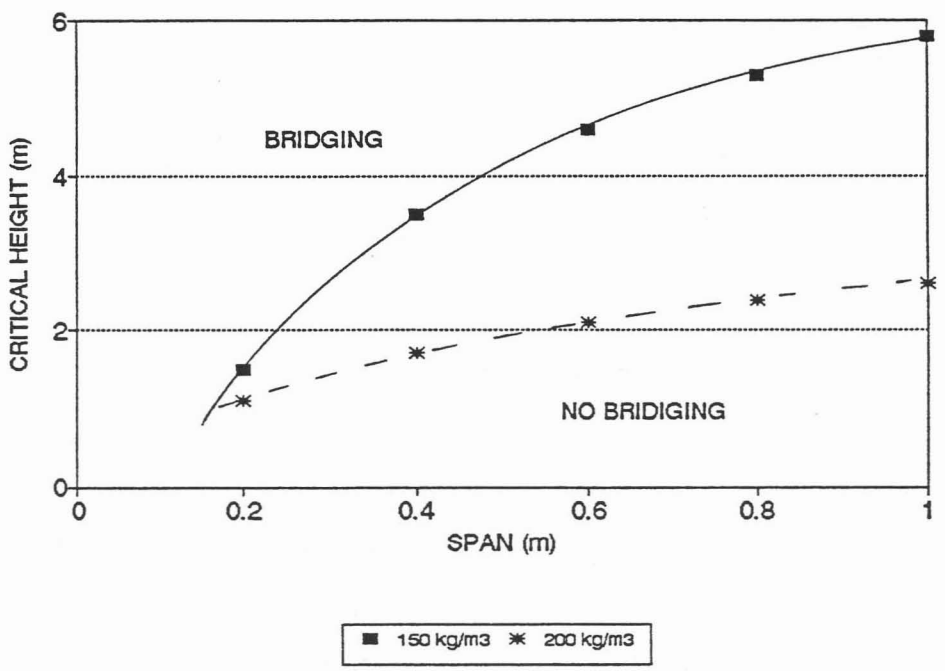

Figure 5.15 Bridging characteristics for mill bagasse

In Figure 5.15 the bridging characteristics for mill bagasse are presented. The following "normal" mill bagasse parameters were used to generate the characteristics: L = 8.0 mm, c = 0.8 and W = 50%. The longer chute dimension t was assumed to be 1.0 m and the chute material polished stainless steel. Since the critical bridging height is very dependent on degree of compaction, two characteristics are given, viz. for ρ_b = 150 and 200 kgm^{-3} respectively. A knowledge of the approximate bulk density is obviously necessary before these graphs can be used. The region above and to the left of each curve represents the situation where bridging can be expected, whereas that below and to the right of the curve is the region where bridging is not expected to occur.

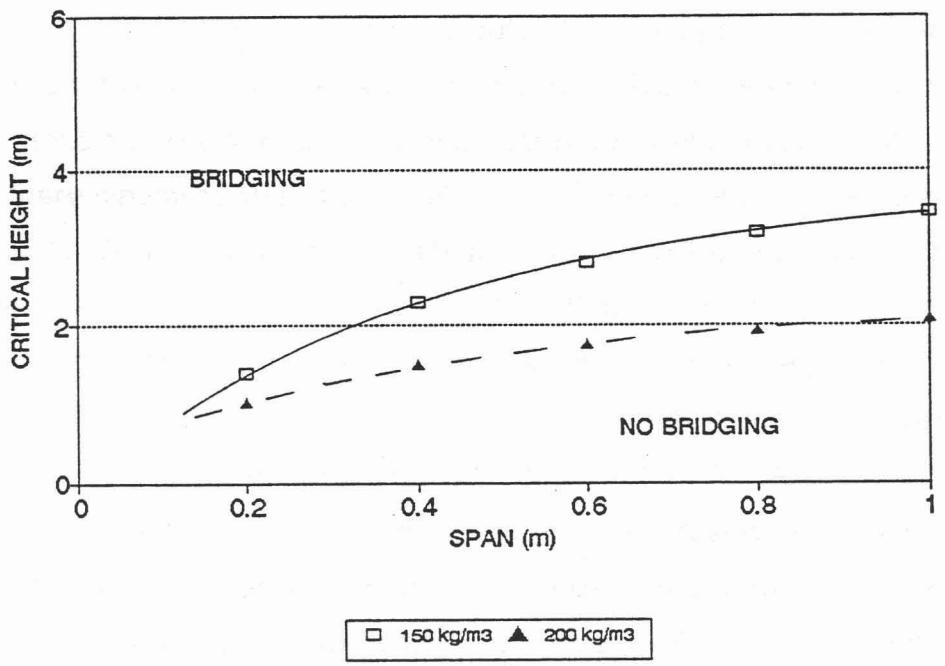

Figure 5.16 Bridging characteristics for diffuser bagasse.

The bridging characteristics for diffuser bagasse are given in Figure 5.16. The same fundamental parameters were used (W = 50%, t = 1.0, ρ_b = 150 and 200 kgm^{-3}) with an average mean fibre length L for diffuser bagasse of 20.0 mm and a coarse-fine ratio c of 2.0. It is noteworthy that

the graphs for diffuser bagasse are significantly lower, indicating a much increased bridging tendency compared to mill bagasse.

Diverging chutes

This chapter will be concluded by a few remarks concerning diverging chutes. Most bagasse chutes in the sugar industry are constructed so that they diverge slightly in the downward direction. A common angle of divergence is one degree.

If the mechanism of bridging proposed in section 5.5 is close to what happens in reality then the author would like to suggest that a small angle of divergence of 1° is not likely to be very effective in reducing the tendency to ***form*** stable bridges, because the pressure on these diverging chute walls will be very similar to that if the walls are parallel. It is proposed that one of the ***benefits in using diverging walls is when a choke, that has occurred, is cleared from below***. The reason for this is demonstrated by the compactibility tests reported in section 4.3. Once bagasse has been compacted to a certain extent (as when it forms a bridge in a chute) it will not regain its orginal volume after the compacting force is removed. In a diverging chute a little downward movement will result in a small increase in volume which tends to cause a significant reduction in the pressure between the bagasse and the wall. Therefore it will be easier to move this bagasse than in a parallel-sided chute.

The author decided to test this hypothesis in his bridging apparatus. In a particular test, for a plate separation of 0.20 m, a stable bridge was obtained at a depth of 0.56 m for parallel plates. When one plate was inclined by an angle of 1.3° to the vertical, so that the bottom opening was wider than the top, and the apparatus was charged with the same amount of material, it was found that a stable bridge was formed at a height of 0.51 m. Care had

been taken to attain the same degree of compaction in both tests. The reason why the height of material in the second case was lower than in the first is because of the greater separation of the plates at the bottom as a result of the 1.3° divergence. In other words, bridging occurred in almost identical fashion to the parallel-sided chute. This result seems to lend support to the above reasoning.

CHAPTER SIX

SUMMARY AND RECOMMENDATIONS

6.1 SUMMARY

The aim of this study was to try and identify, and measure, the key variables that influence the handling characteristics of bagasse and to apply the resulting information to the prediction of its bridging behaviour.

In chapter one some of the problems associated with handling of bagasse were described. An examination of existing bulk solid theories, summarised in chapter two, revealed that these could probably not be applied to a fibrous material like bagasse because conventional test equipment could not be used to measure one of the essential input variables, namely the angle of internal friction.

It was deemed necessary to place the measurement of the range of particle size and shape commonly found in bagasse on a sound, repeatable basis. Since the flow of bagasse is profoundly affected by the inter-locking

tendency of the fibres, in which the fibre length plays a major role, chapter three was devoted to describing the techniques that were developed to measure mean fibre length. Another measure, called the coarse-fine ratio, was defined. This figure describes quantitatively the ratio of the mass of fine particles to that of the coarse ones.

In chapter four the apparatus and techniques that were used to measure bulk properties of bagasse were described. These included

surface friction
change of bulk density under compacting loads
internal shear
translation of vertical to horizontal pressure
tensile strength.

Multivariate expressions for these, in terms of moisture content, bulk density, mean fibre length and coarse-fine ratio, were developed with the help of a statistical package. The attempts to measure internal shear of bagasse produced rather disappointing results. The other properties yielded expressions for which the agreement between observed and predicted values was acceptable.

A fairly intensive study of bridging behaviour was reported in chapter five. Two distinct modes of bridging were identified , one occurring as a result of surface friction and the other due to lateral obstructions. Bridging as a result of surface friction tends to be responsible for problems occurring in transfer equipment. An approximate bridging model for the surface friction mode was presented. It utilises the expressions from chapter four to evaluate the critical bridging height of a plug of bagasse. The model was used to compare predicted critical heights to those measured in the actual bridging tests, with satisfactory results. An example, in which the model is used to calculate the required dimensions of a bagasse chute, is presented. The model was also

employed to generate bridging characteristics for mill and diffuser bagasse from which the critical heights (determining maximum chute lengths) for different chute widths can be estimated.

6.2 ACHIEVEMENTS

The perceived achievements of this study are:

1. The particle characterisation of bagasse, in terms of its mean fibre length and coarse-fine ratio, has been placed on a sound basis. Furthermore, the techniques used to obtain these values are relatively simple and only require inexpensive and readily available equipment.

2. Accurate information on surface friction, and its dependence on bulk density, normal stress, mean fibre length and moisture content has been presented. This has also been obtained through the use of relatively unsophisticated hardware.

3. An indirect measure of the internal friction of bagasse, viz. the translation of vertical to horizontal pressure has been developed.

4. Multivariate expressions for various bulk properties of bagasse, and an approximate surface friction bridging model, which have application in design calculations, have been developed.

5. It was shown by means of the bridging apparatus that there are two distinct mechanisms of bridge formation, viz. bridges supported purely as a result of surface friction and those that are held up by lateral obstructions. In bagasse transfer

equipment the surface friction mode is operative whereas a knowledge of bridging due to lateral obstructions has little practical application.

6. The spreadsheet bridging model, which was described in section 5.5, has been used to develop two sets of bridging characteristics, one for mill bagasse and the other for diffuser bagasse, according to which the likelihood of bridging for different spans can be evaluated. Use of these characteristics, which are depicted insection 5.6, presupposes a knowledge of the approximate bulk density of the bagasse. The spreadsheet model can be used to generate similar characteristics for bagasse of a particular mean fibre length, coarse-fine ratio and moisture content.

6.3 RECOMMENDATIONS

Apart from the particle characteristics studied, the fibre hardness of bagasse is likely to have an effect on its handling characteristics. A way of measuring this would further assist in the understanding of its flow behaviour.

No application of the expression for tensile strength has been discussed. In the phenomenon of bridging caused by lateral supports this property is likely to feature prominently but this appears to have little practical application.

In this study a large cylindrical shear cell was used for measurements of surface friction and internal shear, as well as the translation of vertical to lateral pressure. The large shear cell did not prove very effective for surface friction and internal shear determinations. On the other hand, the surface friction box, the compactibility beaker and the tensile strength trolleys were relatively simple items which gave highly repeatable results. It seems

therefore that, for bulk solid measurements, small, simple equipment is to be preferred. However, a large cylindrical apparatus will be useful in studying the bridging behaviour in chutes of circular cross-section.

The translation of vertical to horizontal pressure as an indirect measure of internal friction is considered a very important measurement for predicting the flow properties of bagasse. A more extensive study of this relationship should improve the reliability of flow/hold-up predictions. Furthermore, the use of bricks is considered, in retrospect, an inappropriate means of increasing the vertical load on a given mass of bagasse because of the uneven load distribution generated. It is recommended that for valid deductions about horizontal and vertical pressures only loading with bagasse be used.

REFERENCES

Allan, GN (1970). Gledhow bagasse conveying system. *Sugar Milling Research Institute Technical Report* 911, 20 March: 5 pp.

Allen, T (1990). *Particle size measurement*. 4th edition. Chapman and Hall, London: 806 pp.

Anderson, CN (1988). Aerodynamics of bagasse particles. *Proc Austr Soc Sugar Cane Technol*: 235-239.

Anonymous (1958). Assessing the degree of cane preparation. *Sugar Research Institue Mackay Technical Report* 48, May: 6 pp.

Aralde, LE, Paz de Vázquez, D and Cárdenas, GJ (1993). Determination of heat transfer coefficient in pneumatic conveying of bagasse. *Int Sugar Jnl.* 95 (1135E): 287-291.

Arnold, PC and Reed, AR (1987). On the machine dependence of flow property measurements on bulk solids. *Bulk Solids Handling* 7 (3): 397-400.

Bernhardt, HW (1993). Shape factors of bagasse particles. *Proc South Afr Sugar Technol Ass* 67: 181-184.

Blight, GE (1988). A comparison of measured pressures in silos with code recommendations. *Bulk Solids Handling* 8 (2): 145-153.

Bruijn, J (1973). Progress report No. 1: Microbial influence of bagasse storage. *Sugar Milling Research Institute Technical Report* 977, 22 February: 13 pp.

Bullock, KJ (1957). *An investigation into the crushing and physical properties of sugar cane and bagasse*. PhD thesis, Vol I and Vol II, Univ. Queensland, May: 400 pp.

Bullock, KJ and Murry, CR (1957). Coefficient of friction of bagasse on iron surfaces. *Proc Queensland Soc Sug Cane Technol* 24: 81-88.

Burger, R and Gonin, CR (1975). A proposed method to evaluate sugar-cane bagasse for useful fibre. *CSIR Special Report HOUT 110*, November: 15 pp.

Carliell, DJ (1984). Swinging bagasse ploughs. *Proc South Afr Sugar Technol Ass* 58: 96-97.

Carr, JF and Walker, DM (1967). An annular shear cell for granular materials. *Powder Technology* 1: 369-373.

Carson, JW (1991). North American advances in the design of silos, bins and hoppers. *Bulk Solids Handling* 11 (1): 37-44.

Cowin, SC (1974). A theory for the flow of granular materials. *Powder Technology* 9: 61-69.

Cullen, RN (1967). Pneumatic separation and conveying of bagacillo. *Proc Queensland Soc Sug Technol Conf* 34: 161-170.

Douglas, TP, Picaro, T and White, ET (1991). Friction between a moving fibre bed and a stationary wall. *Proc Australian Soc Sug Cane Technol*, 313-321.

Eagle Electric Company (Pty) Ltd (1991). *Electronics catalogue*, Cape Town, Telephone (021) 234943: 240 pp.

Ednie, WP (1967). Atlas storage bin and reclaim conveyor system. *Hawaiian Sugarcane Technol Reports* 26: 83-84.

Farley, R and Valentin, FHH (1968). Effect of particle size upon the strength of powders. *Powder Technology* 1: 344-354.

Farmer, J (1977). The theory, design and operation of multiple barrelled screw presses for bagasse. *Proc ISSCT* 16 (3): 2199-2229.

Ferguson, EF (1957). Ash and bagasse handling at Ewa. *Hawaiian Sugarcane Technol Reports* 16: 103-104.

Foster, DH and Hill, JW (1966). Pilot plant diffusion experiments. *Proc Queensland Soc Sug Cane Technol* 33: 111-119.

Foster, DH and Shann, DS (1968). Cane preparation in relation to milling and difffusion. *Proc ISSCT* 13: 142-150.

Gaylord, EH and Gaylord, CN (1984). *Design of steel bins for storage of bulk solids*. Prentice-Hall, London: 359 pp.

Herdan, G (1960). *Small particle statistics*, 2nd edition. Butterworths, London: 418 pp.

Heywood, H (1970). Size, shape and size distribution of particulate materials. *Lecture in Course on Particle Technology*, November. Nordwijk, Netherlands: 14 pp.

Hoeckman, W and Meulewaeter, L (1988). Experimental investigation of some important soy shreds characteristics. *Bulk Solids Handling* 8 (2): 155-161.

Hoekstra, RG (1987). The evaluation of bagasse quality. *Tongaat-Hulett Sugar Technology Department Report*: 14 pp.

Holliday, B (1990). Size distribution of bagacillo. *Tongaat-Hulett Sugar Technology Department Report* R/BA/01/3 T/MP/06, 14 June: 9 pp.

Hugot, E (1986). *Handbook of cane sugar engineering*, 3rd edition. Elsevier, Amsterdam: 1166 pp.

Jackson, JR (1984). Bagasse avalanche screws at Amatikulu. *Proc S Afr Sug Technol Ass* 58: 93-95.

Janssen, HA (1895). Getreidedruck in Silozellen. *Z Ver Dt Ing*, 39: 1045-1049.

Jenike, AW, Elsey, PJ and Woolley, RH (1960). Flow properties of bulk solids. *Proc ASTM* 60: 1168-1190.

Jenike, AW (1964). Storage and flow of solids. *Bulletin 123*, University of Utah, Engineering Experiment Station.

Jenkins, GH (1966). *Introduction to cane sugar technology*. Elsevier, Amsterdam: 478 pp.

Knights, AG and Perreira, DC (1966). Mechanised handling of bagasse. *Proc Brit. West Indies Sug Technol*, 2: 404-407.

Love, DJ and Rein, PW (1980). Percolation behaviour of cane diffuser. *Proc ISSCT* 17 (3): 1900-1924.

Luxford, RW, Magnussen, WH and Wilson, MJ (1977). Development of a bagasse feeder. *Proc Queensland Soc Sug Cane Technol* 44: 369-372.

Marson, JL (1980). *Mathematical modelling of an industrial cane shredder*. MSc Eng thesis, Univ. Natal (Durban), November: 220 pp.

McCabe, WL, Smith, JC and Harriott, P (1985). *Unit operations in chemical engineering*,4th edition. McGraw Hill, New York: 960 pp.

McLean, AG (1988). A closer examination of the variation of wall friction angle with major consolidation stress. *Bulk Solids Handling* 8 (4): 407-411.

Miyagawa, ST (1975). Bagasse feeding with plows and belt conveyor. *Hawaiian Sugarcane Technol Reports* 34: 128-129.

Molerus, O (1975). Theory of yield of cohesive powders. *Powder Technology* 12: 259-275.

Molerus, O (1985). Mechanics of particulate solids - state of the art and current trends. *German Chem. Eng.* 8: 380-388.

Moodley, M (1991). Pith and fibre content of cane. *Sugar Milling Research Institute Technical Report* 1596: 7 pp.

Munro, BM (1964). *An investigation into crushing of bagasse and the influence of imbibition on extraction*. PhD thesis, Univ. Queensland, June: 283 pp.

Murry, CR (1960). *The mechanics of crushing sugar cane*. PhD thesis, Univ. Queensland, September: 265 pp.

Murry, CR and Hutchinson, R (1958). Movement of bagasse in long chutes. *Proc Queensland Soc Sug Cane Technol* 25: 75-81.

Nedderman, RM (1982). The theoretical prediction of stress distributions in hoppers. *Trans IChemE* 60: 259-275.

Pastega, LA (1971). The effects of varying the percentage pol in open cells in prepared cane. *Proc Queensland Soc Sug Technol Conf* 38: 217-223.

Paturau, JM (1989). *By-products of the cane sugar industry*. Elsevier, Amsterdam, 3rd edition: 435 pp.

Plaza, F and Edwards, BP (1994). Shear, friction and the required roll roughness. *Proc Austr Soc Sugar Cane Technol*: 244-248.

Ponce, N, Friedman, P and Leal, D (1983). Geometric properties and density of bagasse particles. *Int Sugar Jnl.* 85 (1018): 291-295.

Precision curve fitter (1994). Distributed by *PRECISION SOFTWARE*, PO Box 84360, Greenside 2034, South Africa.

Press, WH, Flannery, BR, Teukolsky, SA and Vetterling, WT (1990). *Numerical recipes in Pascal*. Cambridge University Press: 574-580.

Ramanujam, D (1956). Influence of structure of cane on the "steaming" quality of bagasse and on mill work. *Proc ISSCT* 9 (2): 63-69.

Rein, PW (1972). *A study of the cane diffusion process*. PhD thesis, Univ. Natal (Durban), October: 330 pp.

Roberts, AW (1991). Bulk solids handling: recent developments and future directions. *Bulk Solids Handling* 11 (1): 17-35.

Russell, GE (1968). *The extraction performance of sugar cane crushing trains*. PhD thesis, Univ. Queensland, July: 341 pp.

Ryder, HG (1969). *Strength of materials*, 3rd edition in SI units. Macmillan, London: 340 pp.

SASTA Laboratory Manual (1985). *Laboratory manual for South African sugar factories including the official methods*, 3rd edition. Interpak Natal, Pietermaritzburg: 436 pp.

Schwedes, J (1983). Evolution of bulk solids technology since 1974. *Bulk Solids Handling* 3 (1): 143-147.

Singh, H, Sharma, SM and Prasad, CRK (1993). Bloated clay aggregates as inert bed material for fluidized combustion of bagasse. *Int Sugar Jnl.* 95 (1130): 46-50.

Sockhill, BD (1956). Pol distribution in final bagasse. *Proc Queensland Soc Sug Technol Conf* 23: 163-167.

Solomon, TJ (1967). *Theoretical and experimental studies on the mechanics of crushing sugar cane*. PhD thesis, Univ. Queensland, April: 290 pp.

Statgraphics 5.0 (1991). Statistical Graphics Corporation, USA.

Status-74 V2.00 (1989). Data acquisition software for IBM and compatible computer systems. Marketed by *Eagle Electronics Company (Pty) Ltd, Cape Town, South Africa*, telephone: (021) 234943.

Terzaghi, K (1943). *Theoretical soil mechanics*. Wiley, New York.

Walker, DM (1966). An approximate theory for pressures and arching in hoppers. *Chem Eng Science* 21: 975-997.

Walters, JK (1972). A theoretical analysis of stresses in silos with vertical walls. *Chem Eng Science* 28: 13-21.

Williams, JC and Birks, AH (1967). The comparison of failure measurements of powders with theory. *Powder Technology* 1: 199-206.

Wilms, H (1985). Calculation of stresses in silos by the method of characteristics. *Bulk Solids Handling* 5(2): 425-429.

APPENDIX A

ELECTRONIC DATALOGGING SYSTEM

A commercially available data acquisition board called Status-74 (Eagle Electric Company, 1991, p.13) was used for data capture. It features an 80 kHz analogue-to-digital throughput, 12 bit resolution, a programmable gain control, 16 analogue input channels, two 12-bit D/A converters and 16 digital I/O lines, and uses an IBM-compatible computer system for data capture, storage and display. It has the capability of reading 16 channels sequentially and the speed of taking readings (sampling) can be set at one of 57 settings between 600 000 and 0.005 Hz. With the aid of a colour monitor the readings of the sampled channels are displayed. The use of appropriate scale factors applied to voltmeter outputs permits the display of actual values. The digital values read on each channel can be observed separately to facilitate calibration. The number of readings to be recorded can be preset. The data could be stored on floppy diskettes and the programme had the capability to change the data format into text mode in which it could be imported into a standard spreadsheet programme such as Quattropro. This was done and initial data analysis was performed within that software programme. The full data analysis procedure is explained in the text.

APPENDIX B

TENSION MEASURING DEVICE

The tension measuring device, which was used for surface friction measurements as well as for tensile strength tests, was constructed of two pieces of spring steel of equal length riveted together at one end with a spacer separating them, as shown in Figure B.1. Tension force was transmitted to the electronic datalogging system by means of a set of strain gauges bonded on each piece of spring steel approximately 15 mm above the rivets. Figure B.1 (a) shows the tension measuring device in its normal position when measurements were being taken while Figure B.1 (b) shows its position during calibration. Mass pieces of known mass were used to calibrate it. The calibration data are presented in Table B.1.

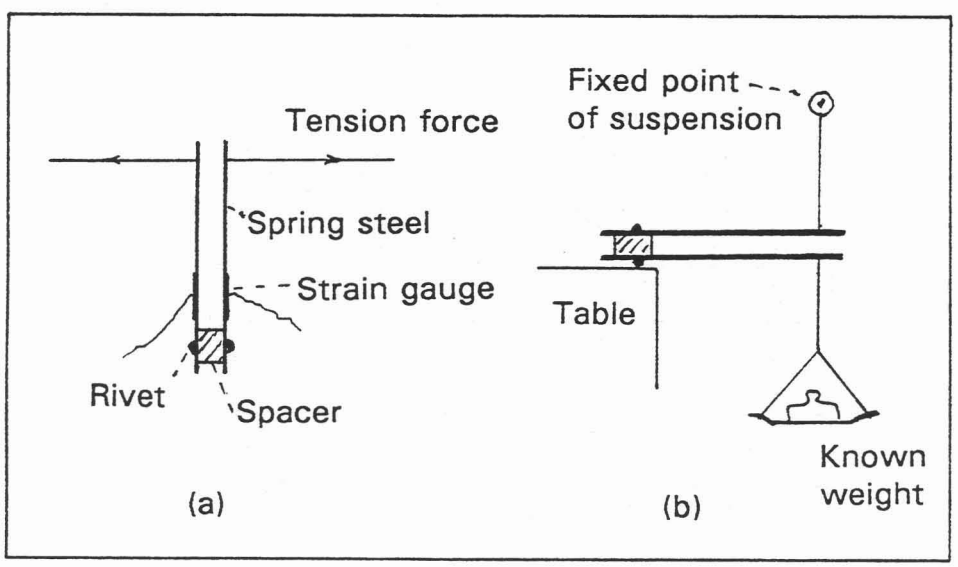

Figure B.1 *Tension measuring device: (a) in normal position during experiments (b) in calibration position*

Table B.1

Calibration details for tensile force meter

CALIBRATION OF TENSILE FORCE METER

OBJECT	MASS (g)	FORCE (N) MEAS	FORCE (N) REGR	INSTR RDG AVE	TENSILE FORCE METER READIN				
0	0.00	0.000	-0.04	3.01	2.99	2.91	3.08	3.16	2.91
PAN	126.54	1.241	1.27	7.96	7.86	7.95	7.78	8.2	8.03
1	21.25	1.450	1.48	8.73	8.72	8.89	8.63	8.8	8.63
2	60.58	1.836	1.84	10.10	9.91	10.28	10.08	10.17	10.08
3	107.23	2.293	2.29	11.81	11.88	11.62	11.71	11.79	12.05
4	354.39	4.718	4.69	20.87	20.76	20.85	20.94	20.68	21.11
5	1430.00	15.270	15.27	60.81	61.10	61.27	60.58	60.33	60.75

Regression Output:

Constant	-0.8364351
Std Err of Y Est	0.0283347
R Squared	0.99997568
No. of Observations	7
Degrees of Freedom	5
X Coefficient(s)	0.26491317
Std Err of Coef.	0.00058432

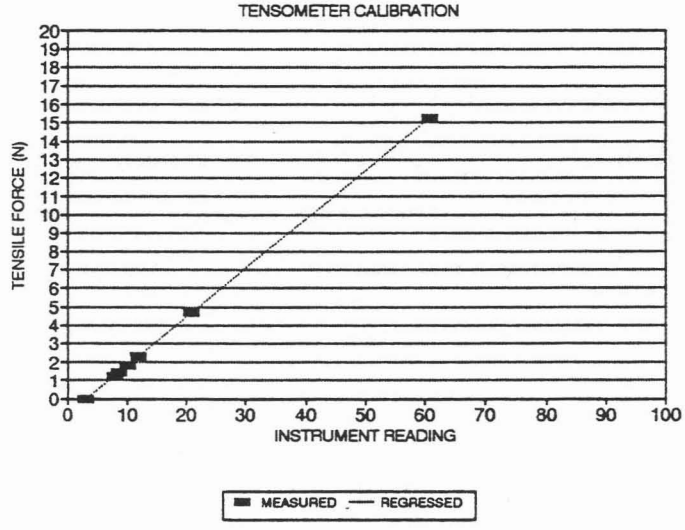

APPENDIX C

CALIBRATION OF TORQUEMETER AND SPEED-MEASURING DEVICE

The torquemeter was used to measure the force required by the stirrer in the cylindrical shear cell to produce internal shear of the bagasse. The measuring element was a load cell fixed to the end of a lever which was bolted to the housing of the hydraulic motor turning the stirrer. The load cell could not be calibrated in its position on the apparatus. As mentioned in the text, this led to an off-set of the torquemeter readings which had to be taken into account in the measurements.

For calibration purposes two platforms were attached to opposite ends of the load cell, one of these resting on the floor. The weight of the other platform which was resting on the top end of the load cell was known. Different weights were placed on the top platform and the electronic output of the loadcell was correlated with these weights. The relation between weight and voltage output is shown in Figure C.1.

The loadcell was thus calibrated with compressive loads, but on the apparatus it was subjected to tensile loads. The manufacturer, however, maintained that its response was the same in tension as in compression. The length of the lever to which the load cell was attached and the diameter of the cylindrical shear surface were taken into account when calculating the internal shear stress.

The speed-measuring device consisted of a circular mild steel disc, mounted co-axially with the shaft of the hydraulic motor, which had accurately machined indentations and protrusions on its circumference . A proximity sensor detected the protrusions which resulted in a given voltage output. For calibration purposes a mark painted on the disc facilitated the counting of

the number of revolutions of the shaft. A stopwatch was used to determine the time taken for the respective number of revolutions. The calibration equation which relates voltage output (V) from the proximity sensor with revolutions per minute (RPM) was

$$RPM = -0.157 + 12.27V \quad . \qquad (C.1)$$

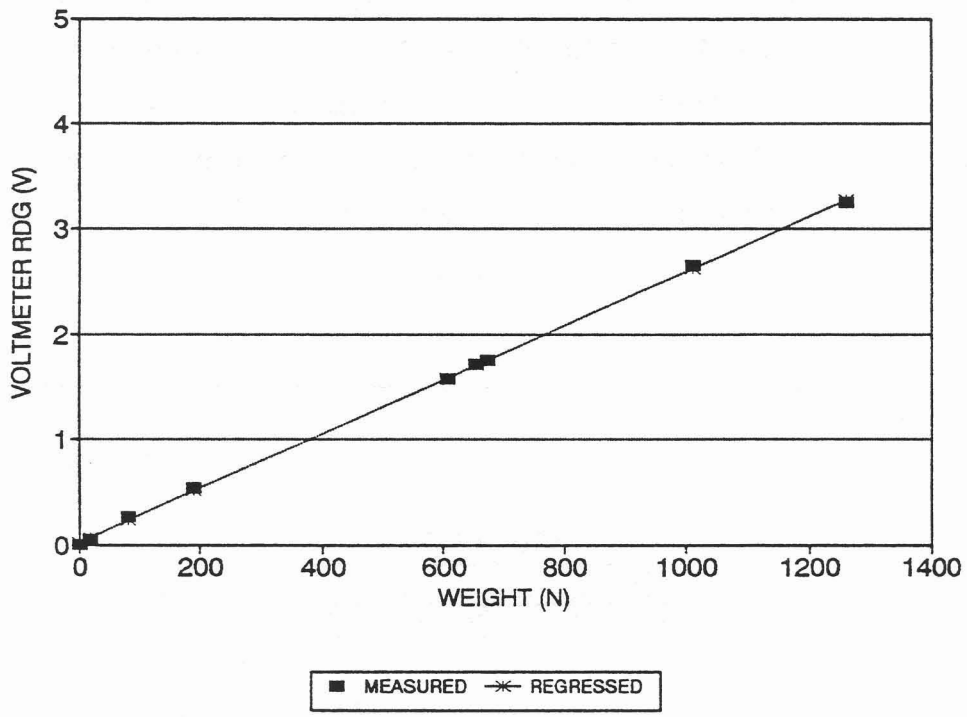

Figure C.1 *Calibration graph of torquemeter loadcell*

APPENDIX D

CONSTRUCTION AND CALIBRATION DETAILS OF PRESSURE TRANSDUCERS

The pressures recorded by bagasse in the shear cell, and also in the bridging apparatus were extremely low (of the order of a few hundred Pa). Hence an instrument that is to be capable of measuring such low pressures must be very sensitive. The transducer that was designed by Mr Vaughn Stone of the Engineering Division at the SMRI was a pneumatic instrument. Its construction is indicated in Figure D.1.

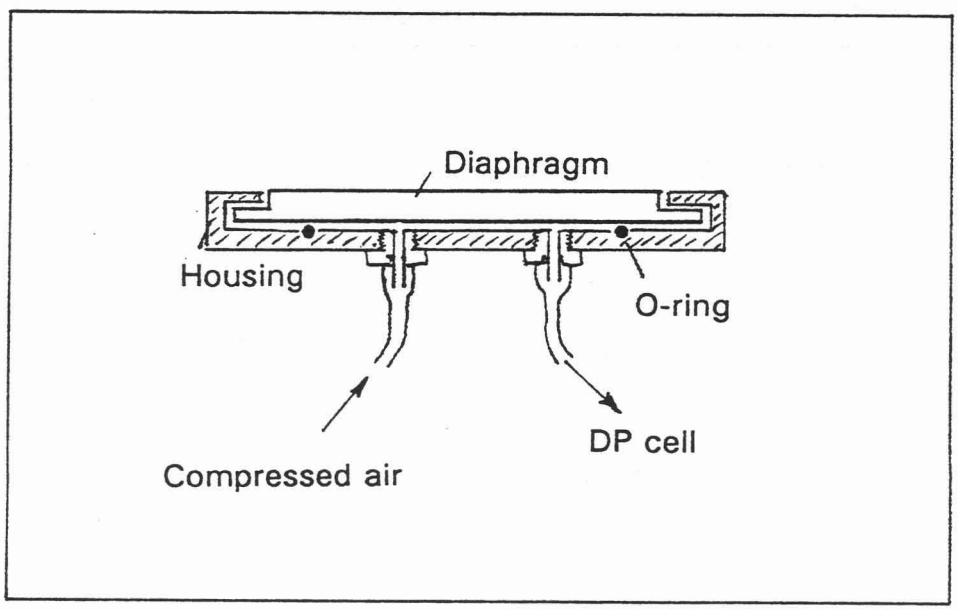

Figure D.1 *Cross-section through bagasse pressure transducer*

The DP cell converted the pneumatic signal to an electronic one. With the transducer in a horizontal position weights were used for calibration. A typical calibration curve is shown in Figure D.2.

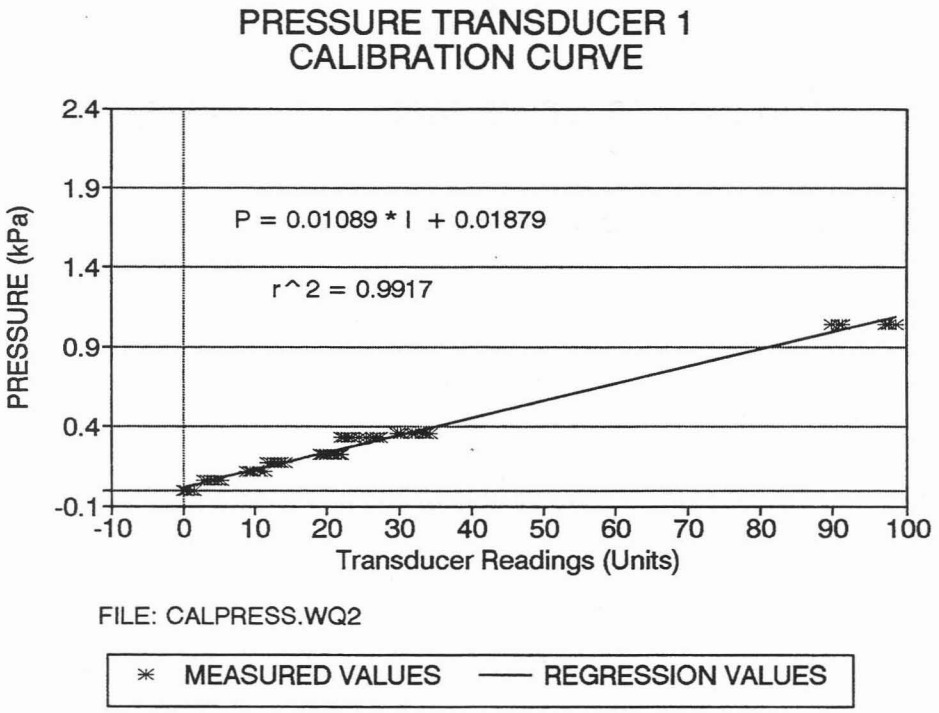

Figure D.2 *Calibration graph for pressure transducer*

APPENDIX E

VARIATION OF LATERAL PRESSURE WITH HEIGHT

The data investigating the variation of lateral bagasse pressure with height are shown in Table E.1.

Table E.1

Measurements to investigate variation of pressure with height

FILE: PRESSHT.WQ2 25-11-94

PRESSURE VS HEIGHT RELATIONSHIP

BAGASSE: MILL (MS6) MOISTURE(%):
DIST. BETWEEN PLATES (cm): 43.5

PRESSURE CALIBRATION EQUN: P = 0.01089*I + 0.01879
(I = TRANSDUCER READING)

MASS kg	HEIGHT cm	BULK DENSITY kg/m3	PRESS. TRANSDUCER RDGS				AVE	PRESS kPa	VERT. STRESS kPa
13.3	30	63.3	1.46	1.46	0.98	0.00	0.98	0.029	
21.6	50	61.7	8.30	7.32	7.32	6.84	7.45	0.100	0.027
33.4	75	63.6	10.25	10.74	11.23	9.77	10.50	0.133	0.066
46.3	102	64.8	12.70	11.72	14.16	13.18	12.94	0.160	0.108
60.8	131	66.3	24.41	23.44	22.95	23.44	23.56	0.275	0.156
128.4	128	67.9	38.57	38.09	37.11	37.60	37.84	0.431	0.378

* LOAD OF 67.6 kg ON WOODEN PLANK

NOTE: VERTICAL STRESS IGNORES SURFACE FRICTION

The bridging apparatus (see section 5.2) was used for the investigation. With the vertical plates separated by a distance of 43.5 cm and the trapdoor

closed bagasse was added to the apparatus and compacted with the garden fork as described in section 5.3. It can be seen from Table E.1 above that the bulk density during the experiment was essentially constant. The variation of pressure with height is depicted in Figure E.1.

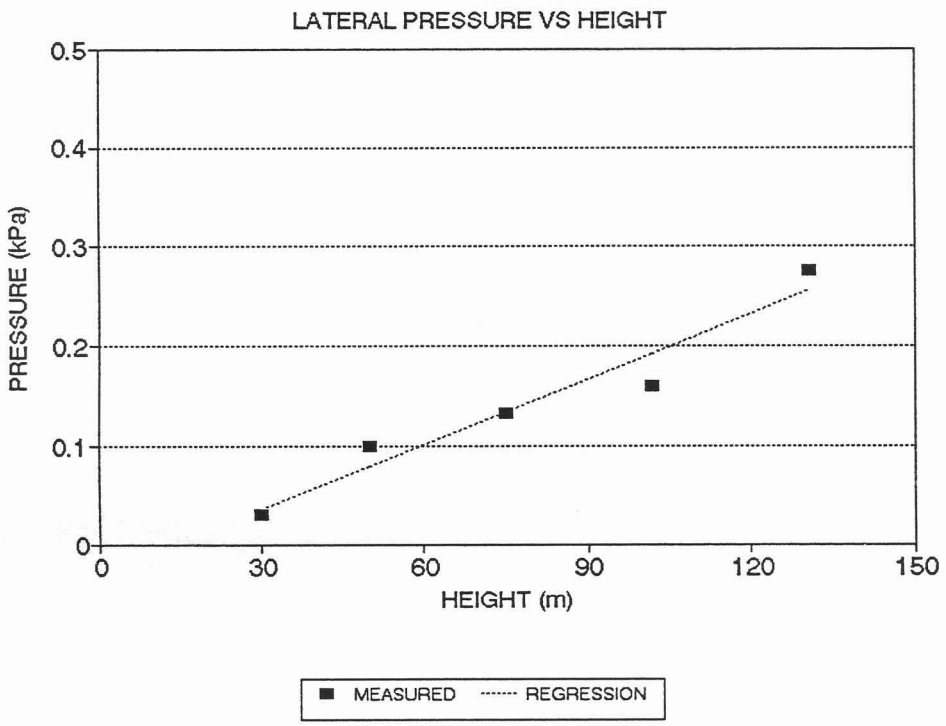

Figure E.1 *Variation of pressure with height*

The pressure transducers (one on each vertical plate) were situated at a height of 30 cm above the trapdoor, thus they measure the lateral pressure of bagasse above that height. This is shown in Figure E.1 which shows that at 30 cm the pressure is nearly zero. A load of 67.6 kg in the form of bricks was added on a wooden plank on top of the bagasse after the final addition of material. This caused some compaction which obviously affected the height. This data point is therefore not shown as part of the graph in Figure E.1.